A fast ionization chamber for the detection of fusion-evaporation residues produced by the exotic beams of SPES: design, tests and first experiment

Giulia Colucci

Heavy Ion Laboratory, University of Warsaw, Warsaw, Poland

Istituto Nazionale di Fisica Nucleare
Laboratori Nazionali di Legnaro

Heavy Ion Laboratory

- A fast ionization chamber for the study of fusion reactions induced by low-intensity radioactive beams

- Effects of non-zero spin in sub-barrier fusion involving odd mass nuclei: the case of $^{36}S+^{50}Ti,^{51}V$

A fast ionization chamber for the study of fusion reactions induced by low-intensity radioactive beams

- **Sub-barrier fusion from stable to radioactive beams**
- **Present status of PISOLO set-up**
- **The Fast Ionization Chamber**
- **Tests with stable beams**
  - **Shaping time and DAQ gate width**
  - **Rates**
  - **Z and Energy resolution**

Effects of non-zero spin in sub-barrier fusion involving odd mass nuclei: the case of $^{36}S+^{50}Ti,^{51}V$

- **A fast ionization chamber for the study of fusion reactions induced by low-intensity radioactive beams**

- **Effects of non-zero spin in sub-barrier fusion involving odd mass nuclei: the case of $^{36}S+^{50}Ti,^{51}V$**

- A fast ionization chamber for the study of fusion reactions induced by low-intensity radioactive beams

- Effects of non-zero spin in sub-barrier fusion involving odd mass nuclei: the case of $^{36}S+^{50}Ti,^{51}V$

  - The $^{36}S+^{50}Ti,^{51}V$ systems
  - Near- and sub-barrier fusion experiment
  - Results

    Excitation function

    Barrier distribution

    Coupled channel (CC) analysis
  - Interpretation of the results
  - Summary

Sub-barrier fusion from stable to radioactive beams

Present status of PISOLO set-up

The Fast Ionization Chamber

Tests with stable beams

- Shaping time and DAQ gate width
- Rates
- Z and Energy resolution

A fast ionization chamber for the study of fusion reactions induced by low-intensity radioactive beams

Istituto Nazionale di Fisica Nucleare
Laboratori Nazionali di Legnaro

Heavy Ion Laboratory

Sub-barrier fusion from stable to radioactive beams

Present status of PISOLO set-up

The Fast Ionization Chamber

Tests with stable beams

- **Shaping time and DAQ gate width**
- **Rates**
- **Z and Energy resolution**

Two interactions: long range repulsive **Coulomb force** and short range attractive **nuclear force**. Cancellation between the two forces generates **Coulomb barrier**.

Sub-barrier region
$|E - V_b| \lesssim 10MeV$

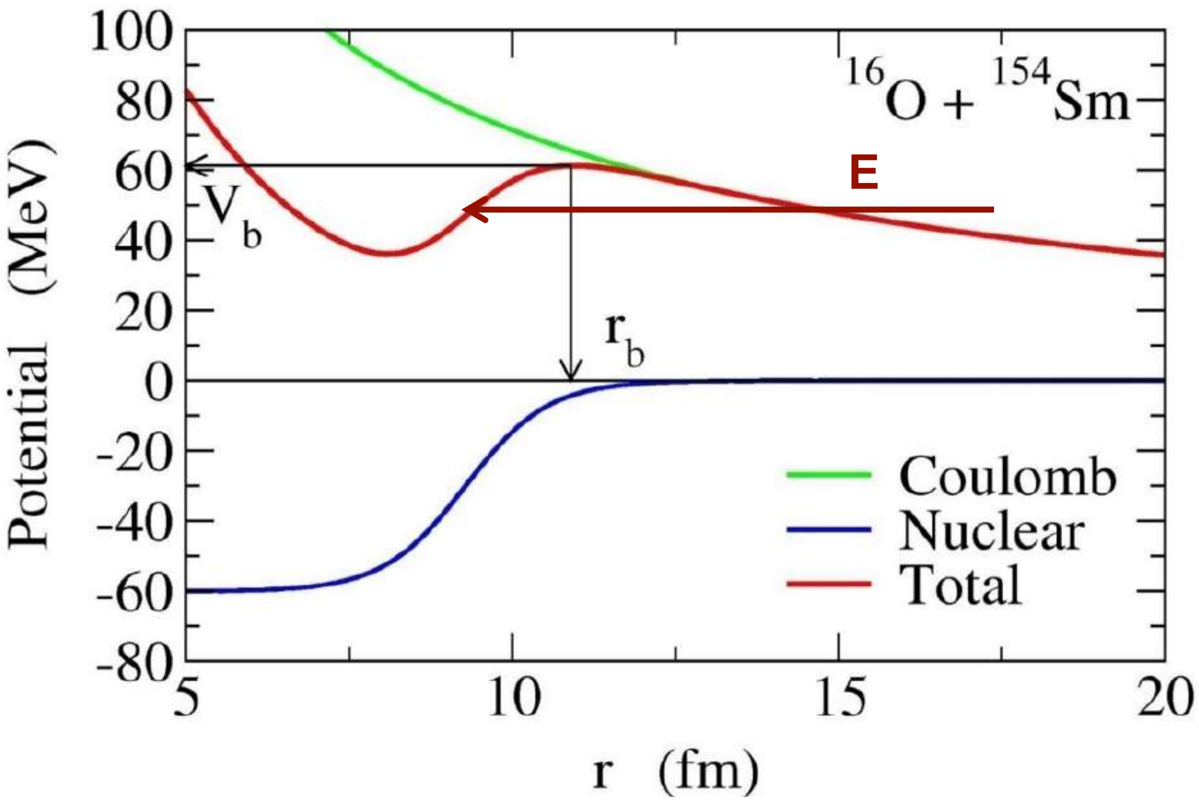

K. Hagino, Progress of Theoretical Physics, Vol. **128**, No. 6, (2012)

Sub-barrier fusion from stable to radioactive beams

Present status of PISOLO set-up

The Fast Ionization Chamber

Tests with stable beams

- **Shaping time and DAQ gate width**
- **Rates**
- **Z and Energy resolution**

Two interactions: long range repulsive **Coulomb force** and short range attractive **nuclear force**. Cancellation between the two forces generates **Coulomb barrier**.

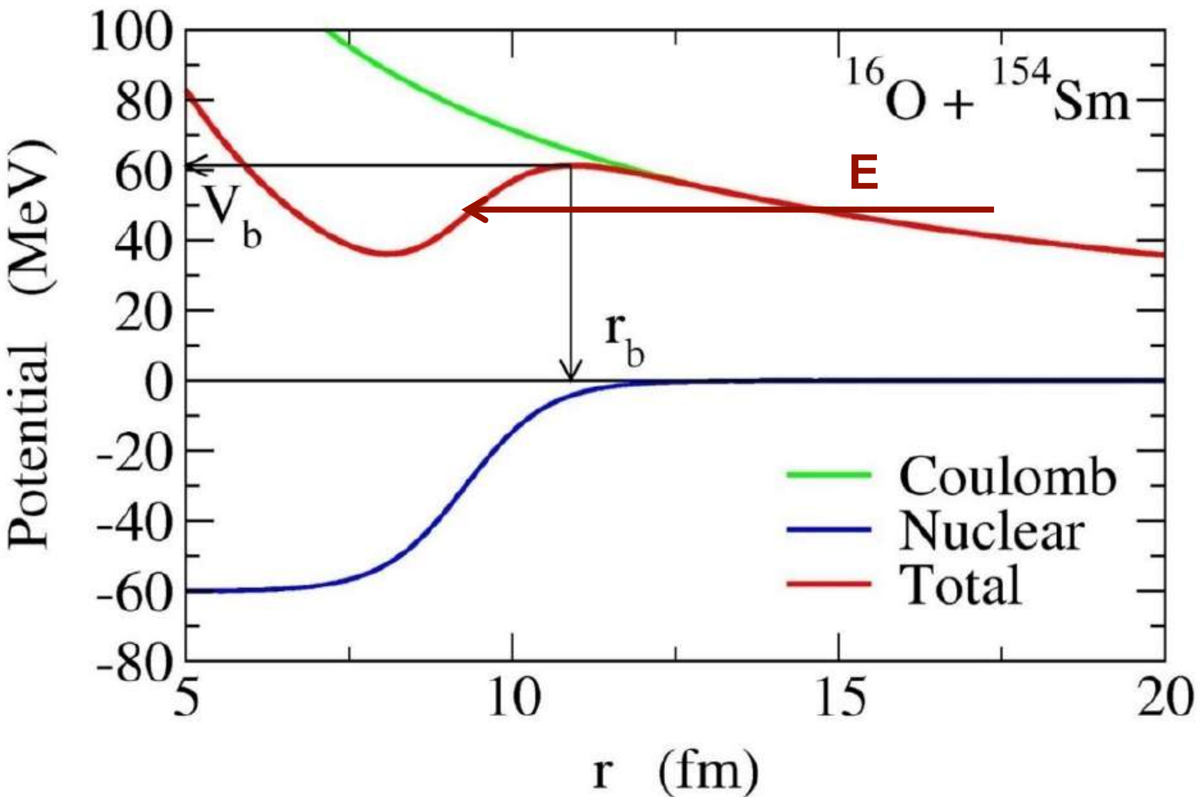

Sub-barrier region
$|E - V_b| \lesssim 10 MeV$

Why sub-barrier fusion?

- Many-particle tunnelling effect
  - Many types of intrinsic degrees of freedom (collective vibrational, rotational states..)
  - Energy dependence of tunnelling probability
- Strong interplay between reaction and structure

K. Hagino, Progress of Theoretical Physics, Vol. **128**, No. 6, (2012)

Sub-barrier fusion from stable to radioactive beams

Present status of PISOLO set-up

The Fast Ionization Chamber

Tests with stable beams

- **Shaping time and DAQ gate width**
- **Rates**
- **Z and Energy resolution**

- One-dimensional model

$$\left[-\frac{\hbar^2}{2\mu}\frac{d^2}{dr^2}+\frac{J(J+1)\hbar^2}{2\mu r^2}+V(r)-E\right]u_n(r)=0$$

$$\Longrightarrow\ \sigma_{fus}=\frac{\pi}{k^2}\sum_J(2J+1)P_l(E)$$

K. Hagino, Progress of Theoretical Physics, Vol. **128**, No. 6, (2012)

Sub-barrier fusion from stable to radioactive beams

Present status of PISOLO set-up

The Fast Ionization Chamber

Tests with stable beams

- **Shaping time and DAQ gate width**
- **Rates**
- **Z and Energy resolution**

- One-dimensional model

$$\left[-\frac{\hbar^2}{2\mu}\frac{d^2}{dr^2}+\frac{J(J+1)\hbar^2}{2\mu r^2}+V(r)-E\right]u_n(r)=0$$

$$\Rightarrow\ \sigma_{fus}=\frac{\pi}{k^2}\sum_J(2J+1)P_l(E)$$

Enhancement due to strong couplings between the relative motion of colliding nuclei and the intrinsic degrees of freedom of target and/or projectile

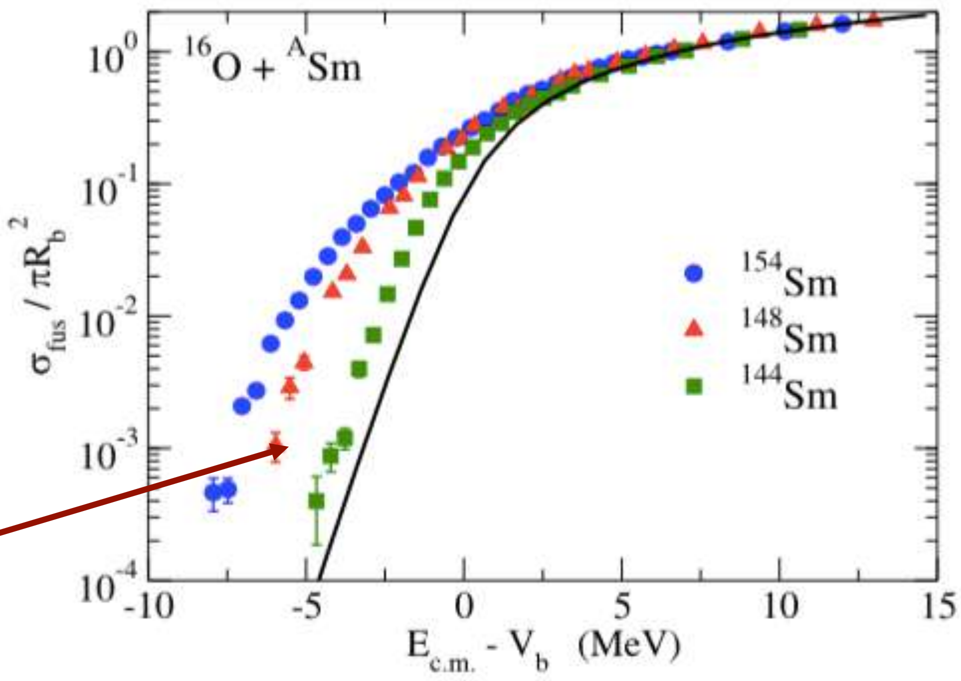

K. Hagino, Progress of Theoretical Physics, Vol. **128**, No. 6, (2012)

Sub-barrier fusion from stable to radioactive beams

Present status of PISOLO set-up

The Fast Ionization Chamber

Tests with stable beams

- **Shaping time and DAQ gate width**
- **Rates**
- **Z and Energy resolution**

- One-dimensional model

$$\left[-\frac{\hbar^2}{2\mu}\frac{d^2}{dr^2}+\frac{J(J+1)\hbar^2}{2\mu r^2}+V(r)-E\right]u_n(r)=0$$

$$\Rightarrow \sigma_{fus}=\frac{\pi}{k^2}\sum_J (2J+1)P_l(E)$$

Enhancement due to strong couplings between the relative motion of colliding nuclei and the intrinsic degrees of freedom of target and/or projectile

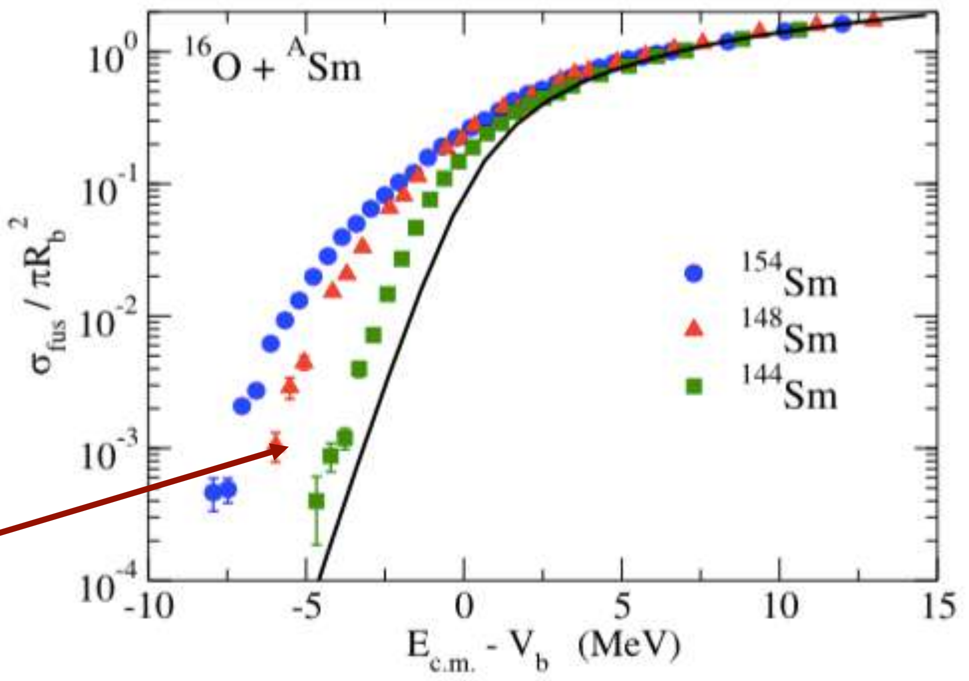

- Coupled channels model

$$H(r,\xi)=-\frac{\hbar^2}{2\mu}\frac{d^2}{dr^2}+V(r)+H_0(\xi)+V_{Coup}(r,\xi)$$

K. Hagino, Progress of Theoretical Physics, Vol. **128**, No. 6, (2012)

Sub-barrier fusion from stable to radioactive beams

Present status of PISOLO set-up

The Fast Ionization Chamber

Tests with stable beams

- **Shaping time and DAQ gate width**
- **Rates**
- **Z and Energy resolution**

- One-dimensional model

$$\left[-\frac{\hbar^2}{2\mu}\frac{d^2}{dr^2}+\frac{J(J+1)\hbar^2}{2\mu r^2}+V(r)-E\right]u_n(r)=0$$

$$\Longrightarrow\ \sigma_{fus}=\frac{\pi}{k^2}\sum_J(2J+1)P_l(E)$$

Enhancement due to strong couplings between the relative motion of colliding nuclei and the intrinsic degrees of freedom of target and/or projectile

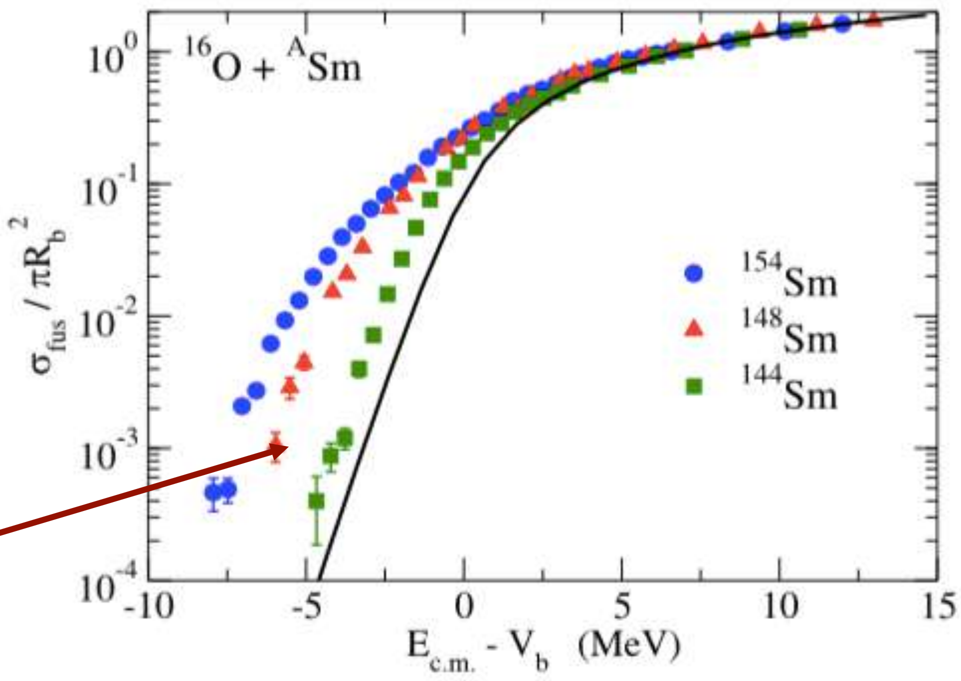

- Coupled channels model

$$H(r,\xi)=-\frac{\hbar^2}{2\mu}\frac{d^2}{dr^2}+V(r)+H_0(\xi)+V_{Coup}(r,\xi)$$

$$\left[-\frac{\hbar^2}{2\mu}\frac{d^2}{dr^2}+\frac{J(J+1)\hbar^2}{2\mu r^2}+V^{(0)}(r)+\epsilon_n-E\right]u_n(r)$$
$$+\sum_m V_{mn}(r)u_m(r)=0$$

Coupling Hamiltonian

K. Hagino, Progress of Theoretical Physics, Vol. **128**, No. 6, (2012)

Sub-barrier fusion from stable to radioactive beams

Present status of PISOLO set-up

The Fast Ionization Chamber

Tests with stable beams

- **Shaping time and DAQ gate width**
- **Rates**
- **Z and Energy resolution**

- One-dimensional model

$$\left[-\frac{\hbar^2}{2\mu}\frac{d^2}{dr^2}+\frac{J(J+1)\hbar^2}{2\mu r^2}+V(r)-E\right]u_n(r)=0$$

$$\Rightarrow\ \sigma_{fus}=\frac{\pi}{k^2}\sum_J(2J+1)P_l(E)$$

Enhancement due to strong couplings between the relative motion of colliding nuclei and the intrinsic degrees of freedom of target and/or projectile

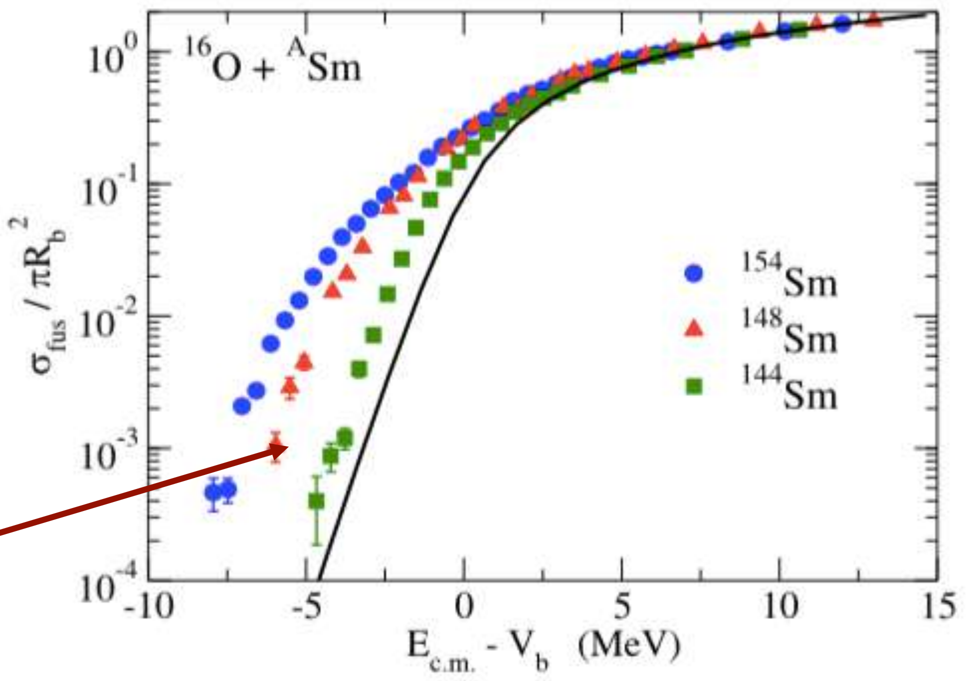

- Coupled channels model

$$H(r,\xi)=-\frac{\hbar^2}{2\mu}\frac{d^2}{dr^2}+V(r)+H_0(\xi)+V_{Coup}(r,\xi)$$

$$\left[-\frac{\hbar^2}{2\mu}\frac{d^2}{dr^2}+\frac{J(J+1)\hbar^2}{2\mu r^2}+V^{(0)}(r)+\epsilon_n-E\right]u_n(r)$$

$$+\sum_m V_{mn}(r)u_m(r)=0 \quad\Rightarrow\quad \sigma_{fus}(E)=\sum_k w_k\sigma_{fus}(E;V_k)$$

Coupling Hamiltonian

K. Hagino, Progress of Theoretical Physics, Vol. **128**, No. 6, (2012)

Istituto Nazionale di Fisica Nucleare
Laboratori Nazionali di Legnaro
HIL Heavy Ion Laboratory

G. Colucci

Sub-barrier fusion from stable to radioactive beams

Present status of PISOLO set-up

The Fast Ionization Chamber

Tests with stable beams

- **Shaping time and DAQ gate width**
- **Rates**
- **Z and Energy resolution**

- One-dimensional model

$$\left[-\frac{\hbar^2}{2\mu}\frac{d^2}{dr^2}+\frac{J(J+1)\hbar^2}{2\mu r^2}+V(r)-E\right]u_n(r)=0$$

$$\Rightarrow\ \sigma_{fus}=\frac{\pi}{k^2}\sum_J(2J+1)P_l(E)$$

Enhancement due to strong couplings between the relative motion of colliding nuclei and the intrinsic degrees of freedom of target and/or projectile

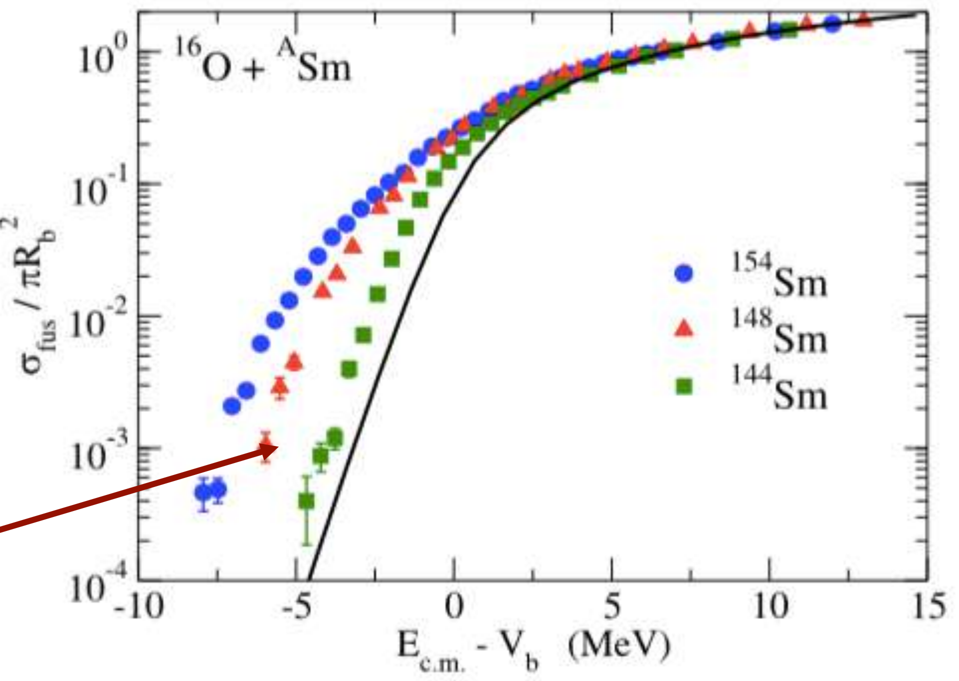

- Coupled channels model

$$H(r,\xi)=-\frac{\hbar^2}{2\mu}\frac{d^2}{dr^2}+V(r)+H_0(\xi)+V_{Coup}(r,\xi)$$

$$\left[-\frac{\hbar^2}{2\mu}\frac{d^2}{dr^2}+\frac{J(J+1)\hbar^2}{2\mu r^2}+V^{(0)}(r)+\epsilon_n-E\right]u_n(r)+\sum_m V_{mn}(r)u_m(r)=0\quad\Rightarrow\quad\sigma_{fus}(E)=\sum_k w_k\sigma_{fus}(E;V_k)$$

Coupling Hamiltonian

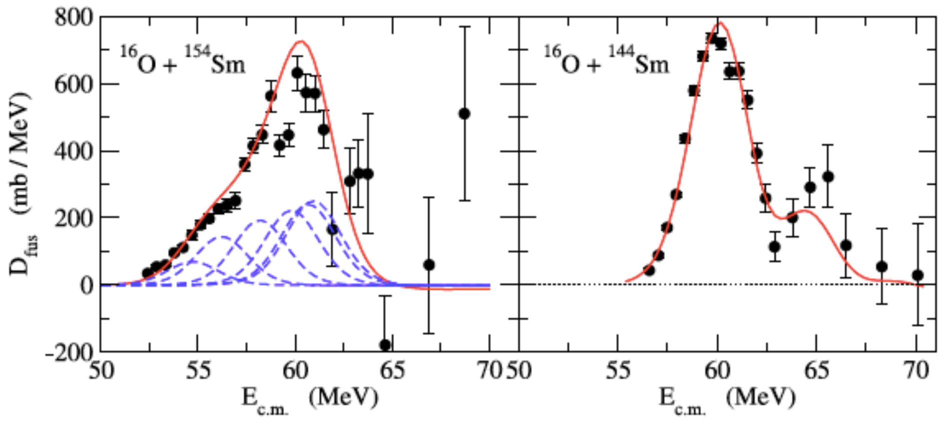

Distribution of barriers due to the channel coupling effects

K. Hagino, Progress of Theoretical Physics, Vol. **128**, No. 6, (2012)

Sub-barrier fusion from stable to radioactive beams

Present status of PISOLO set-up

The Fast Ionization Chamber

Tests with stable beams

- **Shaping time and DAQ gate width**
- **Rates**
- **Z and Energy resolution**

Studies with stable beams showed a connection between dynamics of heavy-ion fusion and nuclear structure

- Collective properties of the nuclei
- Strength and Q-values of transfer reactions
- Coupled-Channels method

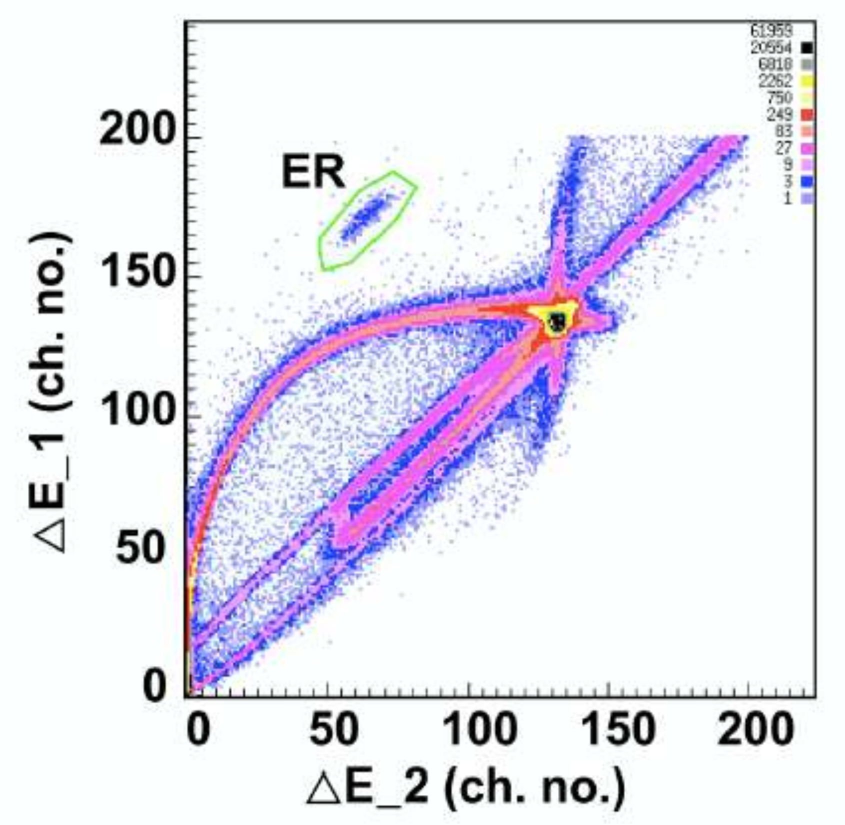

SPES beams will allow to investigate in more detail these issues

→ Nuclear structure changes far from the stability

Interesting effects may show up in the study of fusion reactions near and below the Coulomb barrier, with the SPES exotic beams

Low intensity beams (10^5 pps) → Need set-ups with efficiency close to 100%

J. F. Liang, D. Shapira, Phys.Rev. Lett. **91**. 152701, (2003)

Sub-barrier fusion from stable to radioactive beams

Present status of PISOLO set-up

The Fast Ionization Chamber

Tests with stable beams

- Shaping time and DAQ gate width
- Rates
- Z and Energy resolution

Direct detection of evaporation residues (ER)

- Beam suppression
- ER separation from residual beam

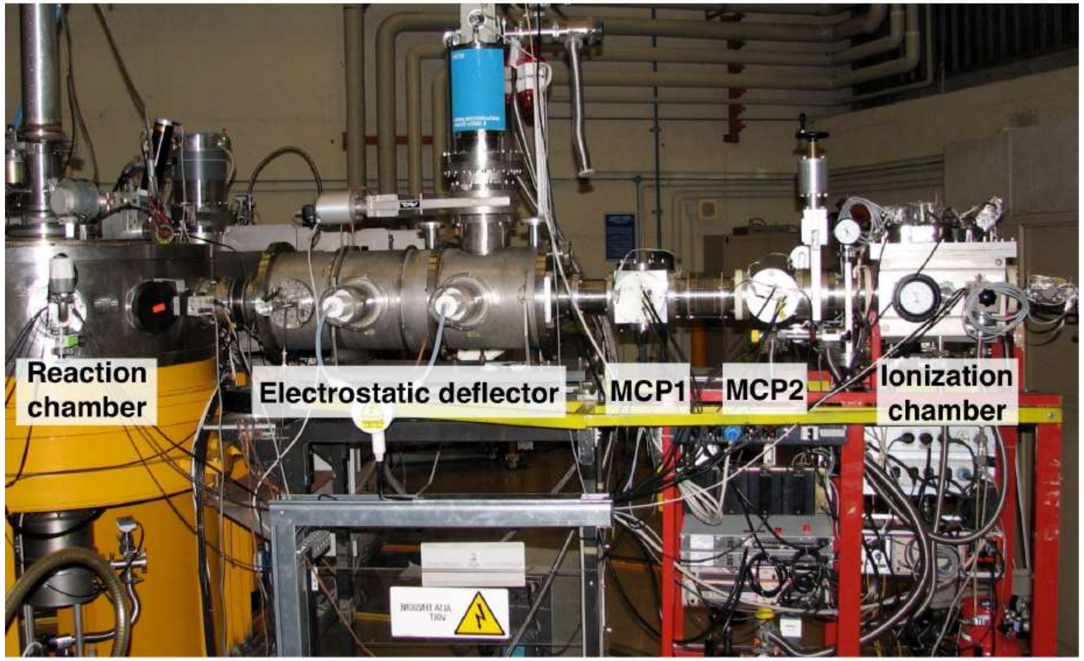

Sub-barrier fusion from stable to radioactive beams

Present status of PISOLO set-up

The Fast Ionization Chamber

Tests with stable beams

- Shaping time and DAQ gate width
- Rates
- Z and Energy resolution

Direct detection of evaporation residues (ER)

- Beam suppression
- ER separation from residual beam

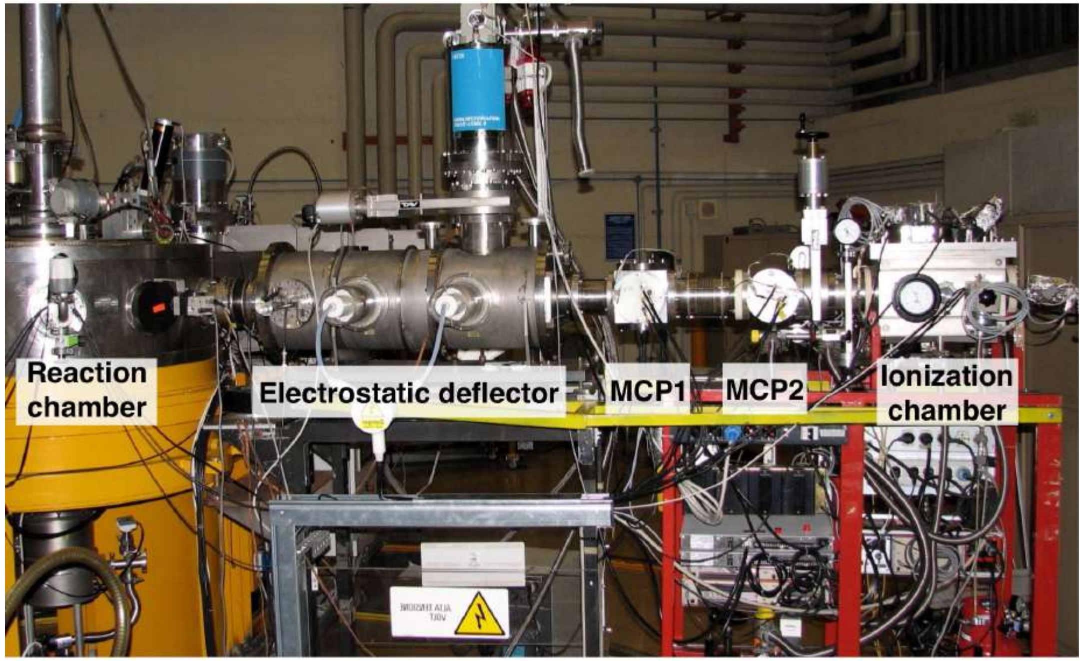

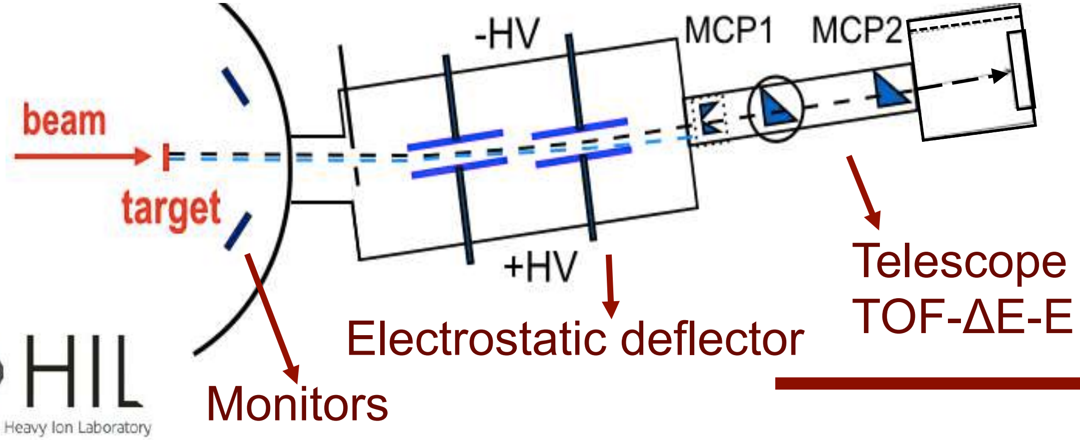

Sub-barrier fusion from stable to radioactive beams

Present status of PISOLO set-up

The Fast Ionization Chamber

Tests with stable beams

- Shaping time and DAQ gate width
- Rates
- Z and Energy resolution

Direct detection of evaporation residues (ER)

- Beam suppression
- ER separation from residual beam

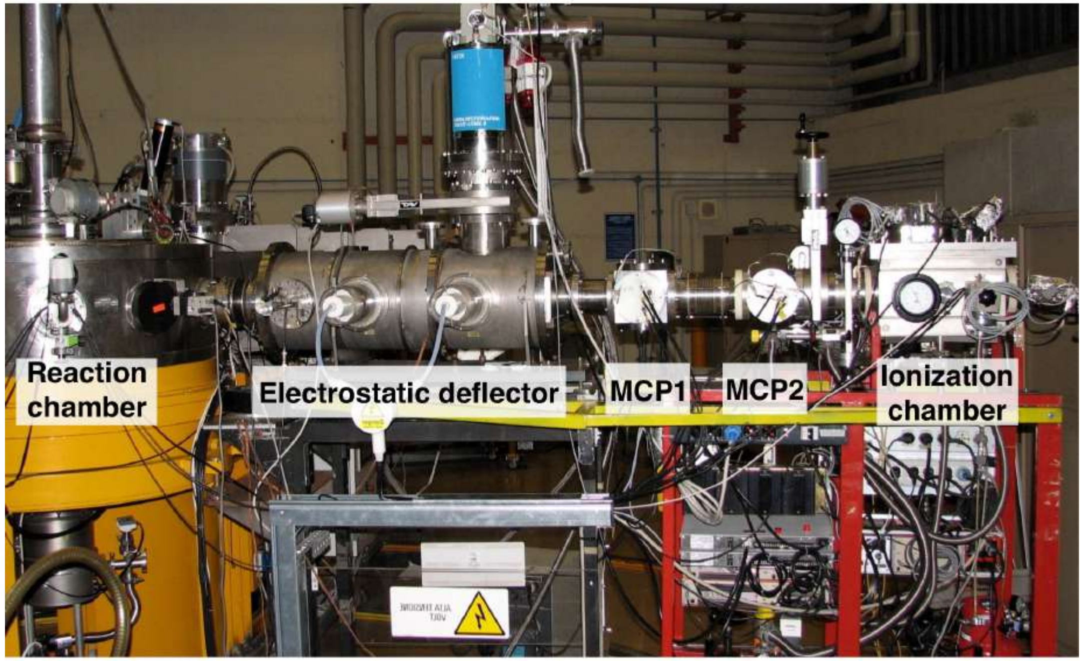

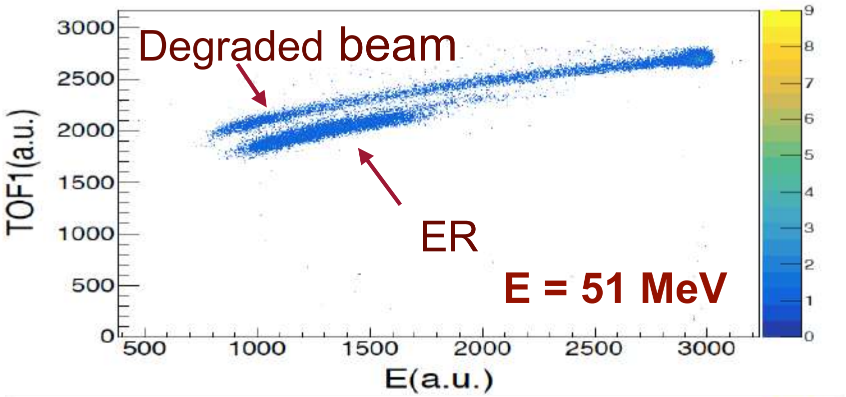

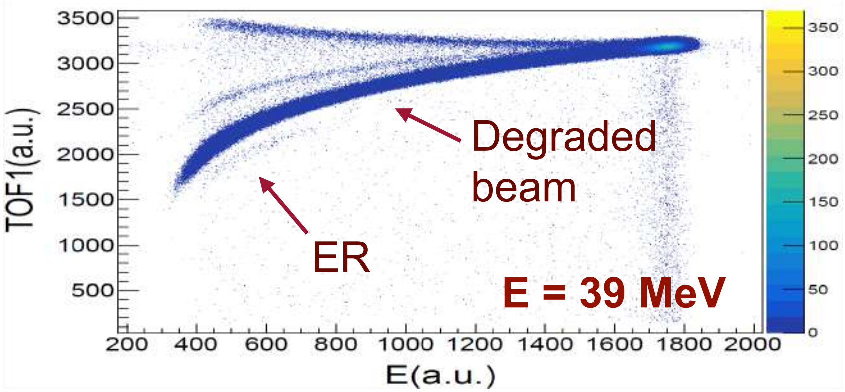

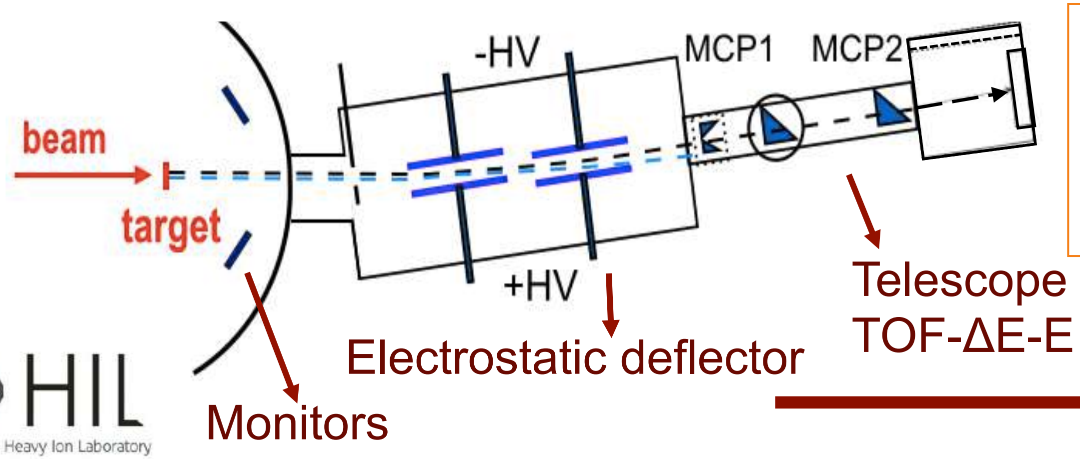

Lowest measurable cross section ≈ **0.5-1.0μb**

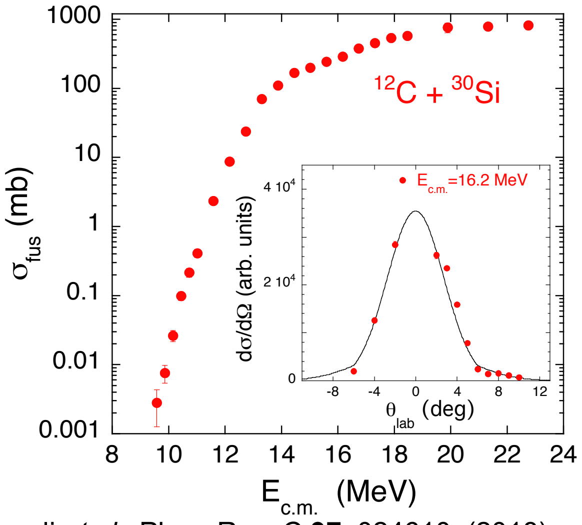

G. Montagnoli *et al.*, Phys. Rev. C **97**, 024610, (2018)

Sub-barrier fusion from stable to radioactive beams

Present status of PISOLO set-up

The Fast Ionization Chamber

Tests with stable beams

- Shaping time and DAQ gate width
- Rates
- Z and Energy resolution

Direct detection of evaporation residues (ER)

→ Beam suppression

→ ER separation from residual beam

Contributes to an overall efficiency of 1% → Limit RIBS

Limits the highest measurable counting rate

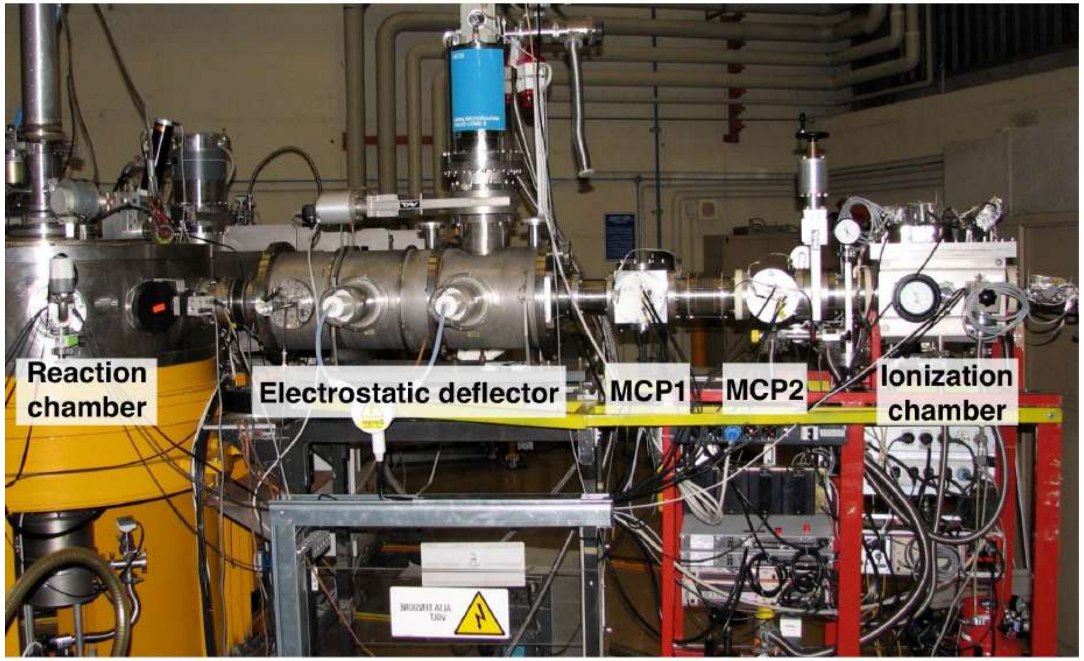

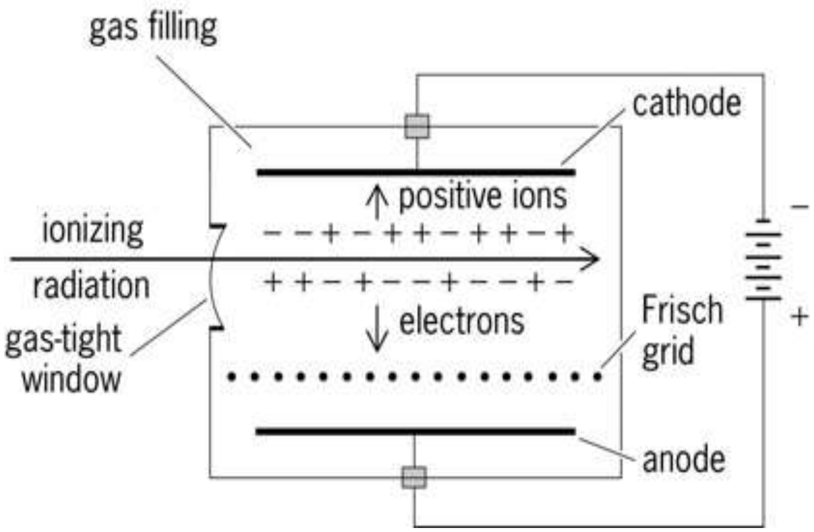

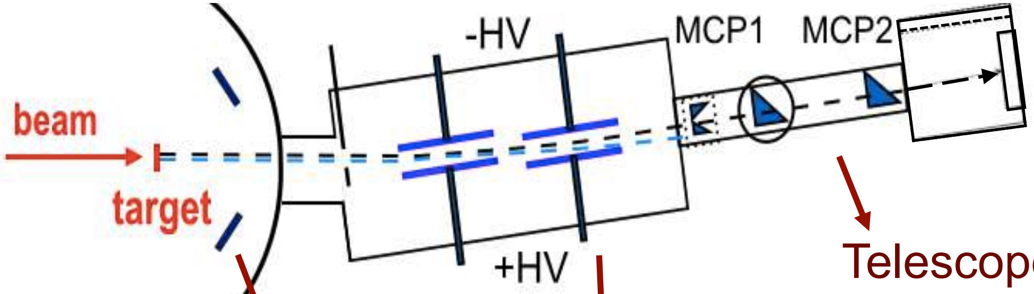

Electrostatic deflector

Telescope TOF-ΔE-E

Monitors

Counting rate $\lesssim$ *2-3* kHz

Sub-barrier fusion from stable to radioactive beams

Present status of PISOLO set-up

The Fast Ionization Chamber

Tests with stable beams

- **Shaping time and DAQ gate width**
- **Rates**
- **Z and Energy resolution**

Direct detection of evaporation residues (ER)

- Beam suppression
- ER separation from residual beam

Low-intensity beams 10^5 ion/s

Fusion excitation function down to around **100 μb**.

With a fast IC

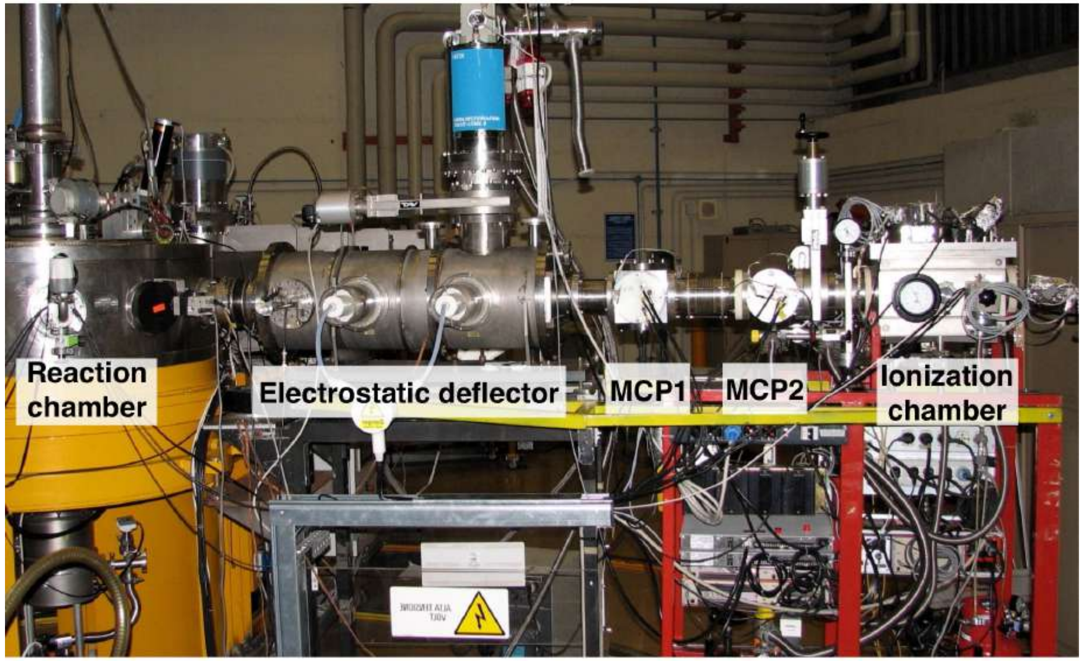

With high intensity beams 10^7- 10^8 ion/s the previous configuration of the set-up will be used

Time of flight

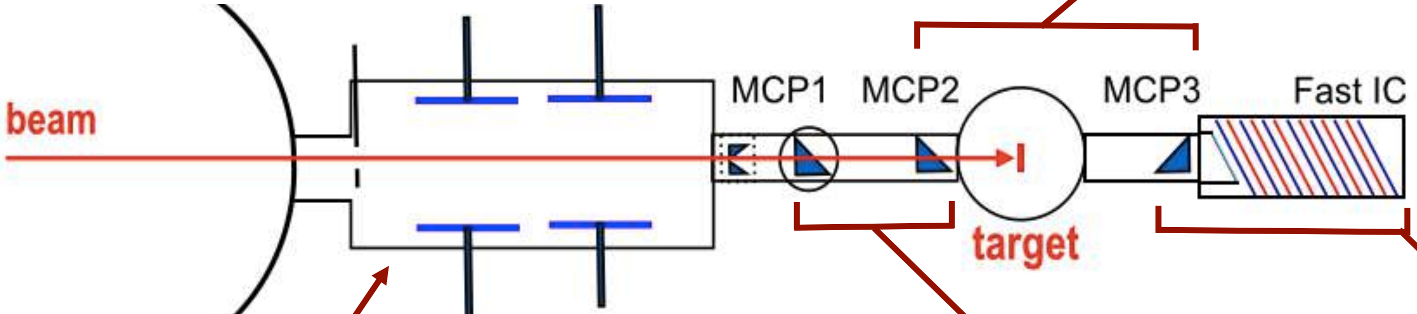

Transmission configuration

Monitor beam quality and direction

Telescope TOF-ΔE

Sub-barrier fusion from stable to radioactive beams

Present status of PISOLO set-up

The Fast Ionization Chamber

Tests with stable beams

- Shaping time and DAQ gate width
- Rates
- Z and Energy resolution

Tilted electrodes → Reduction of drift length – Reduction of charge collection time / Lower probability of recombination

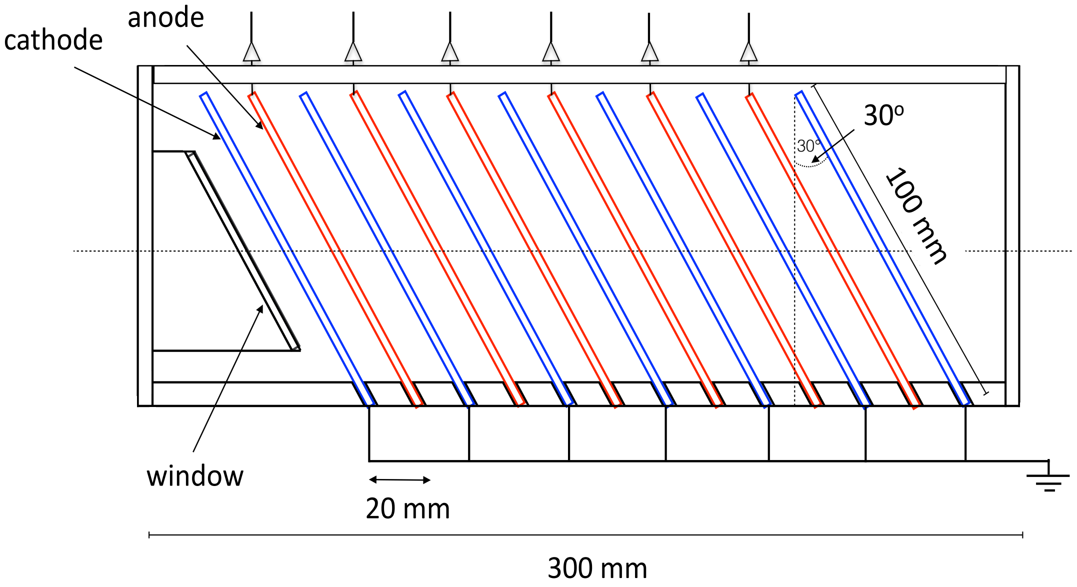

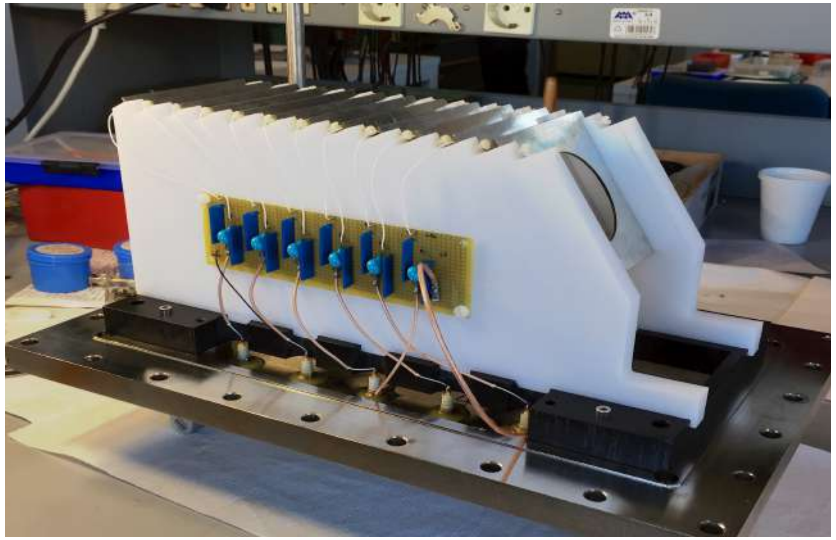

Sub-barrier fusion from stable to radioactive beams

Present status of PISOLO set-up

The Fast Ionization Chamber

Tests with stable beams

- Shaping time and DAQ gate width
- Rates
- Z and Energy resolution

Tilted electrodes → Reduction of drift length → Reduction of charge collection time; Lower probability of recombination

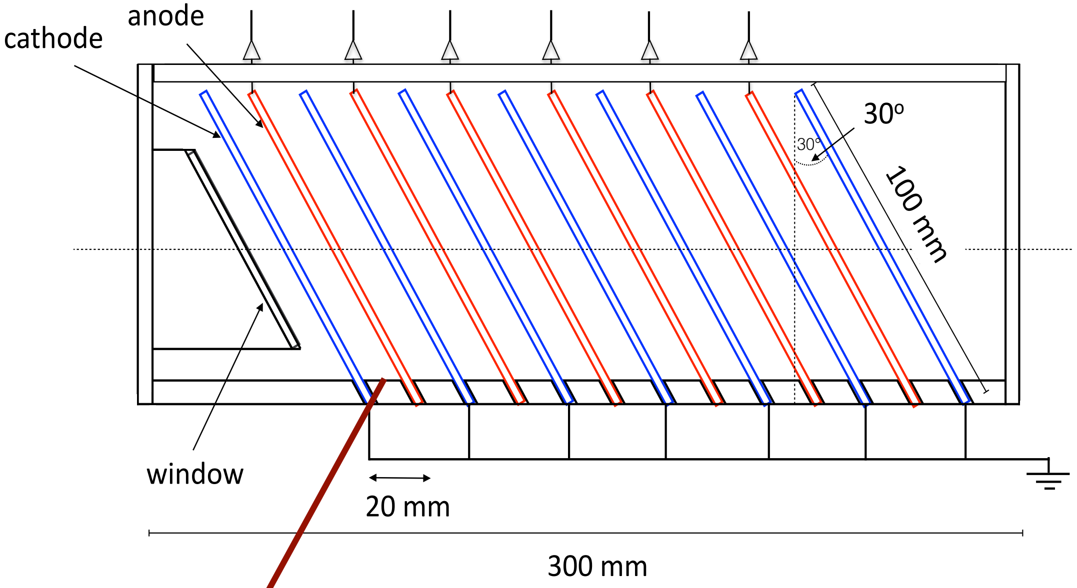

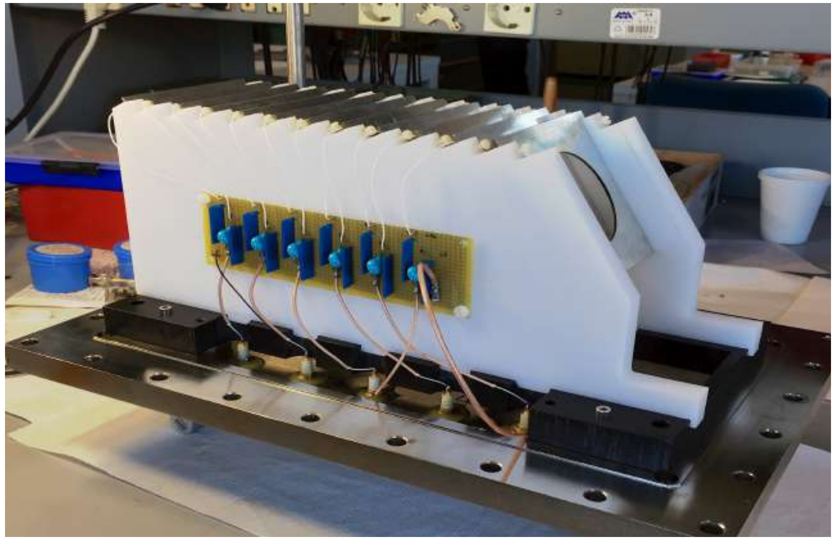

Each cell provides a signal, some of them can be summed giving a ΔE energy loss and the others will give a residual energy signal

Sub-barrier fusion from stable to radioactive beams

Present status of PISOLO set-up

The Fast Ionization Chamber

Tests with stable beams

- **Shaping time and DAQ gate width**
- **Rates**
- **Z and Energy resolution**

Tilted electrodes → Reduction of drift length → Reduction of charge collection time; Lower probability of recombination

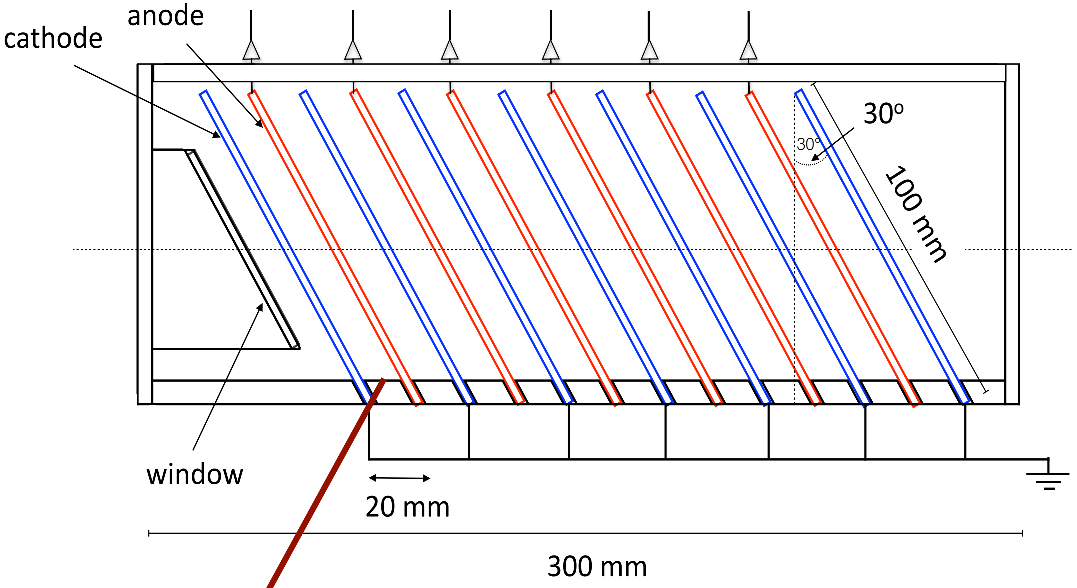

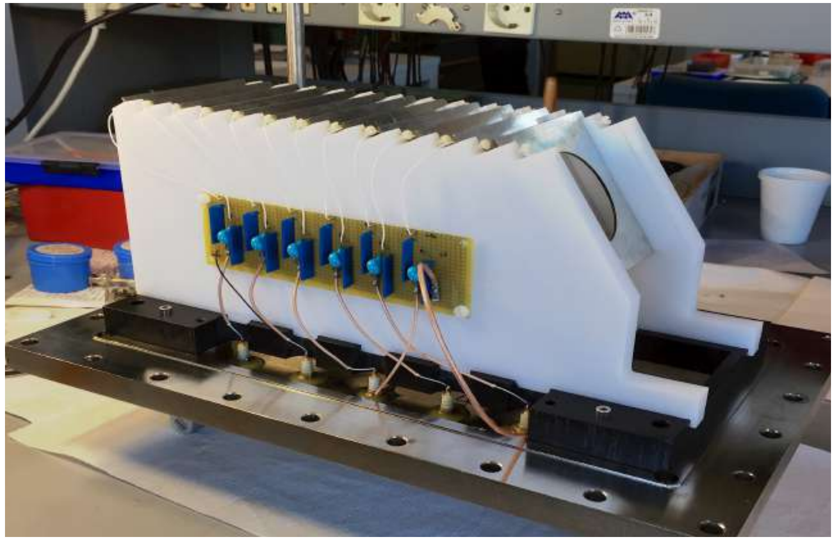

Each cell provides a signal, some of them can be summed giving a ΔE energy loss and the others will give a residual energy signal

Collection time of Fast IC is shorter by a factor ≃ 5 →

By reducing the shaping time from 1 μs to 0.25 μs we expect a usable counting rate up to **≈ 100-200 kHz** according to the results obtained at ORNL

Istituto Nazionale di Fisica Nucleare
Laboratori Nazionali di Legnaro
Heavy Ion Laboratory

Sub-barrier fusion from stable to radioactive beams

Present status of PISOLO set-up

The Fast Ionization Chamber

Tests with stable beams

- **Shaping time and DAQ gate width**
- **Rates**
- **Z and Energy resolution**

6 anodes and 7 cathodes placed at 20 mm steps

Electrodes :
- gold coated tungsten wires (20 μm)
- 1 mm spaced wires
- copper coated fiberglass frames

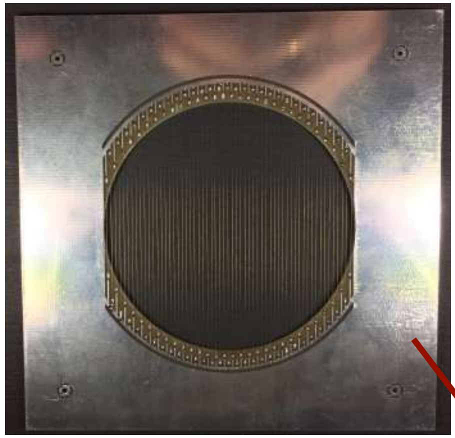

Entrance window:
- tilted at 30°
- 2 μm thick mylar

To avoid significant loss of energy of low-energy particles before they reach the first electrode

Each anode connected to a BNC feedthrough

Delrin support fixed on steel cover

Easy replacement of damaged electrodes and interchange with conventional IC

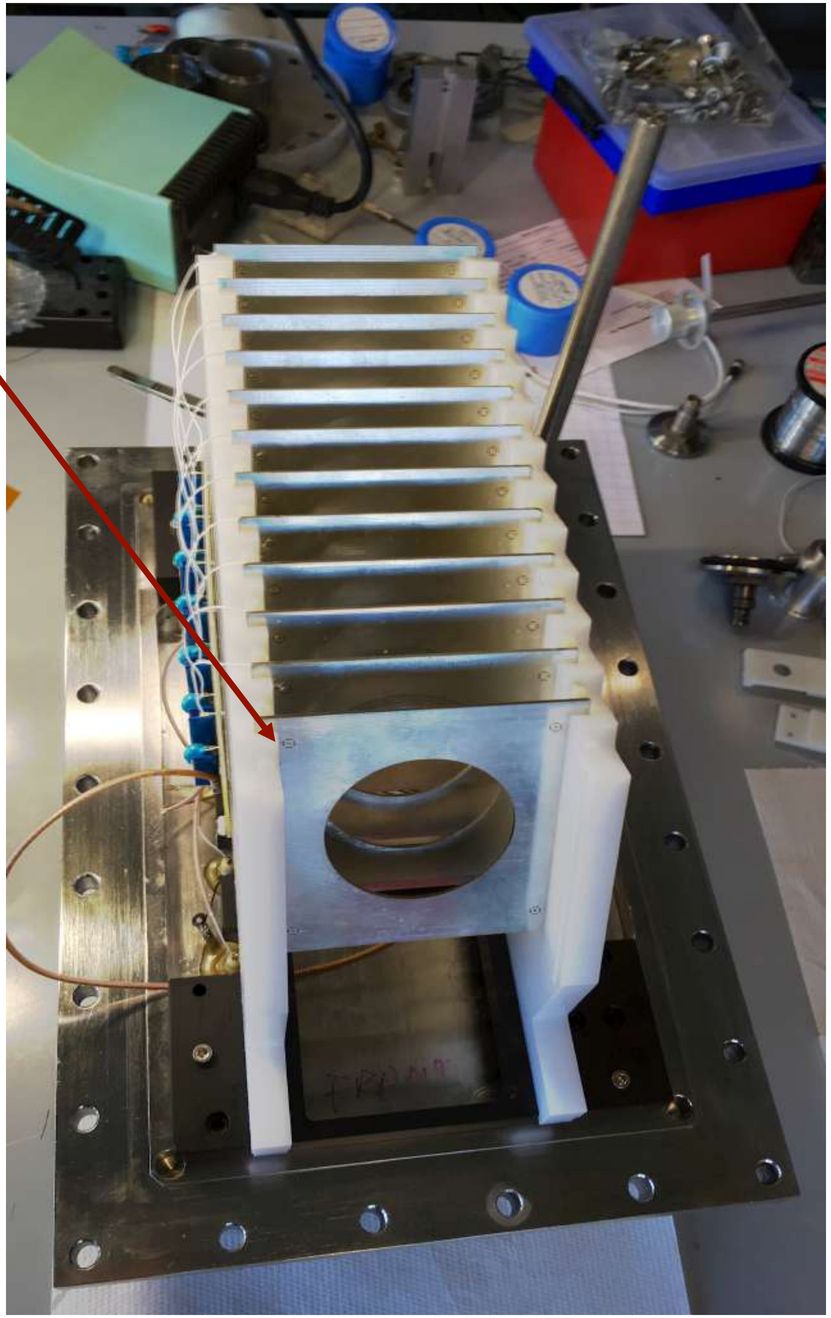

Sub-barrier fusion from stable to radioactive beams

Present status of PISOLO set-up

The Fast Ionization Chamber

Tests with stable beams

- Shaping time and DAQ gate width
- Rates
- Z and Energy resolution

Fast IC in complete configuration with 6 signals ΔE_i

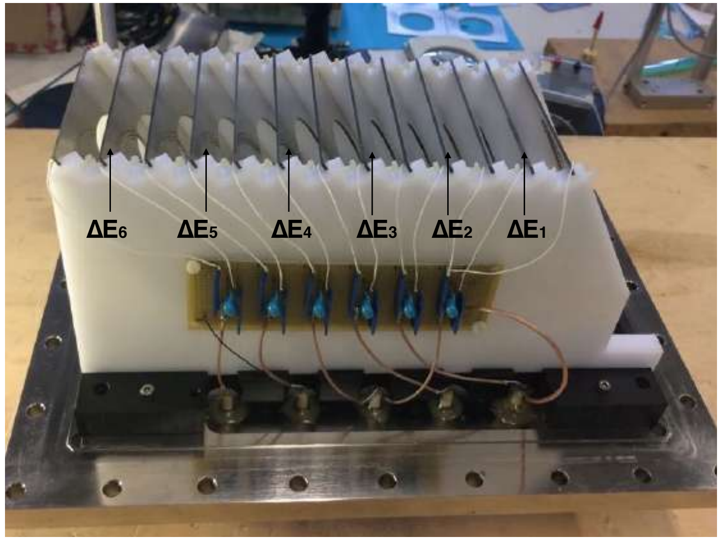

A total of 5 days tests have been performed using the reactions:

- $^{28}Si + ^{100}Mo$ (Fusion)
- $^{58}Ni + ^{28}Si$ (Fusion)
- $^{64}Zn + ^{58}Fe, ^{197}Au$ (Quasi-elastic scattering)

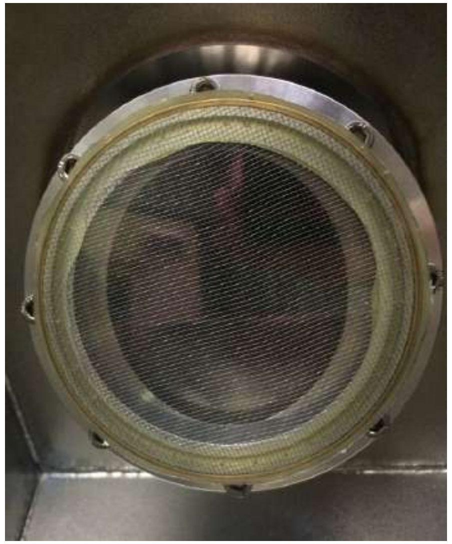

Entrance window

Highest pressure used 200 mbar

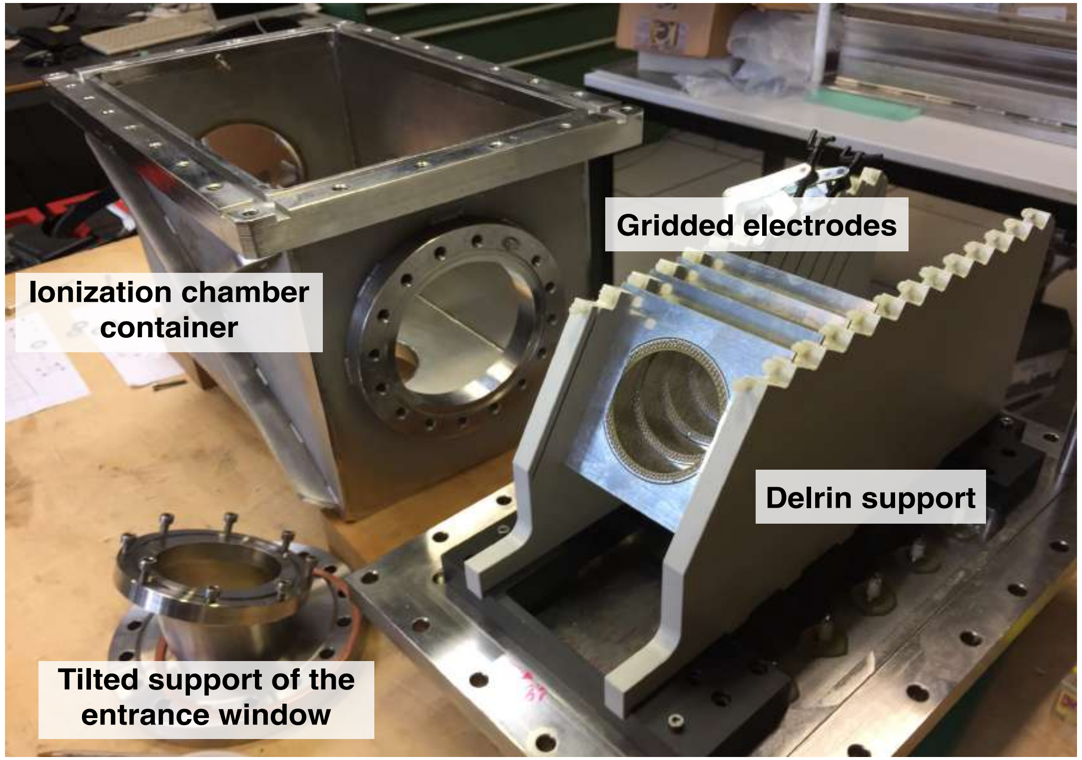

^{28}Si beam at the energy E_{lab}=125 MeV on a ^{100}Mo target

Reduction of shaping time

- Conventional window perpendicular to beam axis
- ORTEC2006 preamplifier
  Canberra 2020 amplifier
- CH4 gas pressure 7.6 mbar

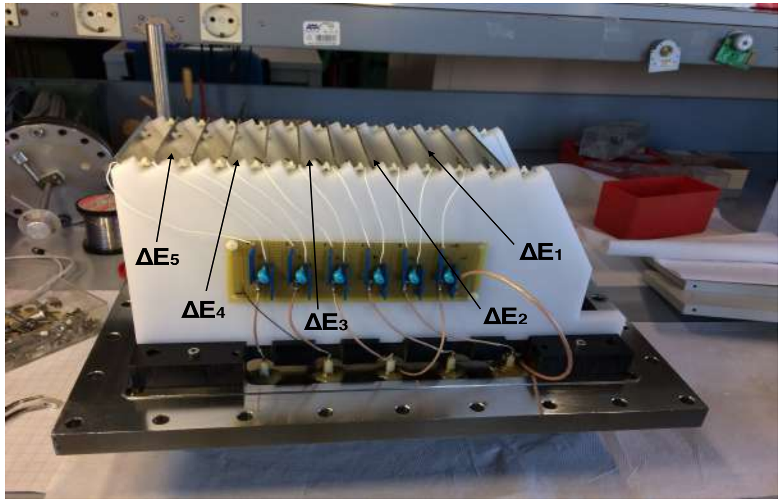

Signals combined in two energy loss signals ΔE and ΔE1

Sub-barrier fusion from stable to radioactive beams

Present status of PISOLO set-up

The Fast Ionization Chamber

Tests with stable beams

- **Shaping time and DAQ gate width**
- Rates
- Z and Energy resolution

^{28}Si beam at the energy E_{lab}=125 MeV on a ^{100}Mo target

Reduction of shaping time

- Conventional window perpendicular to beam axis
- ORTEC2006 preamplifier Canberra 2020 amplifier
- CH_4 gas pressure 7.6 mbar

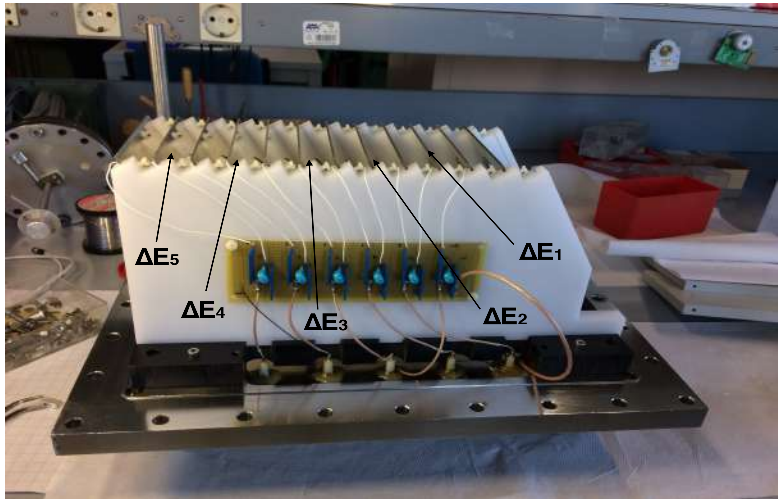

Signals combined in two energy loss signals ΔE and ΔE1

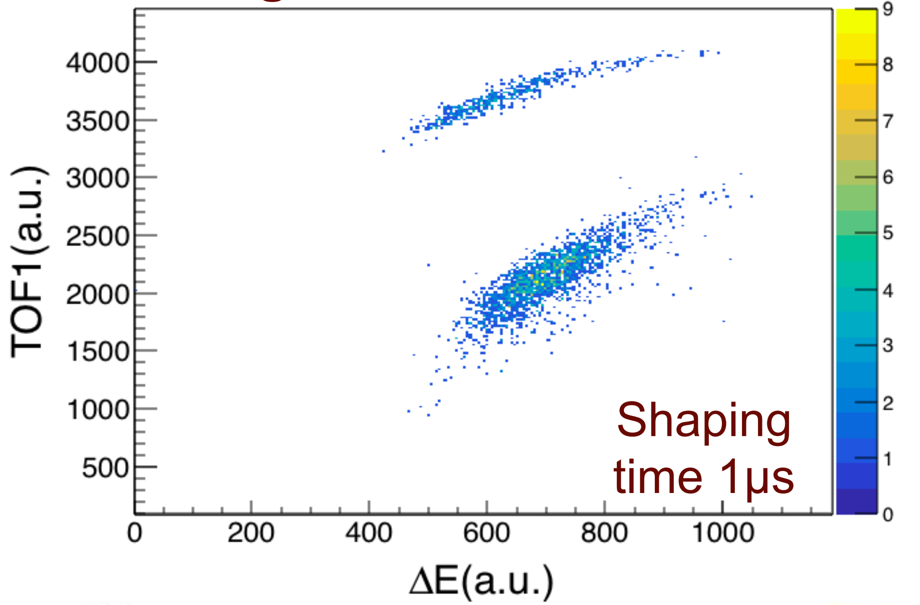

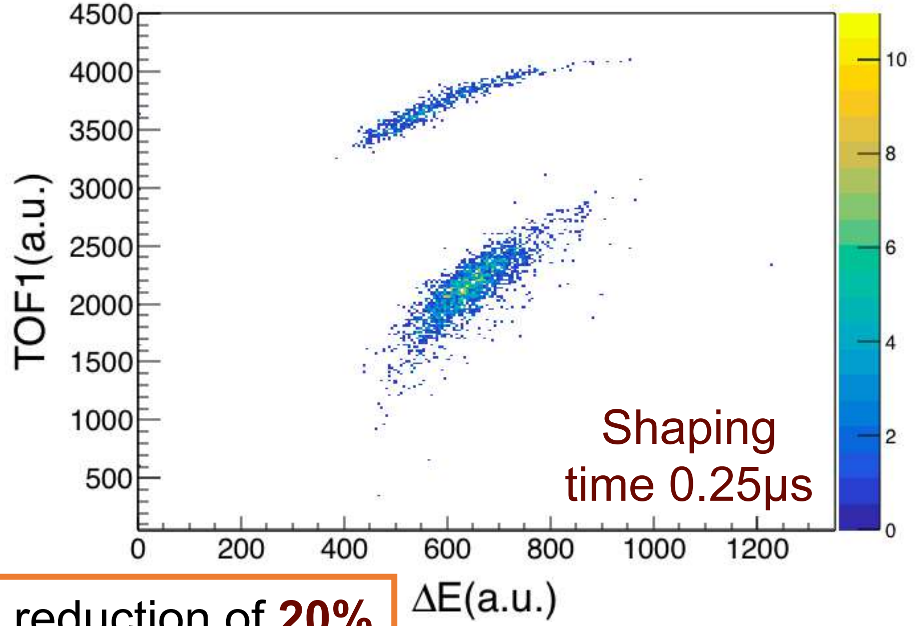

Background reduction of **20%**

G. Colucci

Istituto Nazionale di Fisica Nucleare
Laboratori Nazionali di Legnaro
HIL Heavy Ion Laboratory

Sub-barrier fusion from stable to radioactive beams

Present status of PISOLO set-up

The Fast Ionization Chamber

Tests with stable beams

- **Shaping time and DAQ gate width**
- Rates
- Z and Energy resolution

^{58}Ni beam at the energy E_{lab}=190 MeV on a ^{28}Si target

→ A case resembling future SPES experiments in inverse kinematics

Shorter trigger gate

- Conventional window perpendicular to beam axis
- Mesytec MS-L16 preamplifier
  Mesytec MSCF16 amplifier
  → Shaping time 0.25 μs
- CH_4 gas pressure 30 mbar

Signals combined in two energy loss signals ΔE and ΔE1

Istituto Nazionale di Fisica Nucleare
Laboratori Nazionali di Legnaro
Heavy Ion Laboratory

^{58}Ni beam at the energy E_{lab}=190 MeV on a ^{28}Si target

Sub-barrier fusion from stable to radioactive beams

Present status of PISOLO set-up

The Fast Ionization Chamber

Tests with stable beams

- **Shaping time and DAQ gate width**
- Rates
- Z and Energy resolution

→ A case resembling future SPES experiments in inverse kinematics

Shorter trigger gate

- Conventional window perpendicular to beam axis
- Mesytec MS-L16 preamplifier
  Mesytec MSCF16 amplifier
  → Shaping time 0.25 μs
- CH4 gas pressure 30 mbar

Signals combined in two energy loss signals ΔE and ΔE1

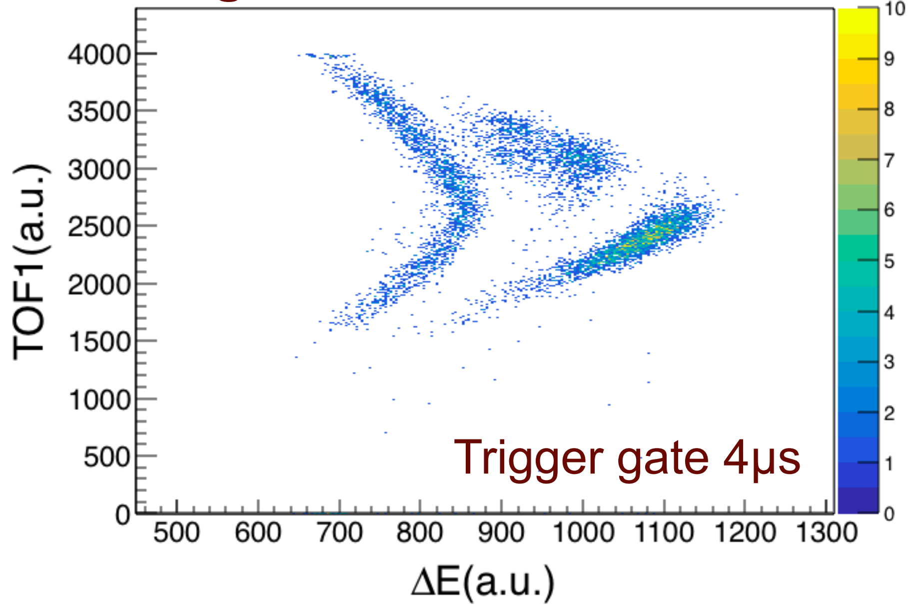

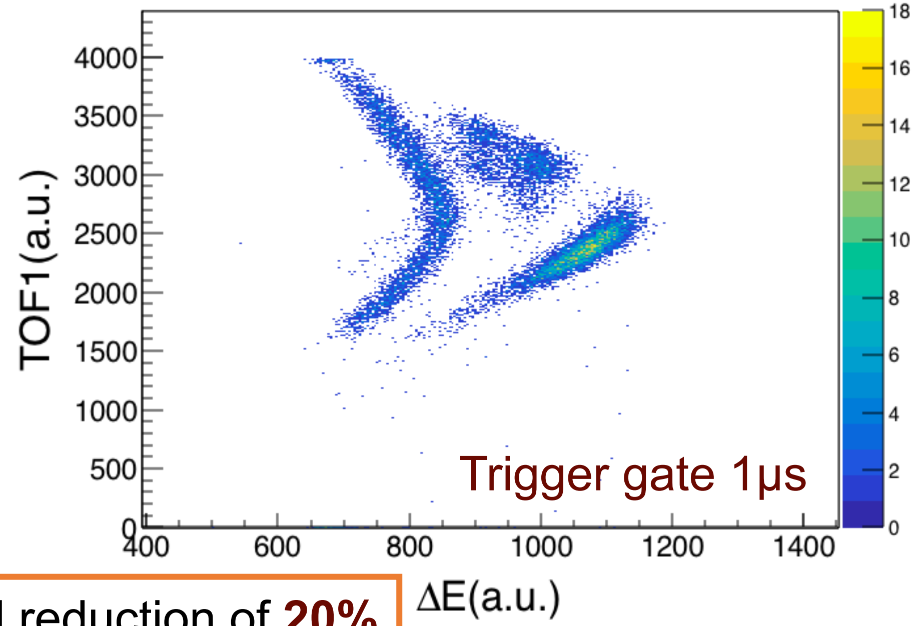

Background reduction of **20%**

Sub-barrier fusion from stable to radioactive beams

Present status of PISOLO set-up

The Fast Ionization Chamber

Tests with stable beams

- Shaping time and DAQ gate width
- **Rates**
- Z and Energy resolution

^{28}Si beam at the energy E_{lab}=125 MeV on a ^{100}Mo target

Counting rate increased by increasing beam current and placing set-up near 0°

CH4 gas pressure 50 mbar

Counting rate of 14 kHz

ER are not affected by the veto, since the pressure of the gas inside the IC stops the ER within the fourth section.

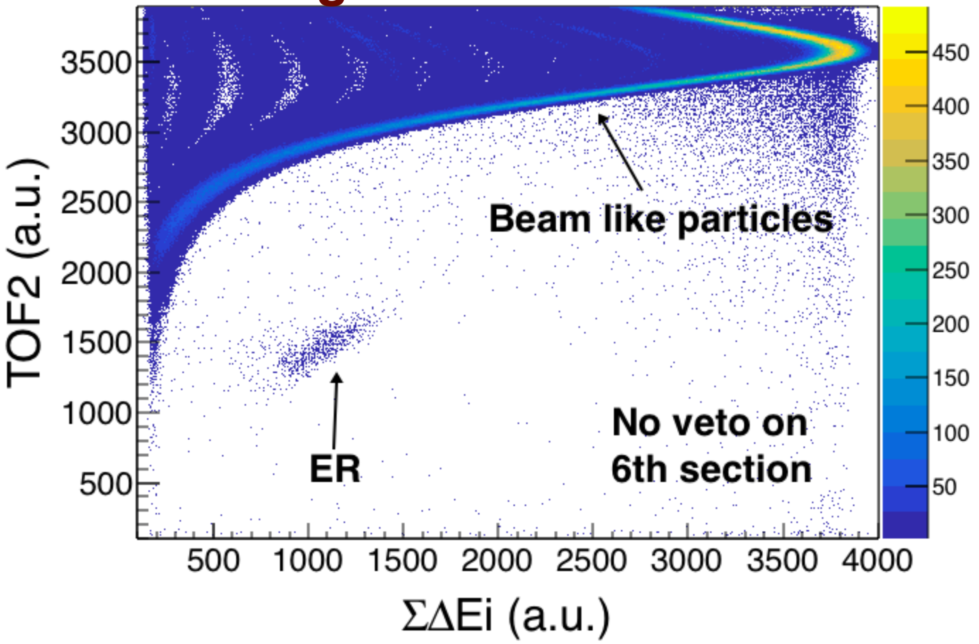

Sixth section of IC used as veto of the DAQ

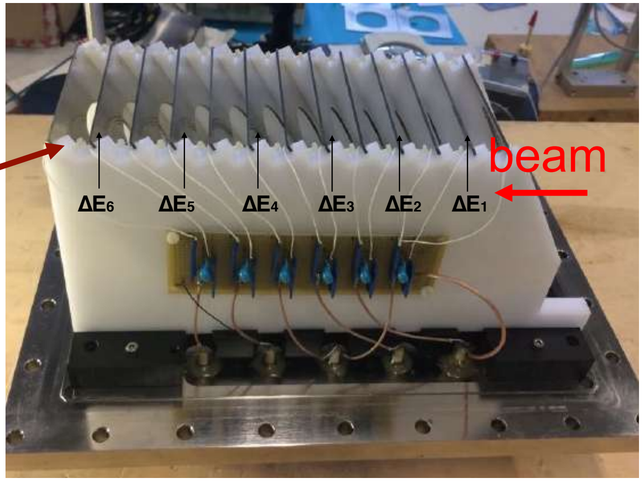

^{28}Si beam at the energy E_{lab}=125 MeV on a ^{100}Mo target

Sub-barrier fusion from stable to radioactive beams

Present status of PISOLO set-up

The Fast Ionization Chamber

Tests with stable beams

- **Shaping time and DAQ gate width**
- **Rates**
- **Z and Energy resolution**

Counting rate increased by increasing beam current and placing set-up near 0°

CH4 gas pressure 50 mbar

Counting rate of 14 kHz

ER are not affected by the veto, since the pressure of the gas inside the IC stops the ER within the fourth section.

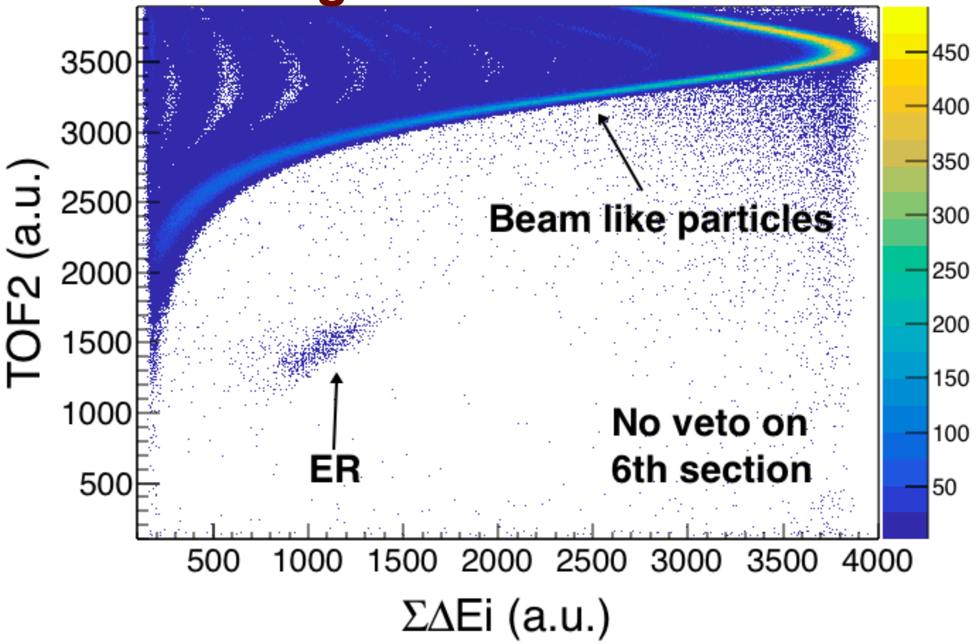

Sixth section of IC used as veto of the DAQ

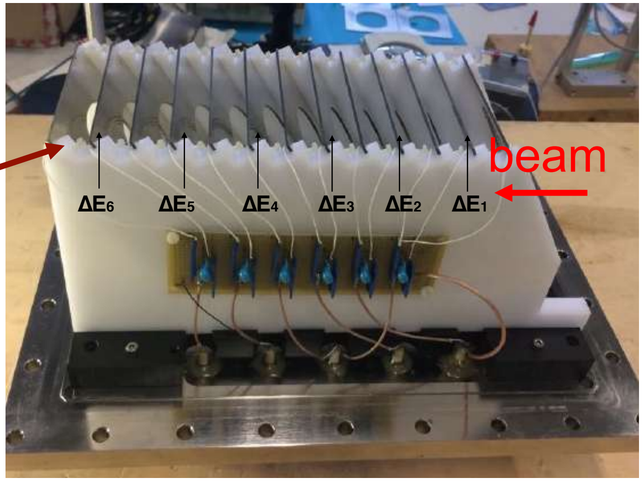

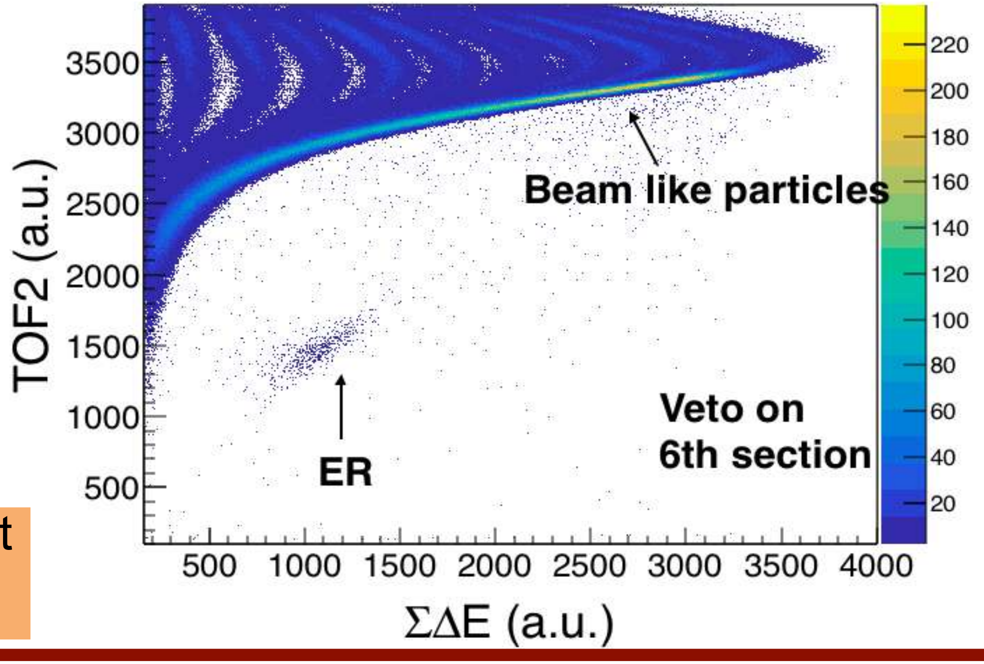

Most energetic part of the beam is not acquired and the noise is reduced

Sub-barrier fusion from stable to radioactive beams

Present status of PISOLO set-up

The Fast Ionization Chamber

Tests with stable beams

- **Shaping time and DAQ gate width**
- **Rates**
- **Z and Energy resolution**

Maximum rate of **139 kHz** reached at 0° and with 5 pnA beam current

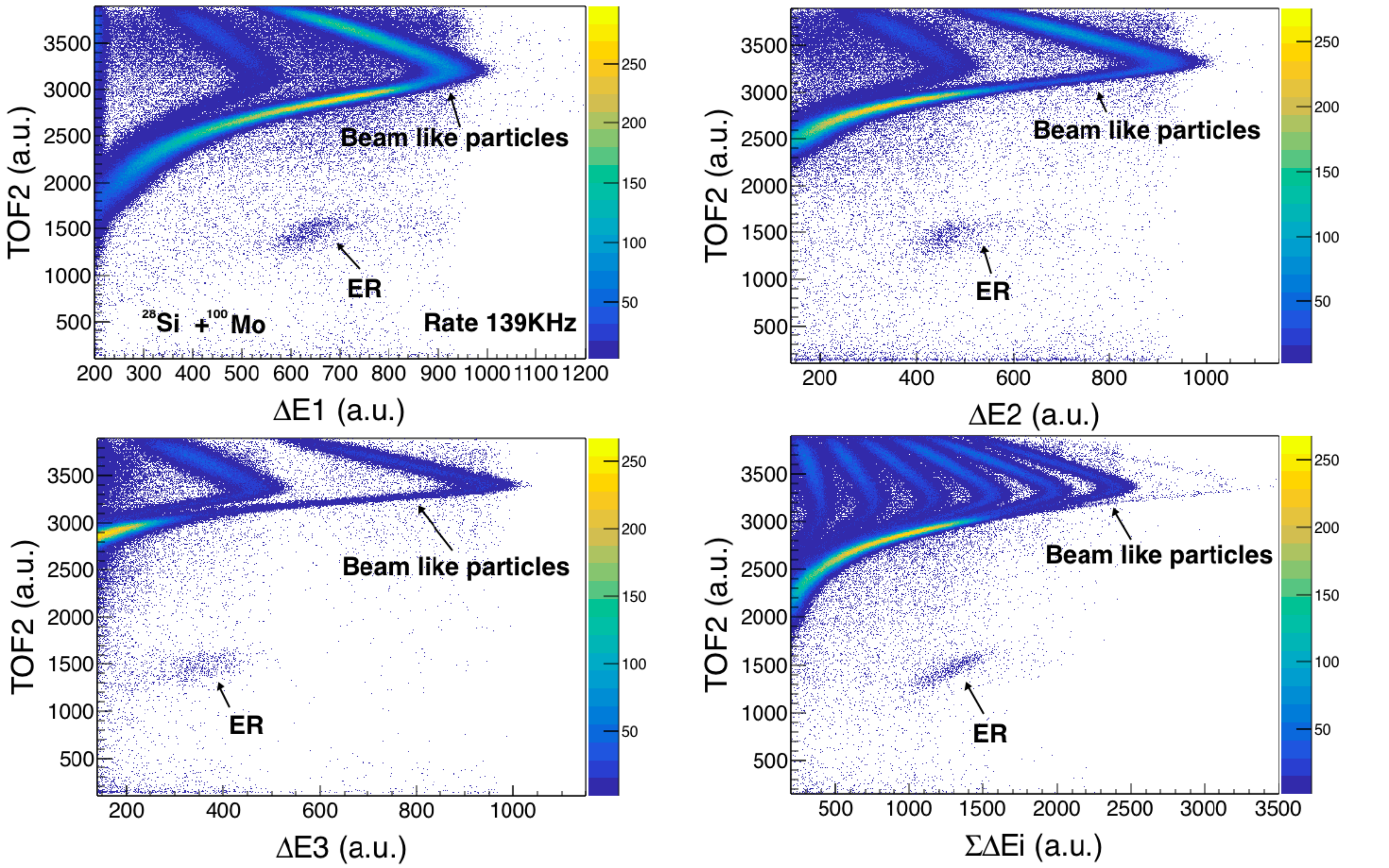

Sub-barrier fusion from stable to radioactive beams

Present status of PISOLO set-up

The Fast Ionization Chamber

Tests with stable beams

- Shaping time and DAQ gate width
- **Rates**
- Z and Energy resolution

Maximum rate of 139 kHz reached at 0° and with 5 pnA beam current

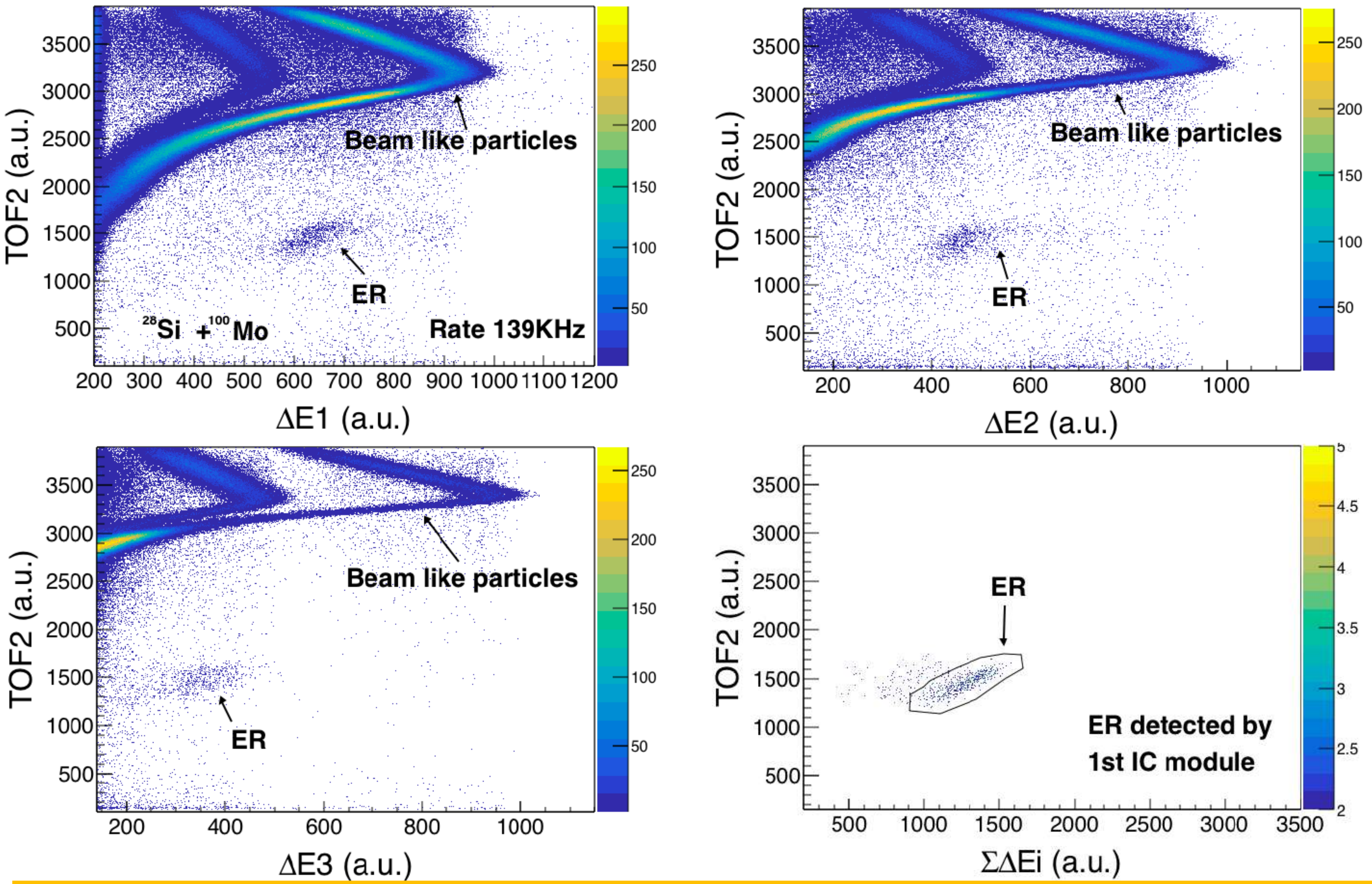

By selecting the ER in the TOF_2-ΔE1 matrix a clear identification of ER is possible.

^{64}Zn at the ALPI-Piave beam energy of E_{lab}=275 MeV on a ^{54}Fe target

Sub-barrier fusion from stable to radioactive beams

Present status of PISOLO set-up

The Fast Ionization Chamber

Tests with stable beams

- Shaping time and DAQ gate width
- Rates
- **Z and Energy resolution**

CH4 gas pressure 200 mbar

Detection angle 30°

→ ^{64}Zn grazing angle 34.5°

^{64}Zn at the ALPI-Piave beam energy of E_{lab}=275 MeV on a ^{54}Fe target

Sub-barrier fusion from stable to radioactive beams

Present status of PISOLO set-up

The Fast Ionization Chamber

Tests with stable beams

- **Shaping time and DAQ gate width**
- **Rates**
- **Z and Energy resolution**

CH4 gas pressure 200 mbar

Detection angle 30°

→ ^{64}Zn grazing angle 34.5°

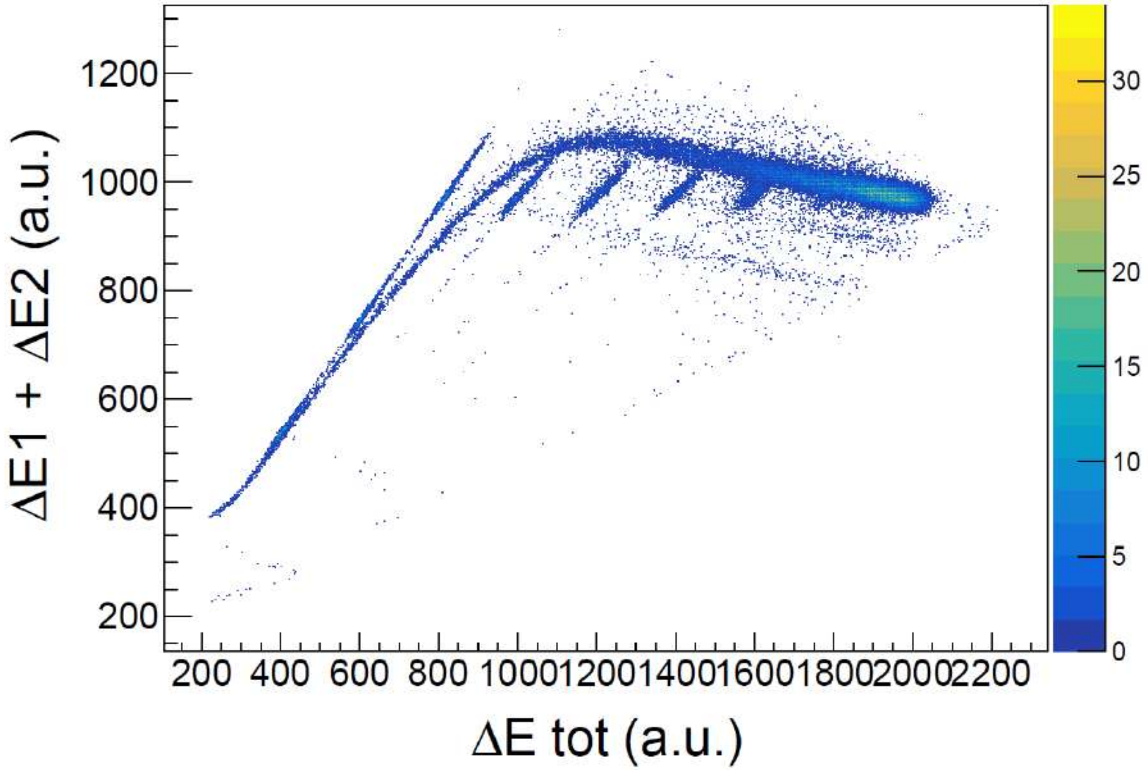

^{64}Zn at the ALPI-Piave beam energy of E_{lab}=275 MeV on a ^{54}Fe target

Sub-barrier fusion from stable to radioactive beams

Present status of PISOLO set-up

The Fast Ionization Chamber

Tests with stable beams

- **Shaping time and DAQ gate width**
- **Rates**
- **Z and Energy resolution**

CH4 gas pressure 200 mbar

Detection angle 30°

→ ^{64}Zn grazing angle 34.5°

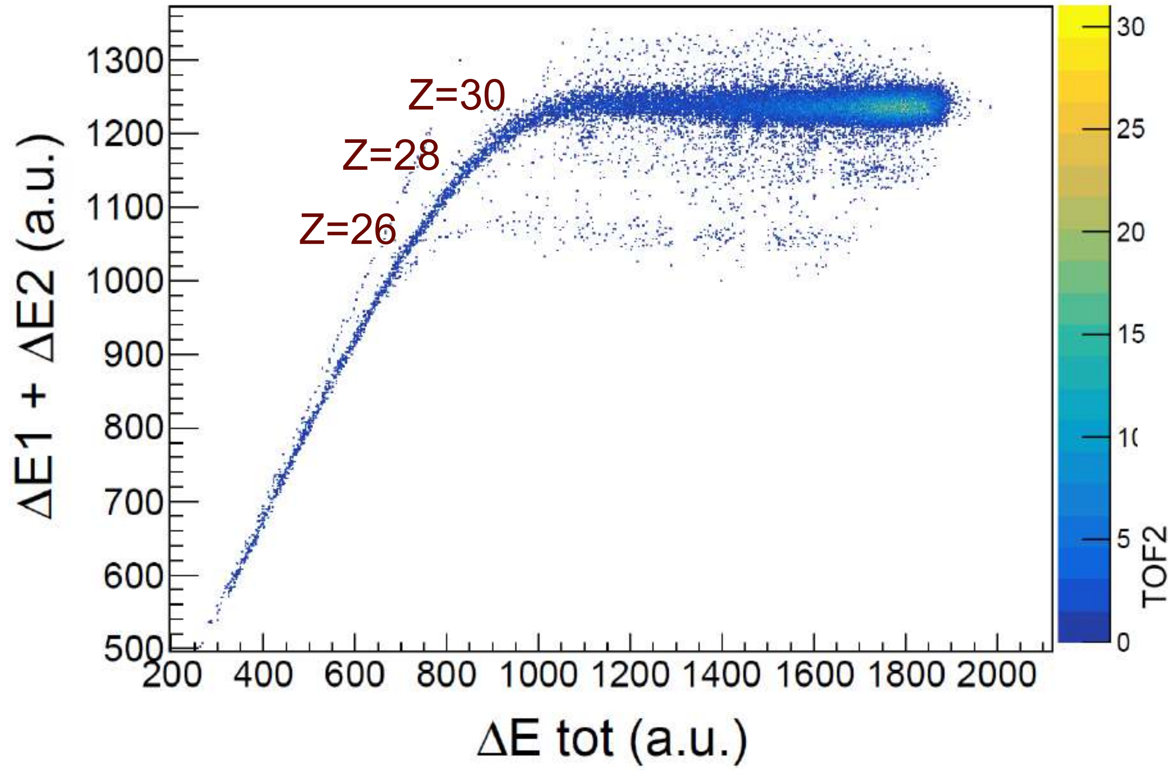

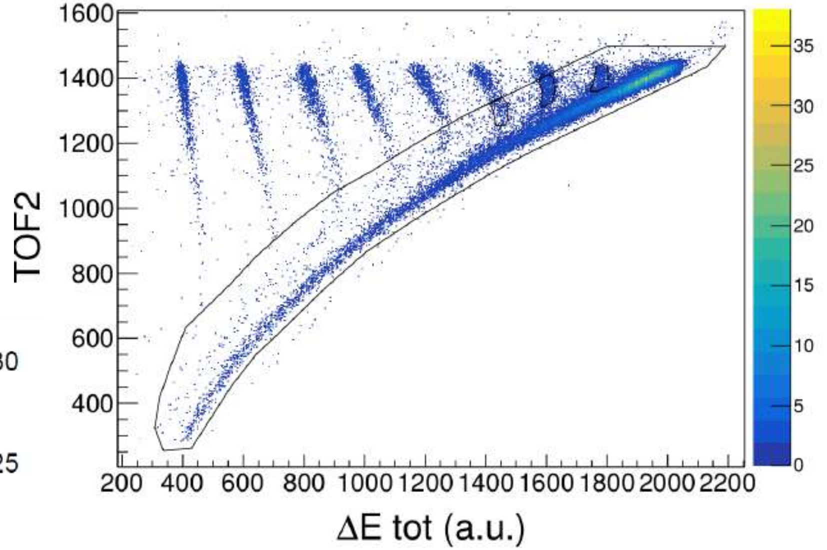

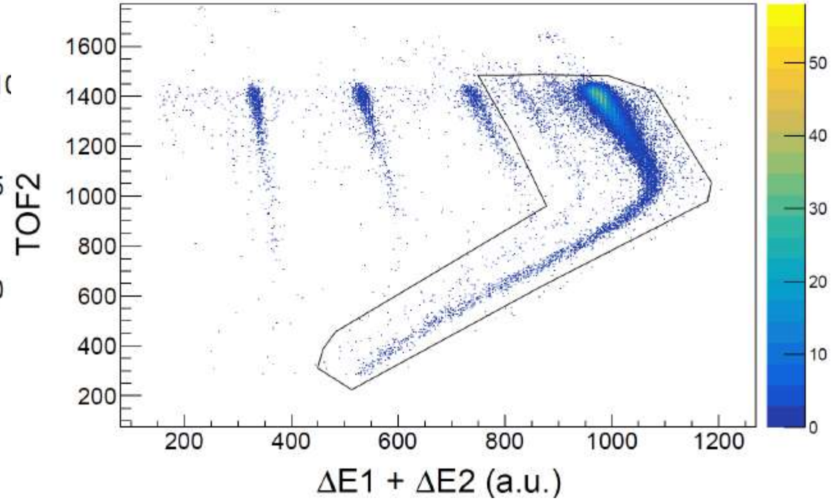

Sub-barrier fusion from stable to radioactive beams

Present status of PISOLO set-up

The Fast Ionization Chamber

Tests with stable beams

- Shaping time and DAQ gate width
- Rates
- **Z and Energy resolution**

^{64}Zn at the ALPI-Piave beam energy of E_{lab}=275 MeV on a ^{54}Fe target

CH4 gas pressure 200 mbar → ^{64}Zn grazing angle 34.5°

Detection angle 30°

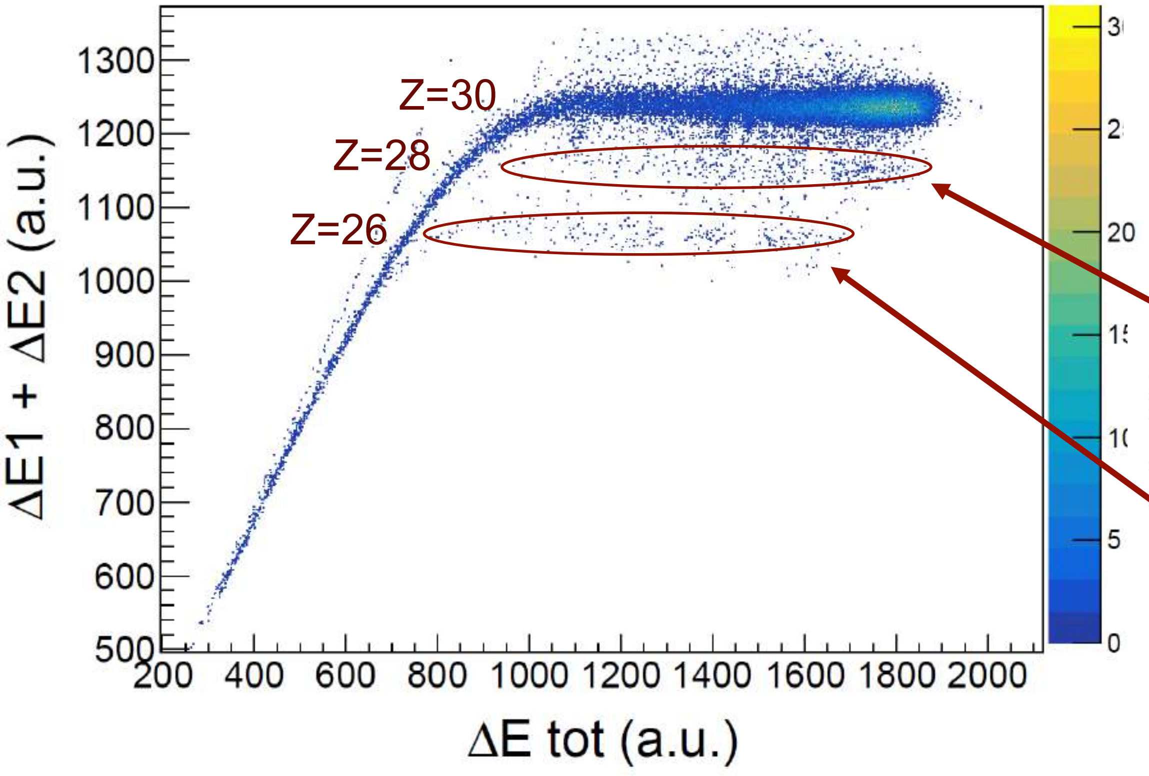

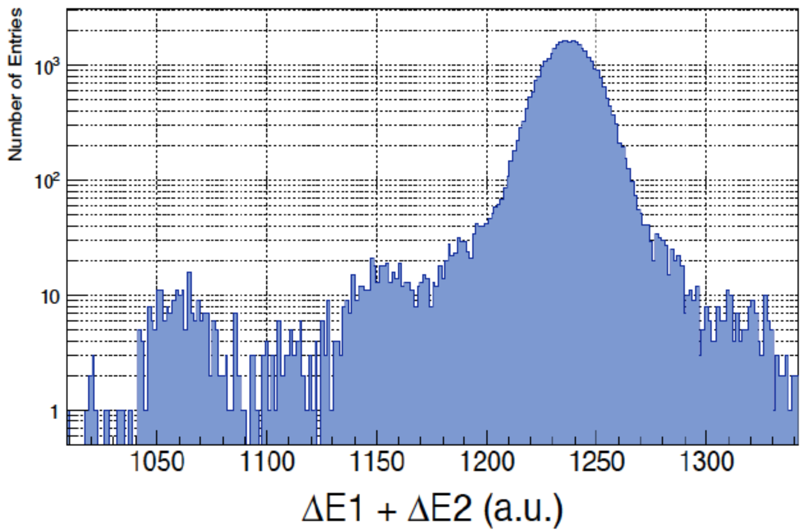

Z resolution of $\frac{\Delta Z}{Z} \approx \frac{1}{38}$

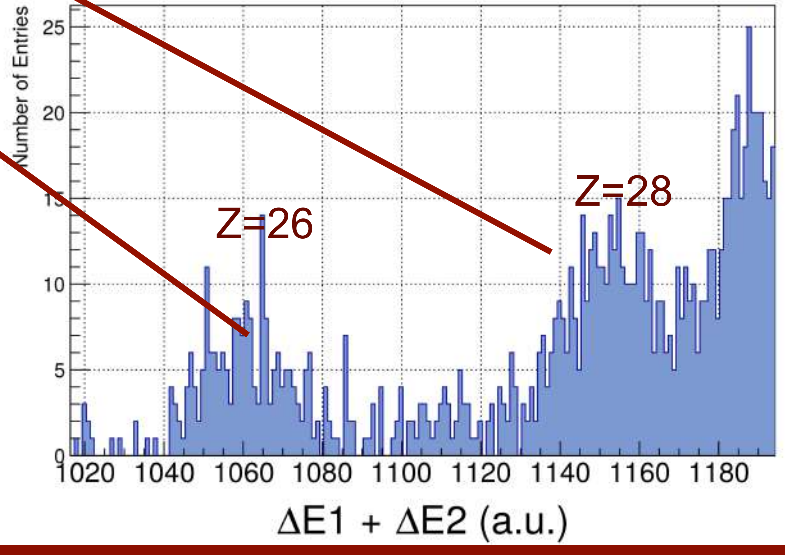

G. Colucci

Istituto Nazionale di Fisica Nucleare
Laboratori Nazionali di Legnaro
Heavy Ion Laboratory

^{64}Zn at the ALPI-Piave beam energy of E_{lab}=275 MeV on a ^{197}Au target

Sub-barrier fusion from stable to radioactive beams

Present status of PISOLO set-up

The Fast Ionization Chamber

Tests with stable beams

- Shaping time and DAQ gate width
- Rates
- Z and Energy resolution

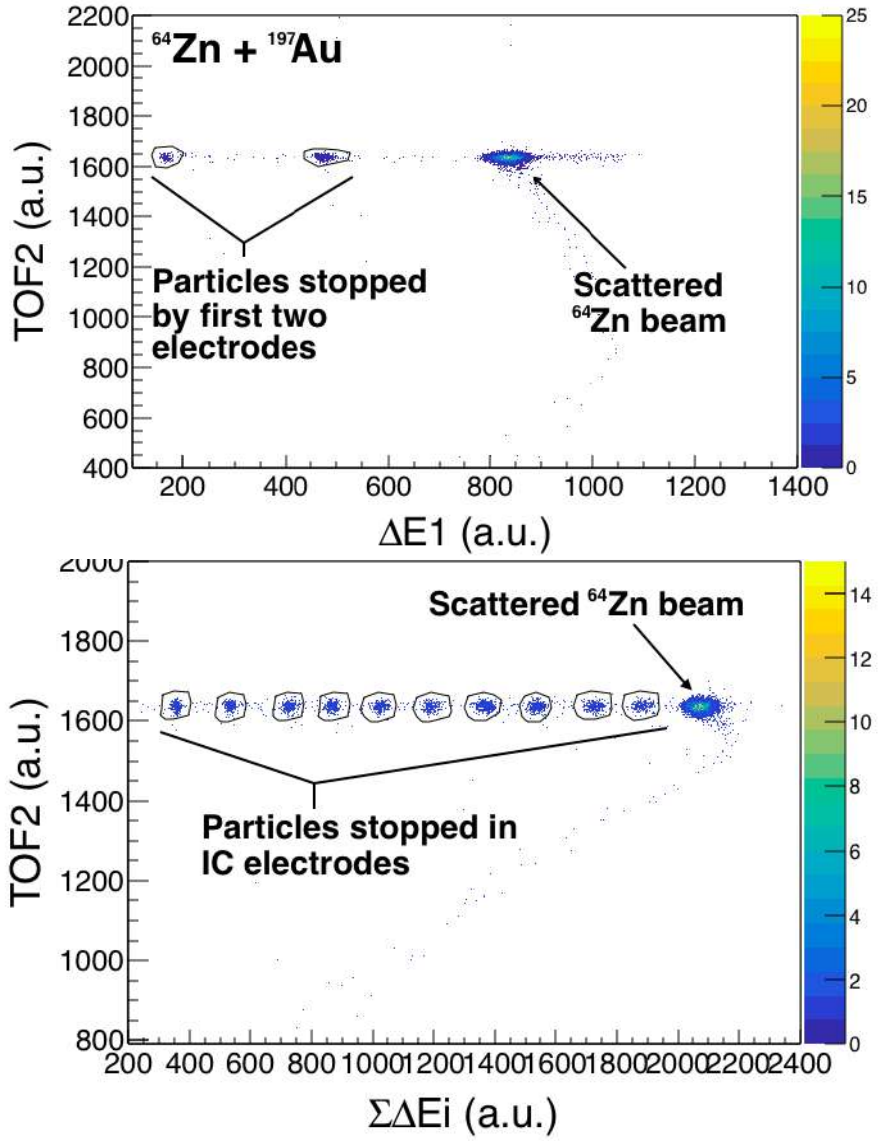

Sub-barrier fusion from stable to radioactive beams

Present status of PISOLO set-up

The Fast Ionization Chamber

Tests with stable beams

- Shaping time and DAQ gate width
- Rates
- **Z and Energy resolution**

^{64}Zn at the ALPI-Piave beam energy of E_{lab}=275 MeV on a ^{197}Au target

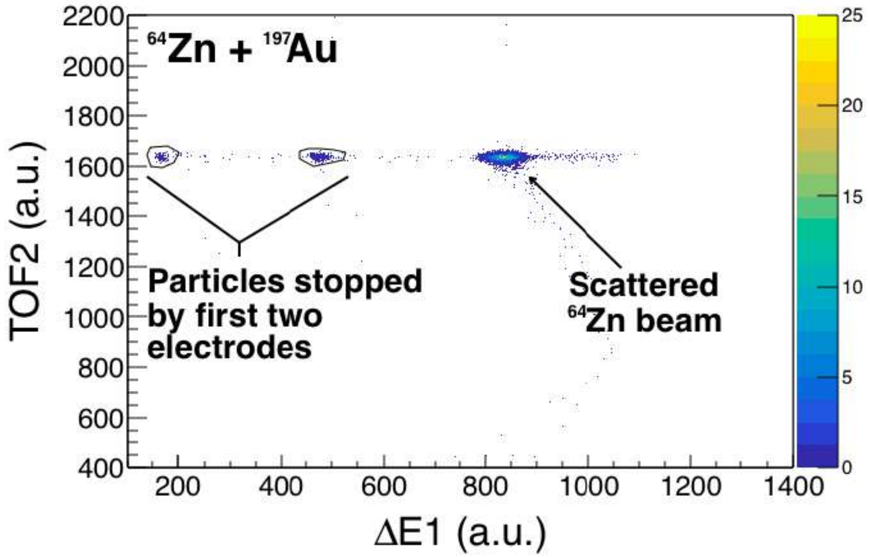

Energy resolution of the single section $\frac{\Delta E}{E} \approx \mathbf{4.35\%}$

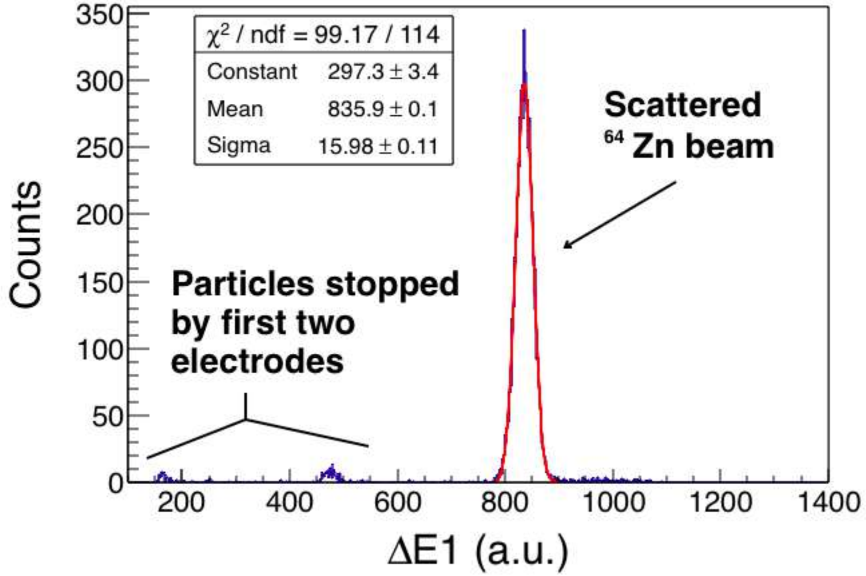

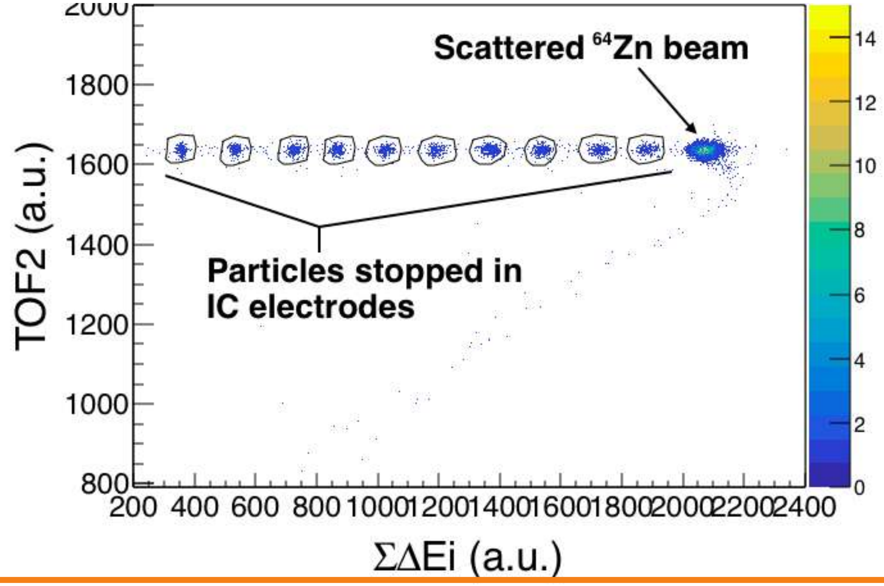

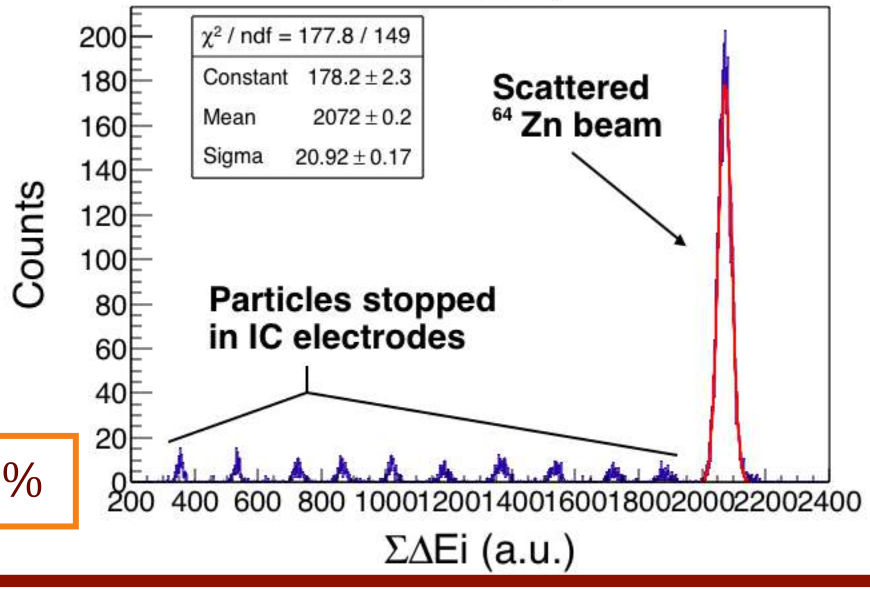

Energy resolution of the total energy signal $\frac{\Delta E}{E} \approx \mathbf{2.09\%}$

Istituto Nazionale di Fisica Nucleare
Laboratori Nazionali di Legnaro

HIL Heavy Ion Laboratory

The $^{36}S+^{50}Ti,^{51}V$ systems

Near- and sub-barrier fusion experiment

Results

- Excitation functions
- Barrier distributions
- Coupled channel (CC) analysis

Interpretation of the results

Summary

Effects of non-zero spin in sub-barrier fusion involving odd mass nuclei: the case of $^{36}S+^{50}Ti,^{51}V$

G. Colucci

When non-zero spin nuclei are involved in fusion process, interesting effects are expected

The $^{36}S+^{50}Ti,^{51}V$ systems

Near- and sub-barrier fusion experiment

Results

- **Excitation functions**
- **Barrier distributions**
- **Coupled channel (CC) analysis**

Interpretation of the results

Summary

When non-zero spin nuclei are involved in fusion process, interesting effects are expected

The $^{36}S+^{50}Ti,^{51}V$ systems

Near- and sub-barrier fusion experiment

Results

- **Excitation functions**
- **Barrier distributions**
- **Coupled channel (CC) analysis**

Interpretation of the results

Summary

Fusion cross section calculated for each magnetic substate of g.s. spin

When non-zero spin nuclei are involved in fusion process, interesting effects are expected

Fusion cross section calculated for each magnetic substate of g.s. spin

↓

Different Coulomb barrier height for each m-substate.

The $^{36}S+^{50}Ti,^{51}V$ systems

Near- and sub-barrier fusion experiment

Results

- Excitation functions
- Barrier distributions
- Coupled channel (CC) analysis

Interpretation of the results

Summary

When non-zero spin nuclei are involved in fusion process, interesting effects are expected

Fusion cross section calculated for each magnetic substate of g.s. spin

↓

Different Coulomb barrier height for each m-substate.

↓

Fusion cross section: average over m-substates

↓

Effects particularly evident **below the Coulomb barrier**.

The $^{36}S+^{50}Ti,^{51}V$ systems

Near- and sub-barrier fusion experiment

Results

- **Excitation functions**
- **Barrier distributions**
- **Coupled channel (CC) analysis**

Interpretation of the results

Summary

When non-zero spin nuclei are involved in fusion process, interesting effects are expected

Fusion cross section calculated for each magnetic substate of g.s. spin

↓

Different Coulomb barrier height for each m-substate.

↓

Fusion cross section: average over m-substates

↓

Effects particularly evident **below the Coulomb barrier**.

The $^{9}Be+^{144}Sm$ system

→ Non-zero spin of $3/2^+$

The $^{36}S+^{50}Ti,^{51}V$ systems

Near- and sub-barrier fusion experiment

Results

- **Excitation functions**
- **Barrier distributions**
- **Coupled channel (CC) analysis**

Interpretation of the results

Summary

When non-zero spin nuclei are involved in fusion process, interesting effects are expected

Fusion cross section calculated for each magnetic substate of g.s. spin

↓

Different Coulomb barrier height for each m-substate.

↓

Fusion cross section: average over m-substates

↓

Effects particularly evident **below the Coulomb barrier**.

CC calculations consider m= 1/2 and 3/2

M3Y+ rep interaction

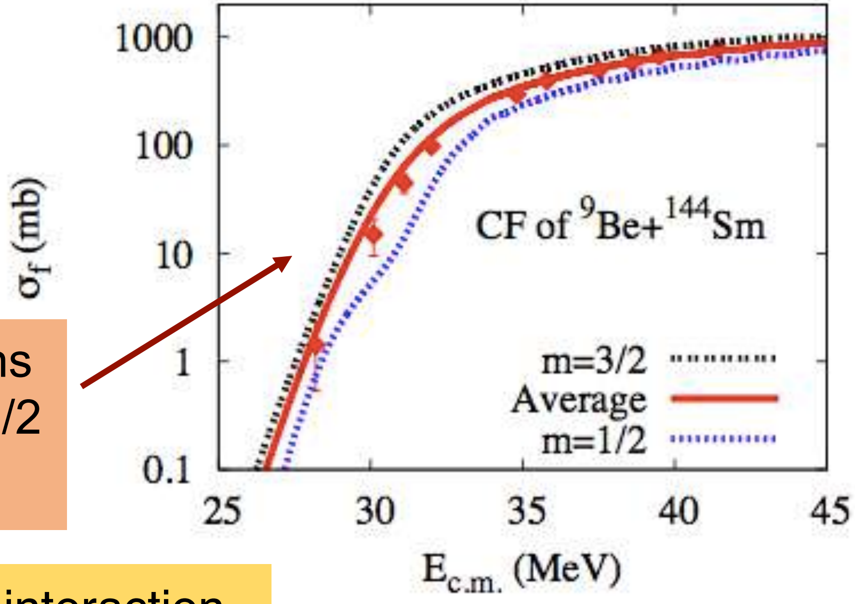

H. Esbensen, Phys. Rev. C 81 , 034606 (2010).
P. R. S. Gomes et al., Phys. Rev. C 73 , 064606 (2006).

The $^{9}Be+^{144}Sm$ system

→ Non-zero spin of $3/2^{+}$

When non-zero spin nuclei are involved in fusion process, interesting effects are expected

The $^{36}S+^{50}Ti,^{51}V$ systems

Near- and sub-barrier fusion experiment

Results

- **Excitation functions**
- **Barrier distributions**
- **Coupled channel (CC) analysis**

Interpretation of the results

Summary

Fusion cross section calculated for each magnetic substate of g.s. spin

↓

Different Coulomb barrier height for each m-substate.

↓

Fusion cross section: average over m-substates

↓

Effects particularly evident **below the Coulomb barrier**.

CC calculations consider m= 1/2 and 3/2

M3Y+ rep interaction

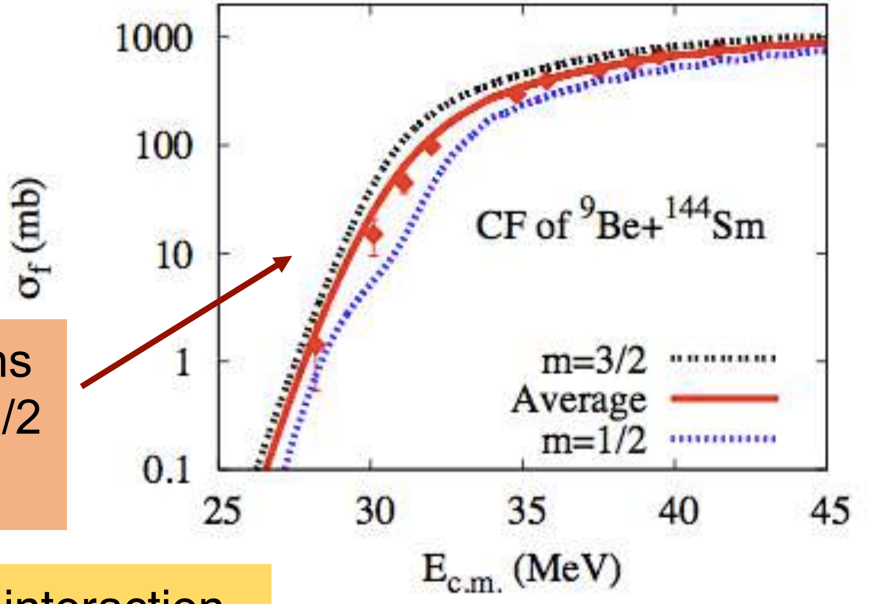

H. Esbensen, Phys. Rev. C 81 , 034606 (2010).
P. R. S. Gomes et al., Phys. Rev. C 73 , 064606 (2006).

The $^{9}Be+^{144}Sm$ system

→ Non-zero spin of $3/2^+$

Entrance potentials largely different for the two magnetic substates

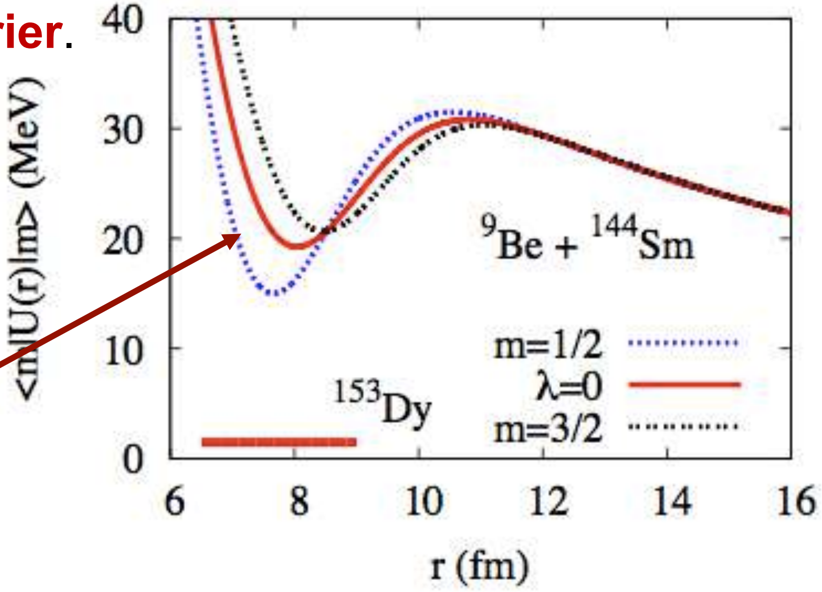

Coulomb barrier for the m= 3/2 lower and thinner than for m= 1/2.

The case of the systems ^{36}S+^{50}Ti and ^{36}S+^{51}V

The ^{36}S+^{50}Ti,^{51}V systems

Near- and sub-barrier fusion experiment

Results

- **Excitation functions**
- **Barrier distributions**
- **Coupled channel (CC) analysis**

Interpretation of the results

Summary

The case of the systems $^{36}S+^{50}Ti$ and $^{36}S+^{51}V$

The $^{36}S+^{50}Ti,^{51}V$ systems

Near- and sub-barrier fusion experiment

Results

- **Excitation functions**
- **Barrier distributions**
- **Coupled channel (CC) analysis**

Interpretation of the results

Summary

Nucleus	E (MeV)	λ^{π}	
^{50}Ti	1.55	2^+	$\beta_2 = 0.16$
	4.41	3^-	$\beta_3 = 0.14$
	2.68	4^+	
^{36}S	3.29	2^+	

The $^{36}S+^{50}Ti,^{51}V$ systems

Near- and sub-barrier fusion experiment

Results

- Excitation functions
- Barrier distributions
- Coupled channel (CC) analysis

Interpretation of the results

Summary

The case of the systems $^{36}S+^{50}Ti$ and $^{36}S+^{51}V$

Nucleus	E (MeV)	λ^{π}	
^{50}Ti	1.55	2^+	$\beta_2 = 0.16$
	4.41	3^-	$\beta_3 = 0.14$
	2.68	4^+	
^{36}S	3.29	2^+	

Nucleus	E (MeV)	Spin I
^{51}V	0	$7/2^-$ (g.s.)
	0.32	$5/2^-$
	0.93	$3/2^-$
	1.61	$11/2^-$
	1.81	$9/2^-$
	2.41	$3/2^-$

Strong B(E2) transitions to the g.s.

A different barrier is expected for each of the four m-substates of the ground state

The $^{36}S+^{50}Ti,^{51}V$ systems

Near- and sub-barrier fusion experiment

Results

- **Excitation functions**
- **Barrier distributions**
- **Coupled channel (CC) analysis**

Interpretation of the results

Summary

The case of the systems $^{36}S+^{50}Ti$ and $^{36}S+^{51}V$

Nucleus	E (MeV)	λ^{π}	
^{50}Ti	1.55	2^+	$\beta_2 = 0.16$
	4.41	3^-	$\beta_3 = 0.14$
	2.68	4^+	
^{36}S	3.29	2^+	

Nucleus	E (MeV)	Spin I
^{51}V	0	$7/2^-$ (g.s.)
	0.32	$5/2^-$
	0.93	$3/2^-$
	1.61	$11/2^-$
	1.81	$9/2^-$
	2.41	$3/2^-$

Strong B(E2) transitions to the g.s.

A different barrier is expected for each of the four m-substates of the ground state

$^{36}S+^{50}Ti$

V_0 (MeV)	r_0 (fm)	a_0 (fm)	V_B (MeV)	R_B (fm)	$\hbar\omega$ (MeV)
62.43	1.17	0.66	46.90	10.05	3.41

$^{36}S+^{51}V$

V_0 (MeV)	r_0 (fm)	a_0 (fm)	V_B (MeV)	R_B (fm)	$\hbar\omega$ (MeV)
62.96	1.17	0.66	49.00	10.05	3.47

Barriers differ by 2 MeV

Comparison between the two systems → No previous data were available

The $^{36}S+^{50}Ti,^{51}V$ systems

Near- and sub-barrier fusion experiment

Results

- **Excitation functions**
- **Barrier distributions**
- **Coupled channel (CC) analysis**

Interpretation of the results

Summary

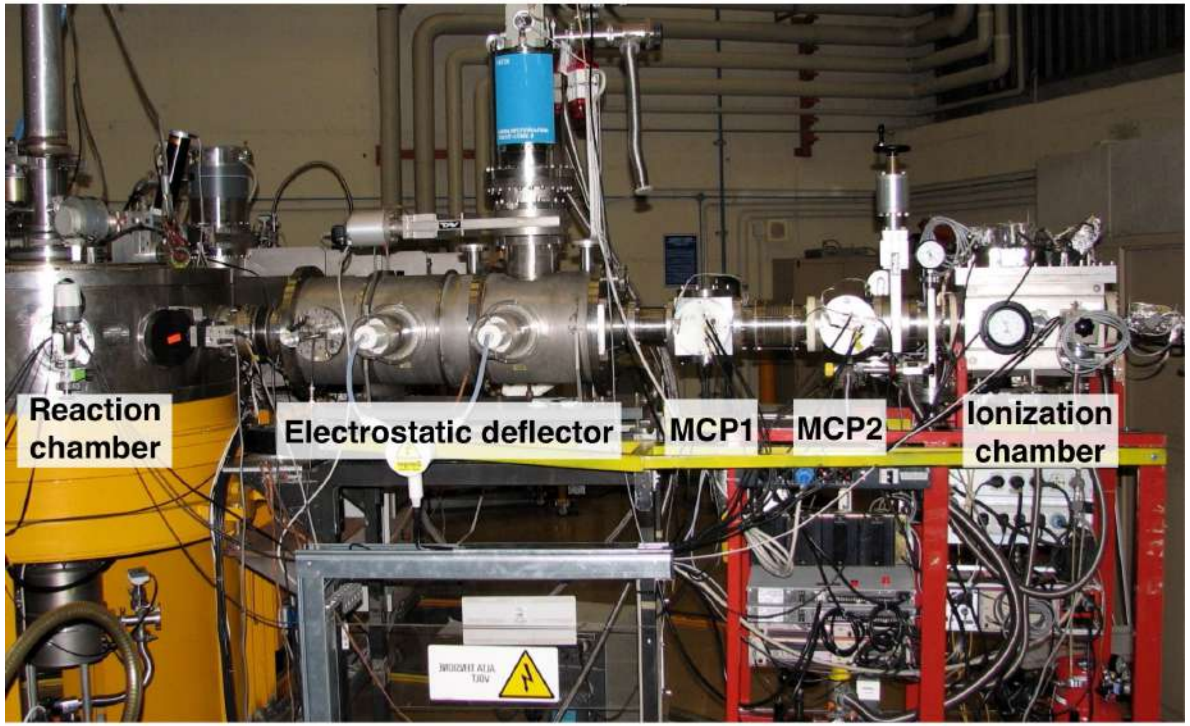

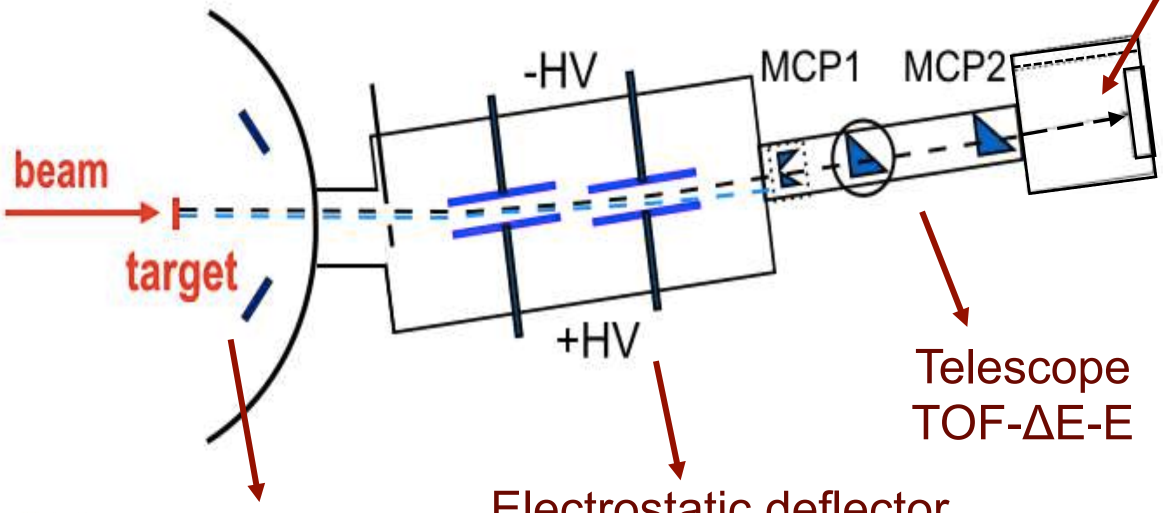

Direct detection of evaporation residues (ER)

- Beam suppression
- ER separation from residual beam

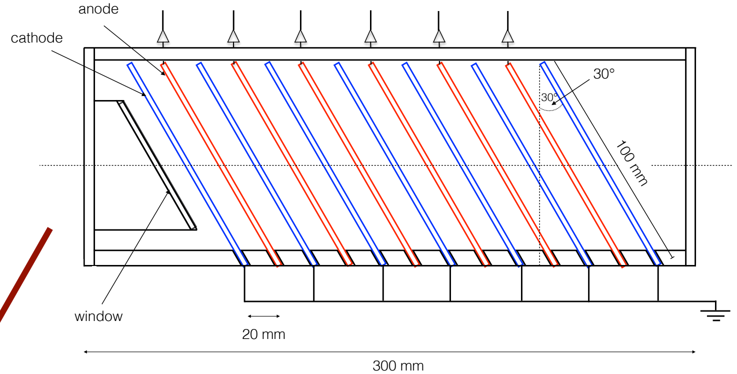

Fast IC

$^{50}TiO_2$ and ^{51}V targets of 50 μg/cm^2 thickness (15 μg/cm^2 carbon backing)

Energy ranges:
E_{lab} = 73 – 100 MeV for ^{50}Ti
E_{lab} = 76 – 100 MeV for ^{51}V

$^{36}S+^{50}Ti$ system

The $^{36}S+^{50}Ti,^{51}V$ systems

Near- and sub-barrier fusion experiment

Results

- **Excitation functions**
- **Barrier distributions**
- **Coupled channel (CC) analysis**

Interpretation of the results

Summary

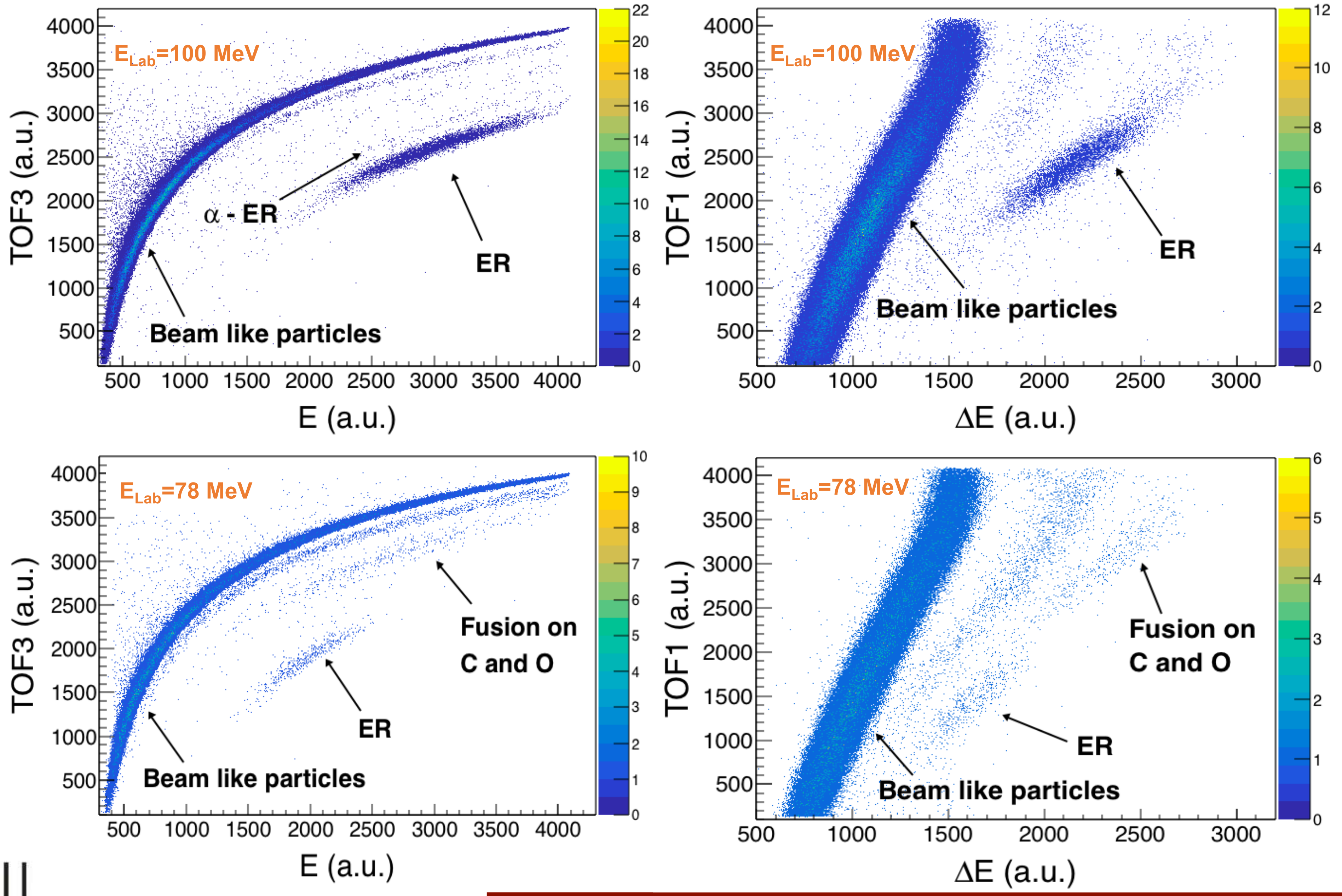

The $^{36}S+^{50}Ti,^{51}V$ systems

Near- and sub-barrier fusion experiment

Results

- **Excitation functions**
- **Barrier distributions**
- **Coupled channel (CC) analysis**

Interpretation of the results

Summary

$^{36}S+^{50}Ti$ system

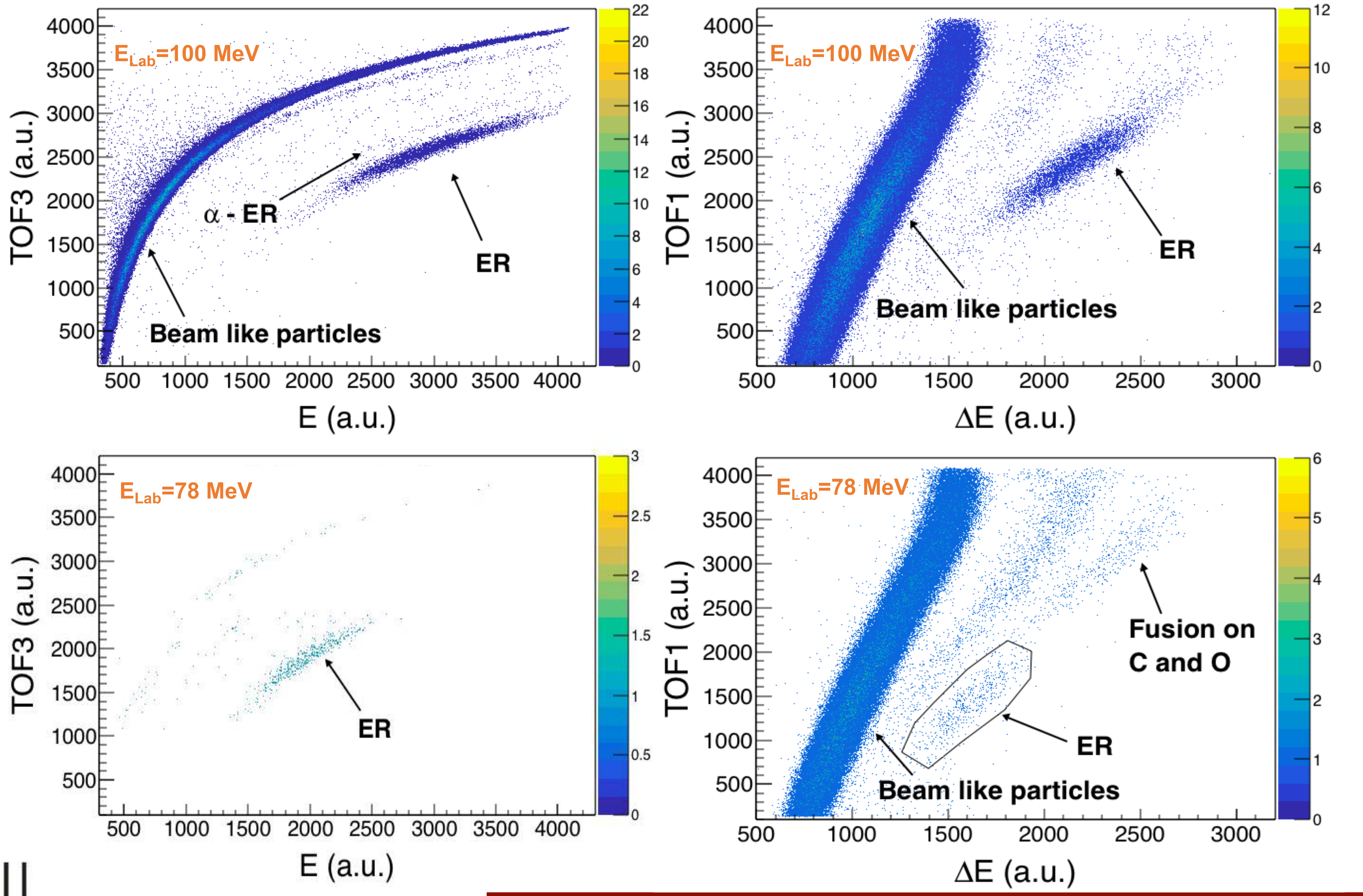

Istituto Nazionale di Fisica Nucleare
Laboratori Nazionali di Legnaro
Heavy Ion Laboratory

The $^{36}S+^{50}Ti,^{51}V$ systems

Near- and sub-barrier fusion experiment

Results

- Excitation functions
- Barrier distributions
- Coupled channel (CC) analysis

Interpretation of the results

Summary

$^{36}S+^{51}V$ system

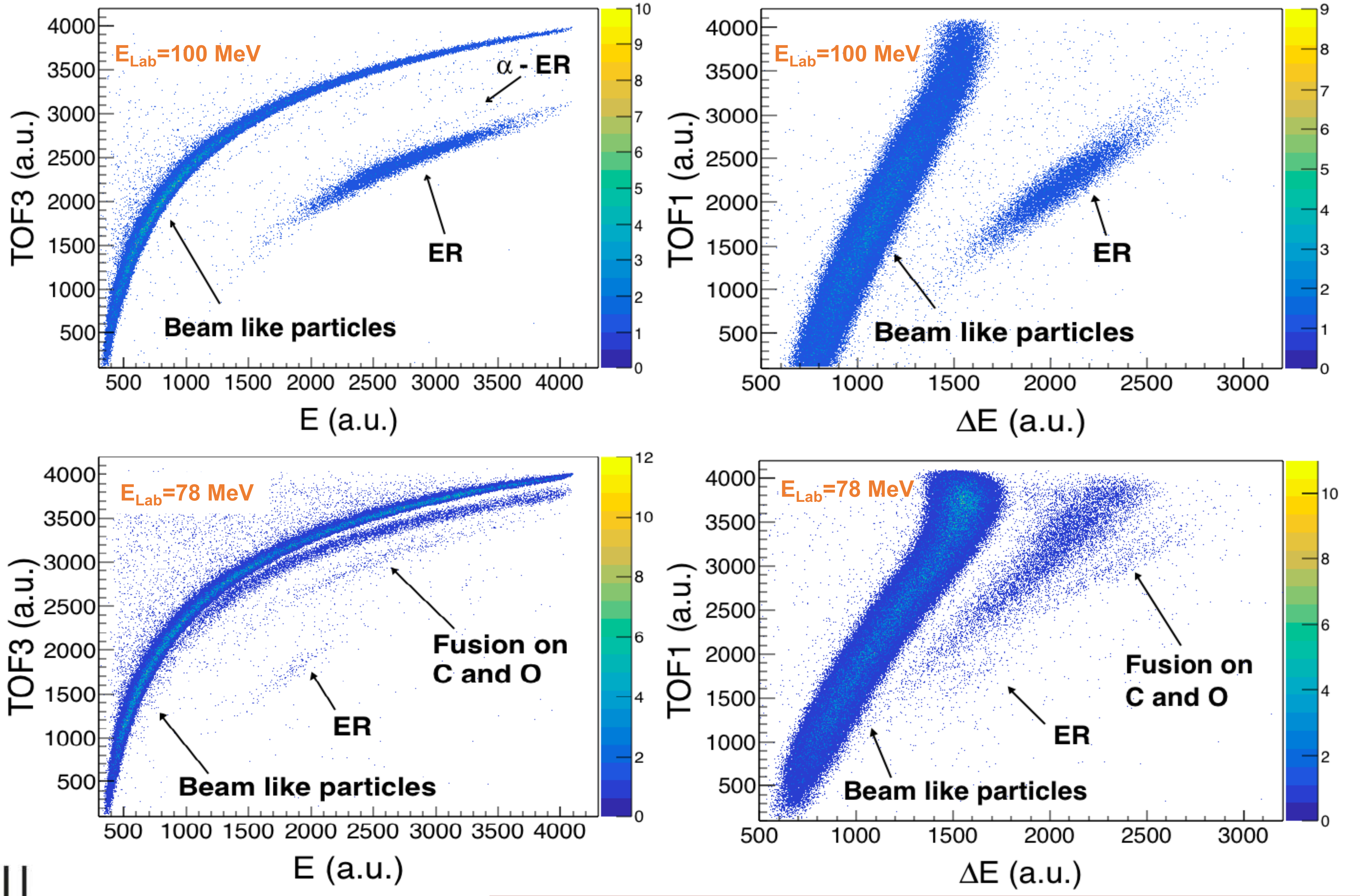

G. Colucci

Istituto Nazionale di Fisica Nucleare
Laboratori Nazionali di Legnaro
Heavy Ion Laboratory

The $^{36}S+^{50}Ti,^{51}V$ systems

Near- and sub-barrier fusion experiment

Results

- **Excitation functions**
- **Barrier distributions**
- **Coupled channel (CC) analysis**

Interpretation of the results

Summary

$^{36}S+^{51}V$ system

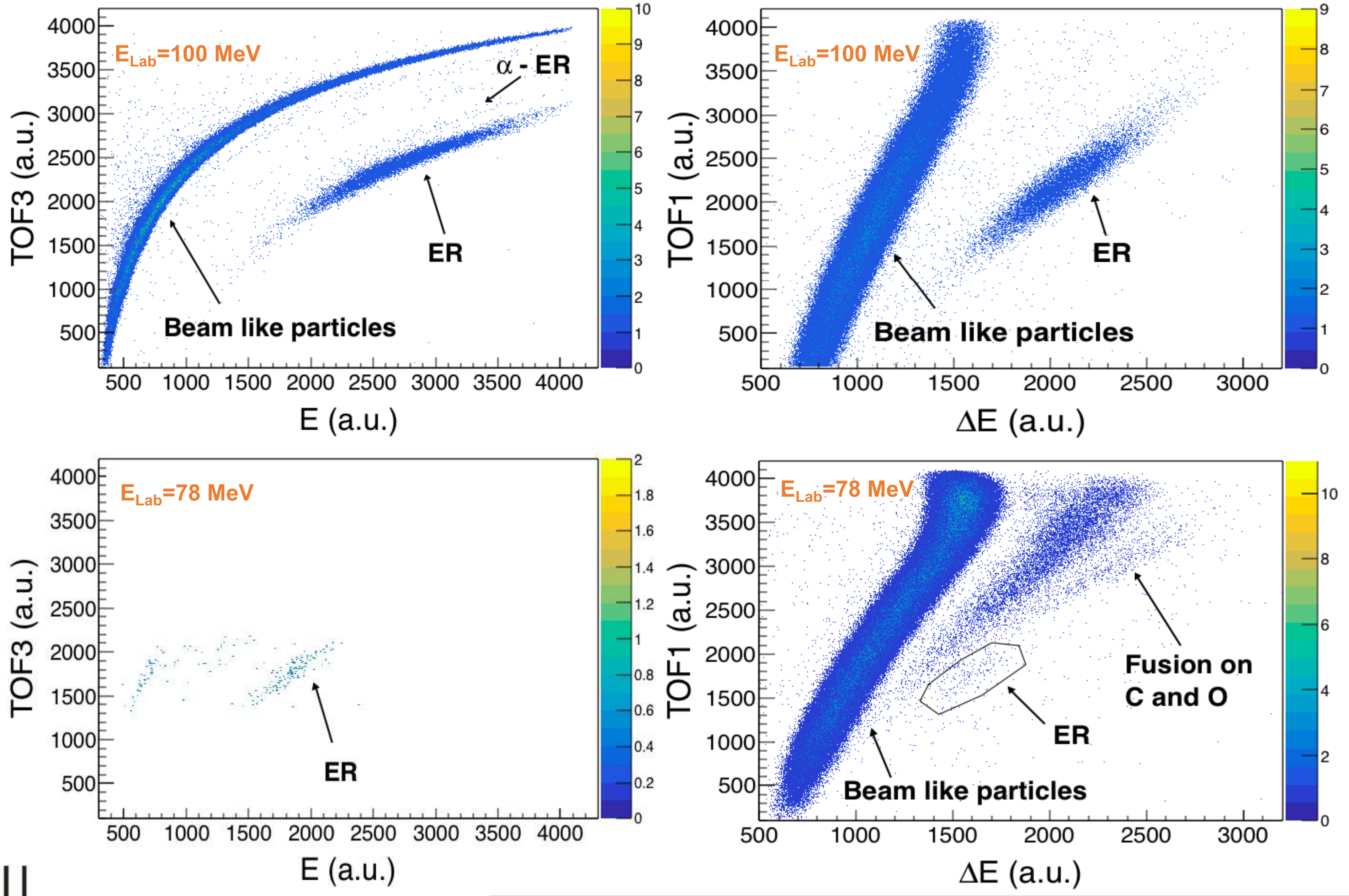

The $^{36}S+^{50}Ti,^{51}V$ systems

Near- and sub-barrier fusion experiment

Results

- **Excitation functions**
- Barrier distributions
- Coupled channel (CC) analysis

Interpretation of the results

Summary

- Excitation function has been extended down to **20-30 μb**

The $^{36}S+^{50}Ti,^{51}V$ systems

Near- and sub-barrier fusion experiment

Results

- **Excitation functions**
- Barrier distributions
- Coupled channel (CC) analysis

Interpretation of the results

Summary

- Excitation function has been extended down to **20-30 μb**

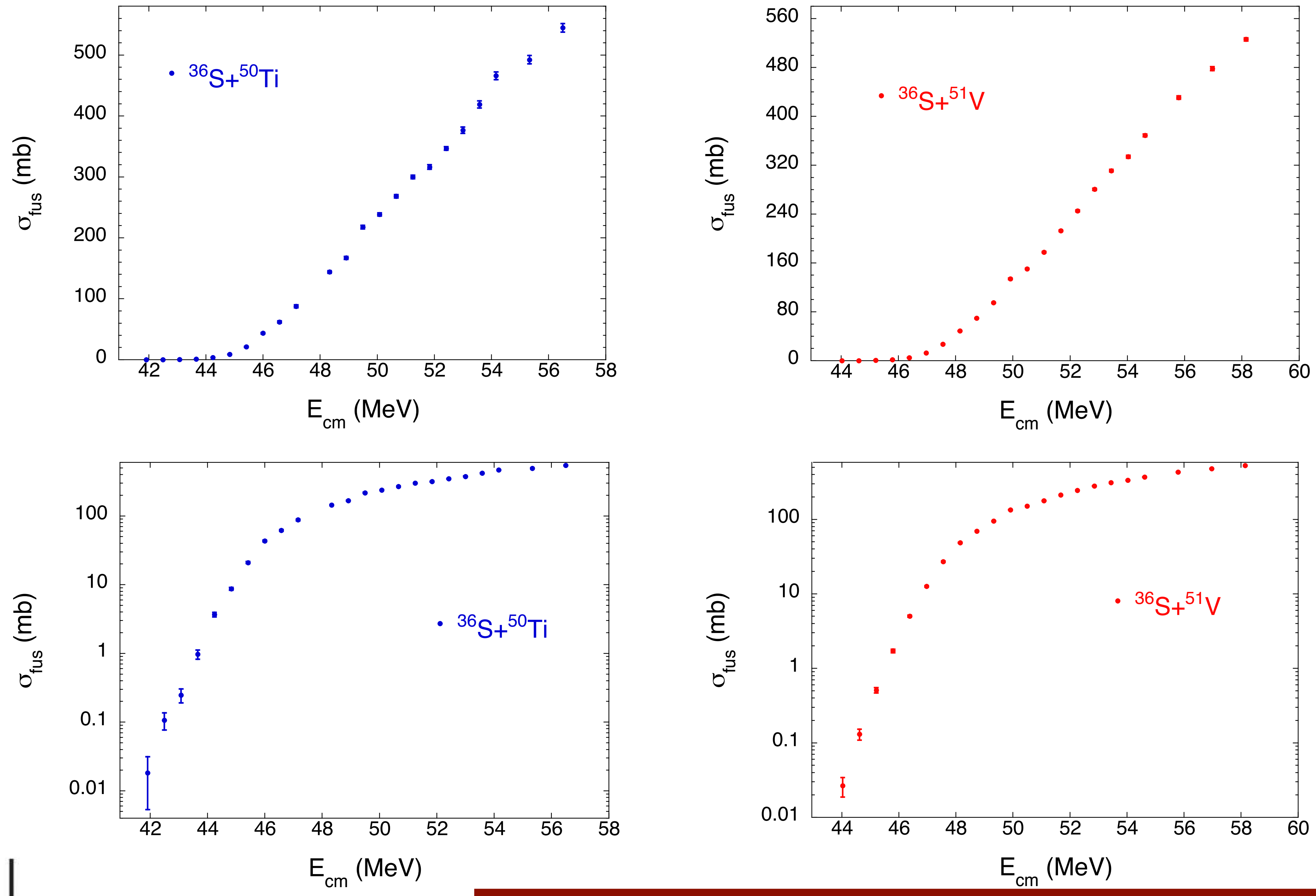

Istituto Nazionale di Fisica Nucleare
Laboratori Nazionali di Legnaro
Heavy Ion Laboratory

- Excitation function has been extended down to **20-30 μb**

- The comparison of the excitation functions shows a very similar behaviour of the two systems

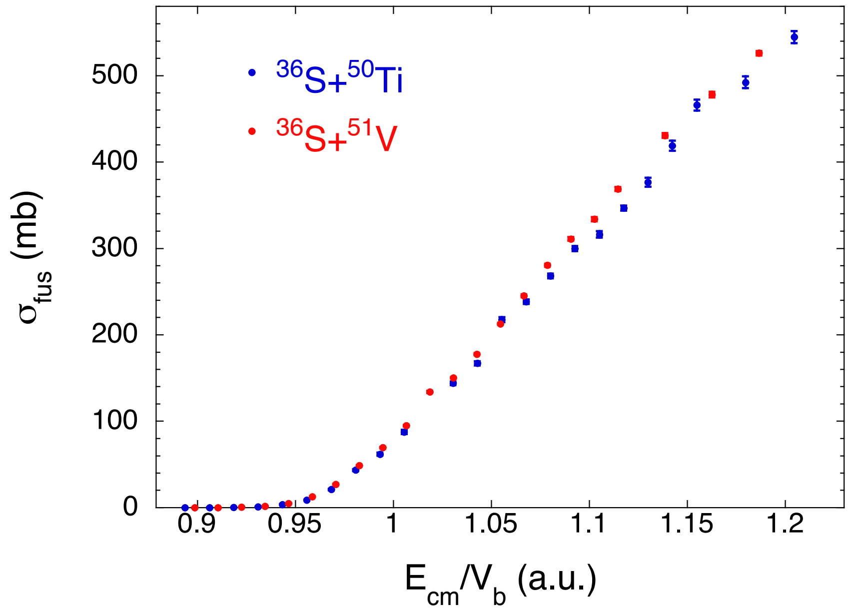

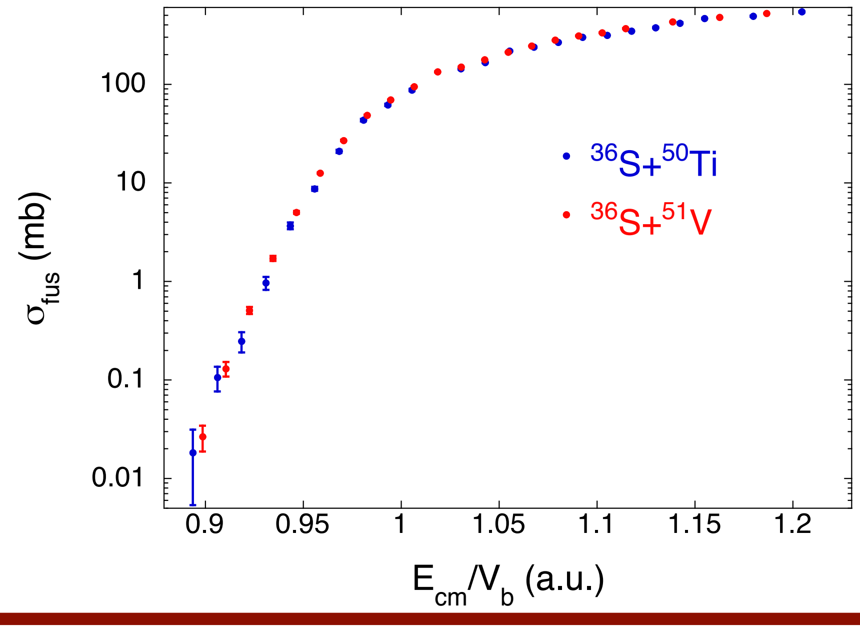

The $^{36}S+^{50}Ti,^{51}V$ systems

Near- and sub-barrier fusion experiment

Results

- **Excitation functions**
- **Barrier distributions**
- **Coupled channel (CC) analysis**

Interpretation of the results

Summary

Istituto Nazionale di Fisica Nucleare
Laboratori Nazionali di Legnaro
Heavy Ion Laboratory

The $^{36}S+^{50}Ti,^{51}V$ systems

Near- and sub-barrier fusion experiment

Results

- **Excitation functions**
- Barrier distributions
- Coupled channel (CC) analysis

Interpretation of the results

Summary

- Excitation function has been extended down to **20-30 μb**
- The comparison of the excitation functions shows a very similar behaviour of the two systems

Comparison of barrier distributions

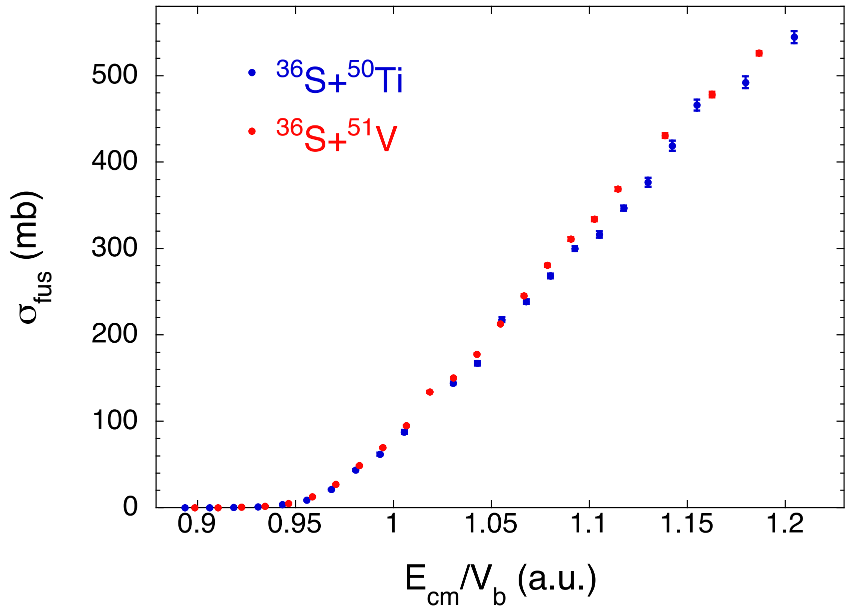

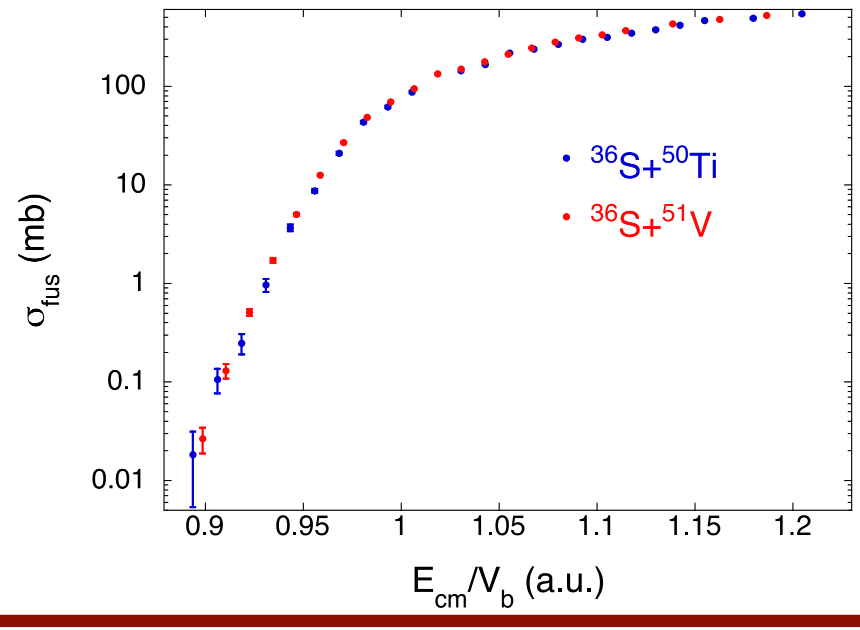

The ^{36}S+^{50}Ti,^{51}V systems

Near- and sub-barrier fusion experiment

Results

- Excitation functions
- **Barrier distributions**
- Coupled channel (CC) analysis

Interpretation of the results

Summary

- Excitation function has been extended down to **20-30 μb**

- The comparison of the excitation functions shows a very similar behaviour of the two systems

  → Comparison of barrier distributions

- Also the shapes of the two distributions are very similar.

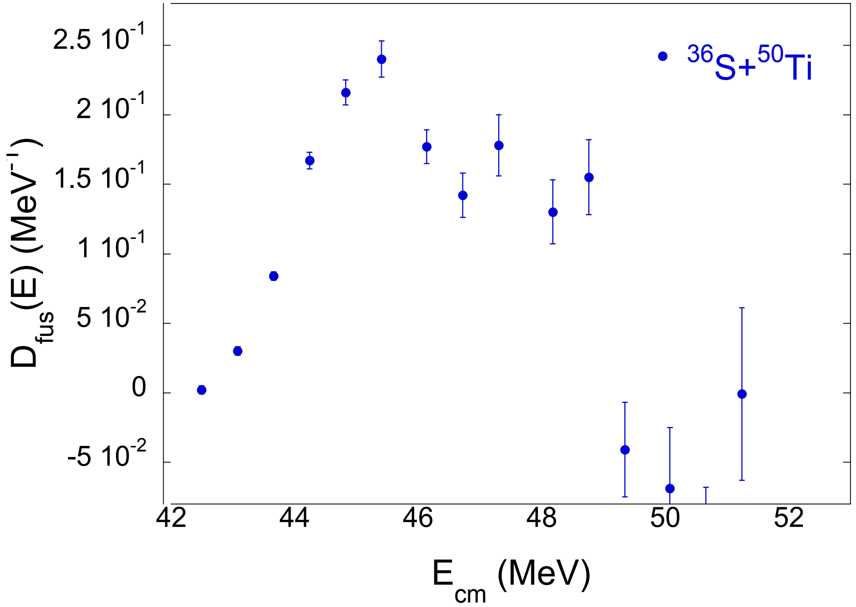

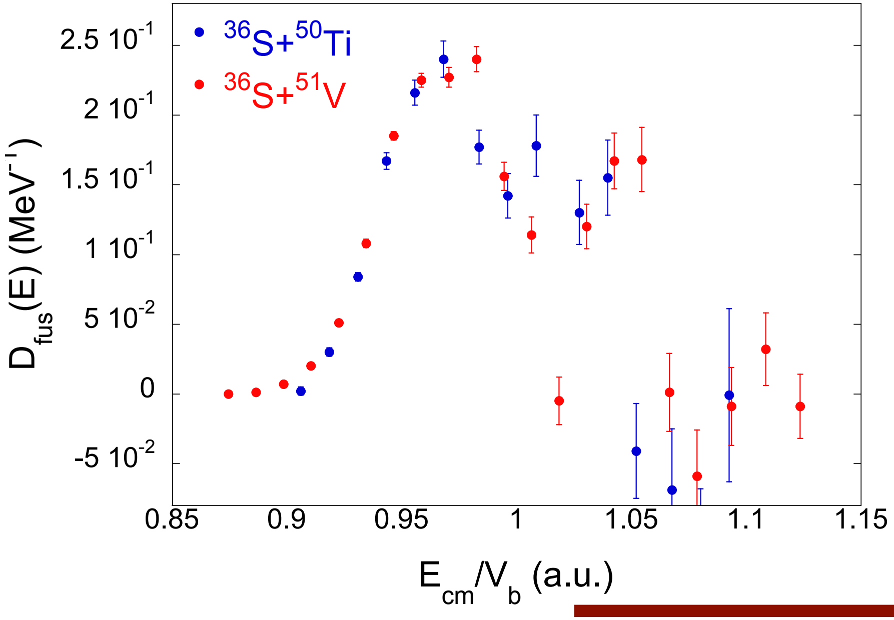

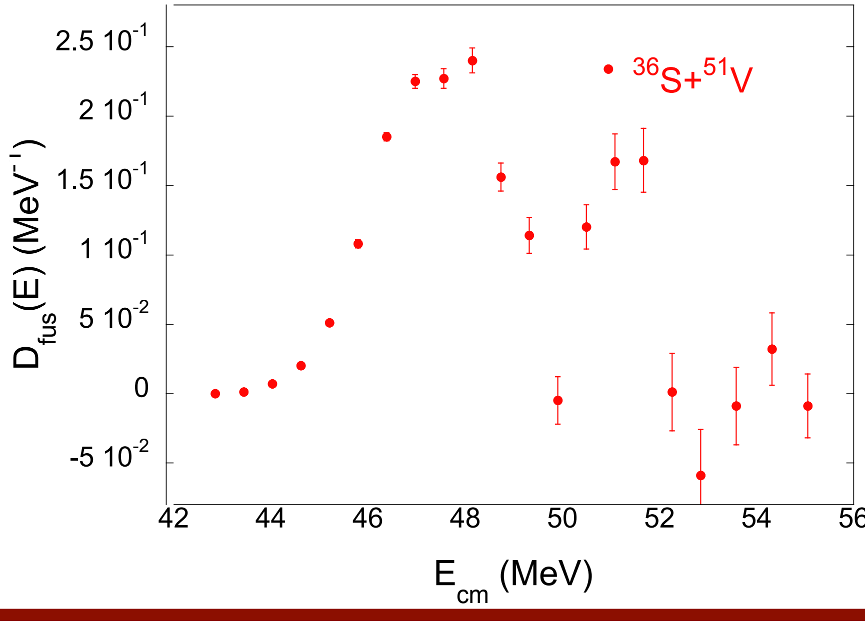

The $^{36}S+^{50}Ti,^{51}V$ systems

Near- and sub-barrier fusion experiment

Results

- Excitation functions
- **Barrier distributions**
- Coupled channel (CC) analysis

Interpretation of the results

Summary

- Excitation function has been extended down to **20-30 μb**
- The comparison of the excitation functions shows a very similar behaviour of the two systems

  → Comparison of barrier distributions

- Also the shapes of the two distributions are very similar.

A coupled-channels analysis is necessary

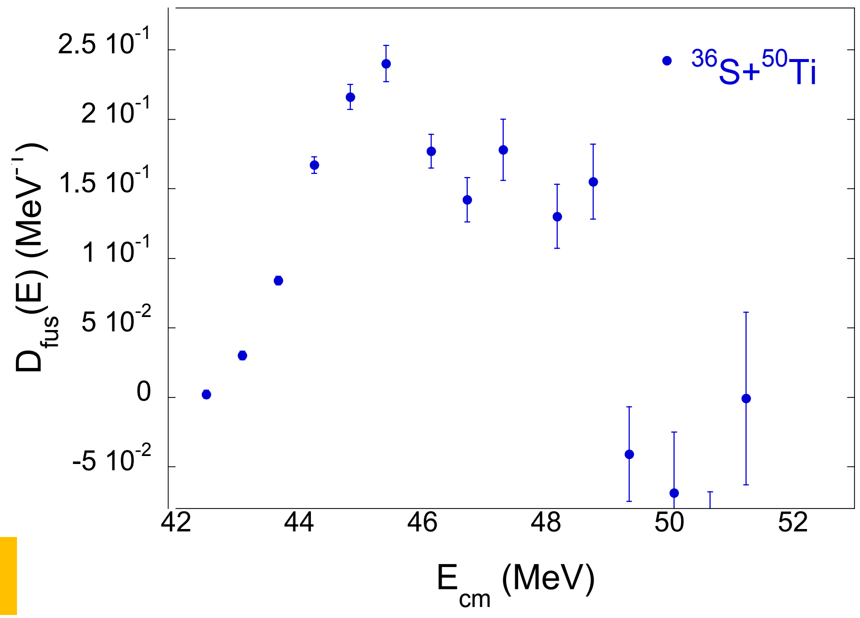

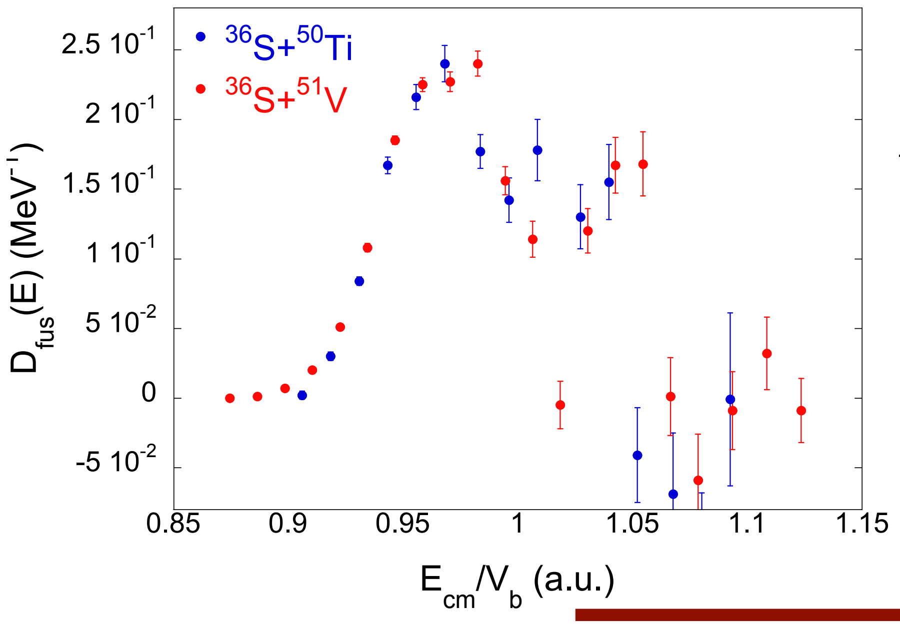

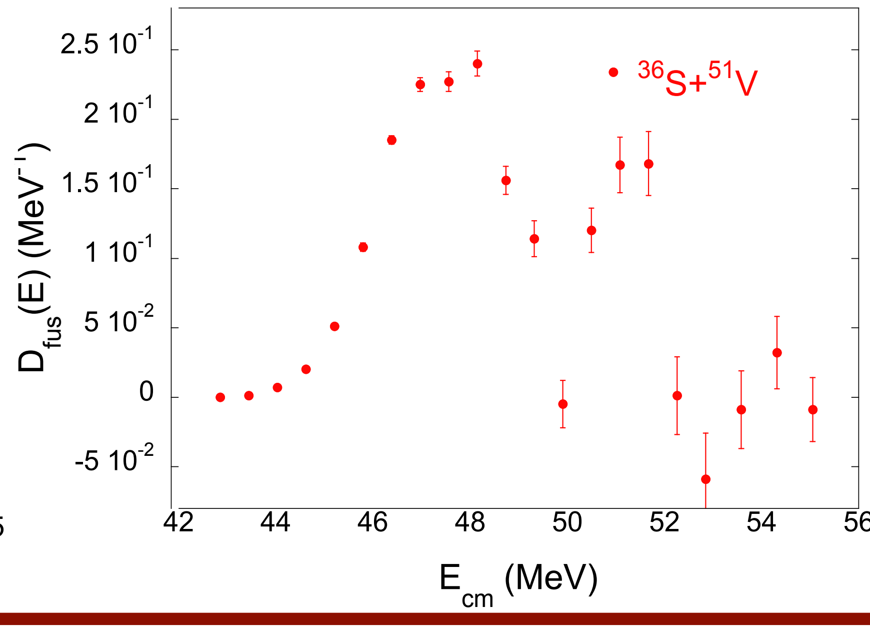

The $^{36}S+^{50}Ti,^{51}V$ systems

Near- and sub-barrier fusion experiment

Results

- Excitation functions
- Barrier distributions
- Coupled channel (CC) analysis

Interpretation of the results

Summary

The CC calculations include the collective vibrational excitations of both target and projectile nuclei.

Nucleus	E (MeV)	λ^{π}	β_{λ}
^{50}Ti	1.55	2^+	0.166
	4.41	3^-	0.138
	2.68	4^+	0.050
^{36}S	3.29	2^+	0.167

Istituto Nazionale di Fisica Nucleare
Laboratori Nazionali di Legnaro

Heavy Ion Laboratory

The ^{36}S+^{50}Ti,^{51}V systems

Near- and sub-barrier fusion experiment

Results

- Excitation functions
- Barrier distributions
- **Coupled channel (CC) analysis**

Interpretation of the results

Summary

The CC calculations include the collective vibrational excitations of both target and projectile nuclei.

One-phonon excitation of the lowest quadrupole vibrational states 2^+

Nucleus	E (MeV)	λ^π	β_λ
^{50}Ti	1.55	2^+	0.166
	4.41	3^-	0.138
	2.68	4^+	0.050
^{36}S	3.29	2^+	0.167

The $^{36}S+^{50}Ti,^{51}V$ systems

Near- and sub-barrier fusion experiment

Results

- Excitation functions
- Barrier distributions
- **Coupled channel (CC) analysis**

Interpretation of the results

Summary

The CC calculations include the collective vibrational excitations of both target and projectile nuclei.

↳ One-phonon excitation of the lowest quadrupole vibrational states 2^+

CC calculations well reproduce the experimental data at energies both below and above the Coulomb barrier.

Nucleus	E (MeV)	λ^π	β_λ
^{50}Ti	1.55	2^+	0.166
	4.41	3^-	0.138
	2.68	4^+	0.050
^{36}S	3.29	2^+	0.167

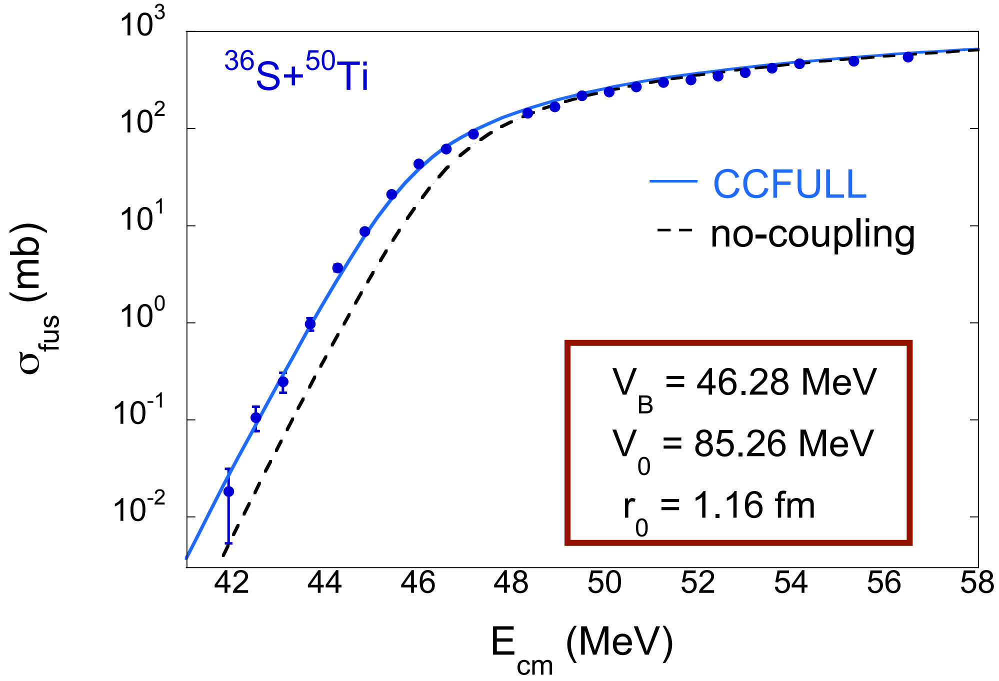

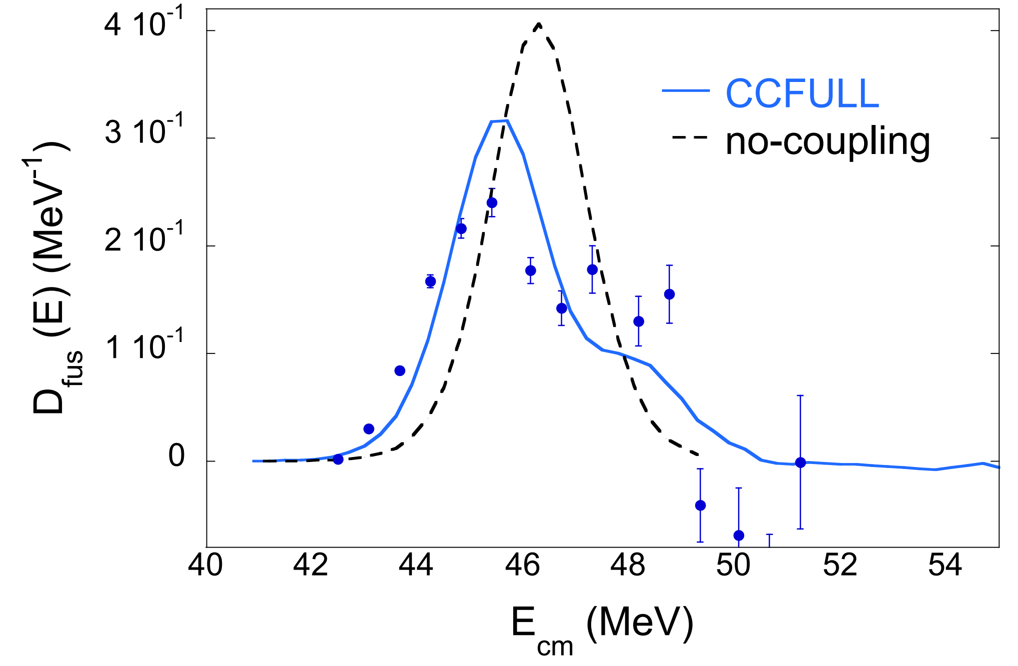

The $^{36}S+^{50}Ti,^{51}V$ systems

Near- and sub-barrier fusion experiment

Results

- **Excitation functions**
- **Barrier distributions**
- **Coupled channel (CC) analysis**

Interpretation of the results

Summary

Modified CCFULL code: evaluates the fusion cross section for each m-substate and provides their average as output.

Nucleus	E (MeV)	Spin I
^{51}V	0	$7/2^-$ (g.s.)
	0.32	$5/2^-$
	0.93	$3/2^-$
	1.61	$11/2^-$
	1.81	$9/2^-$
	2.41	$3/2^-$
^{36}S	3.29	2^+

The $^{36}S+^{50}Ti,^{51}V$ systems

Near- and sub-barrier fusion experiment

Results

- Excitation functions
- Barrier distributions
- **Coupled channel (CC) analysis**

Interpretation of the results

Summary

Modified CCFULL code: evaluates the fusion cross section for each m-substate and provides their average as output.

A total of eight couplings have been included

Nucleus	E (MeV)	Spin I
^{51}V	0	$7/2^-$ (g.s.)
	0.32	$5/2^-$
	0.93	$3/2^-$
	1.61	$11/2^-$
	1.81	$9/2^-$
	2.41	$3/2^-$
^{36}S	3.29	2^+

Istituto Nazionale di Fisica Nucleare
Laboratori Nazionali di Legnaro

Heavy Ion Laboratory

The $^{36}S+^{50}Ti,^{51}V$ systems

Near- and sub-barrier fusion experiment

Results

- Excitation functions
- Barrier distributions
- **Coupled channel (CC) analysis**

Interpretation of the results

Summary

Modified CCFULL code: evaluates the fusion cross section for each m-substate and provides their average as output.

A total of eight couplings have been included

CC calculations well reproduce the experimental data at energies both below and above the Coulomb barrier.

Nucleus	E (MeV)	Spin I
^{51}V	0	$7/2^-$ (g.s.)
	0.32	$5/2^-$
	0.93	$3/2^-$
	1.61	$11/2^-$
	1.81	$9/2^-$
	2.41	$3/2^-$
^{36}S	3.29	2^+

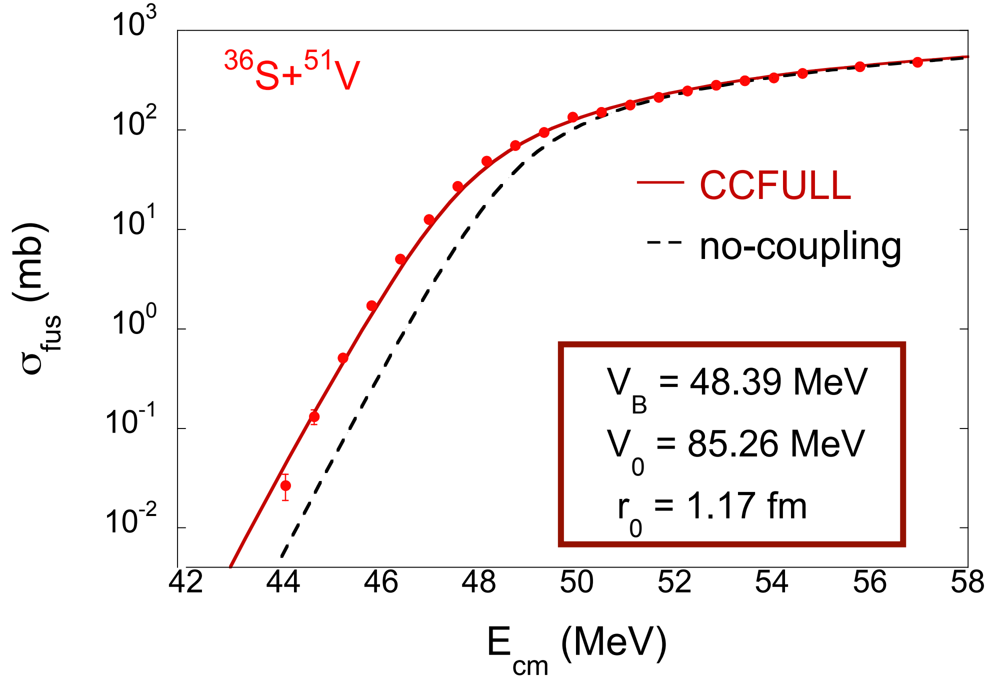

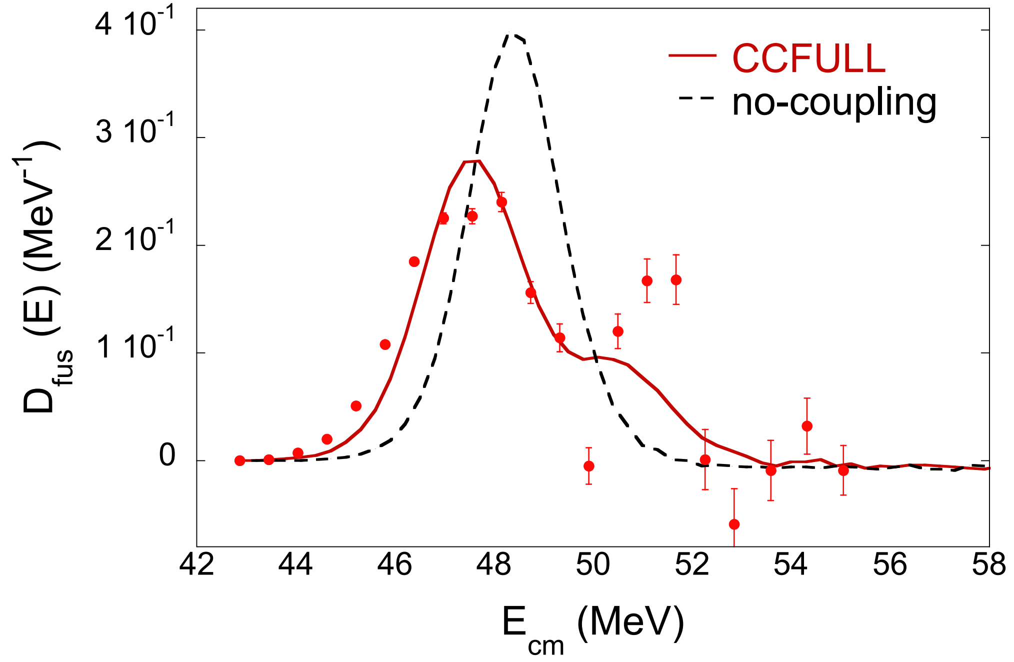

The $^{36}S+^{50}Ti,^{51}V$ systems

Near- and sub-barrier fusion experiment

Results

- Excitation functions
- Barrier distributions
- Coupled channel (CC) analysis

Interpretation of the results

Summary

Barrier distribution and excitation functions look very similar for the two systems

The extra proton in the $1f_{7/2}$ shell of the ^{51}V does not have any significant influence on sub-barrier fusion behaviour of the system

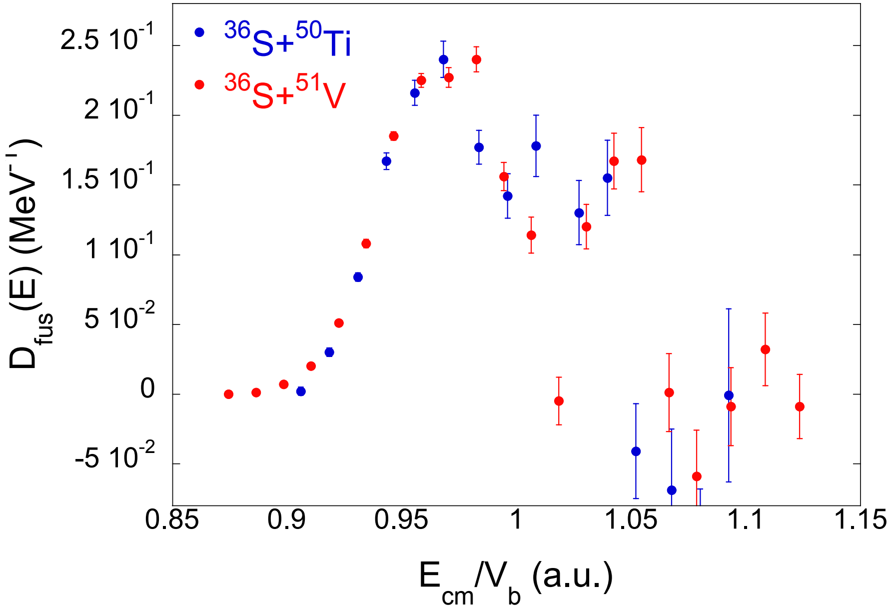

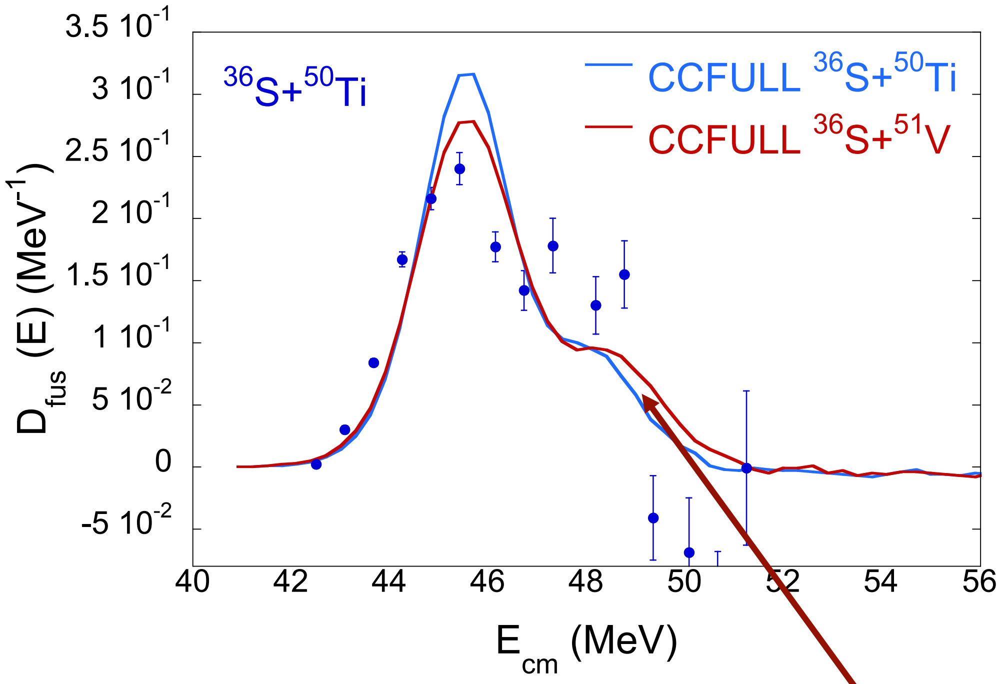

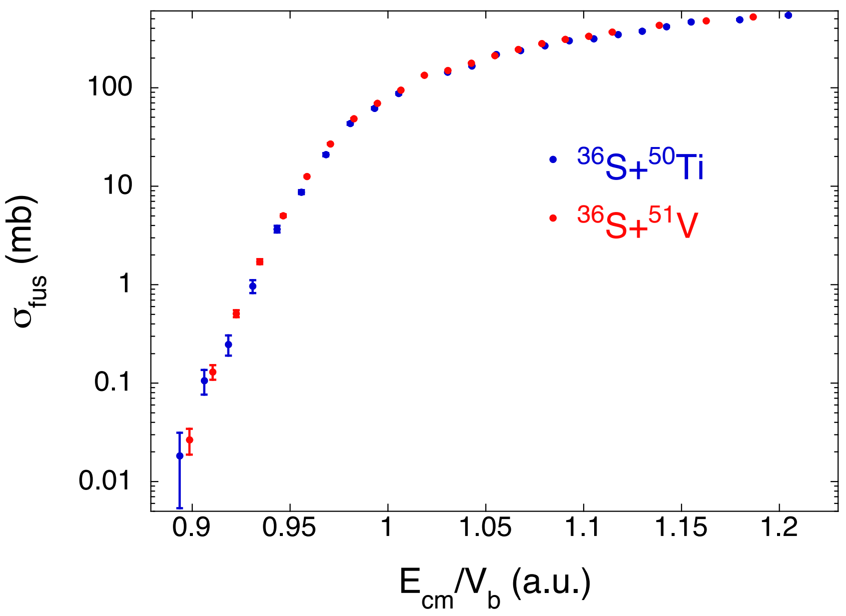

Small difference between the two calculated barrier distributions around 51–52 MeV

The $^{36}S+^{50}Ti,^{51}V$ systems

Near- and sub-barrier fusion experiment

Results

- Excitation functions
- Barrier distributions
- Coupled channel (CC) analysis

Interpretation of the results

Summary

- The 13 tilted grid electrodes (transparency of 98% each) significantly decrease the drift time of the electrons to anodes with respect to a conventional IC with transverse field
  - Reduction of shaping time to 0.25μs
  - Shorter gate width of the DAQ of 1μs
  - Highest counting rate of 140 kHz with the veto provided by the last IC section
- Z-resolution of 1/38 obtained for ^{64}Zn ions at about 3 MeV/A.
- Energy resolution of 2.06 % with ^{64}Zn ions at the energy of 2.3 MeV/A

The Fast IC has been used in one sub-barrier fusion experiment with stable beams

- Sub-barrier fusion of the two systems $^{36}S+^{50}Ti,^{51}V$ has been measured at LNL to investigate the possible effect of the non-zero spin of the ^{51}V ground state
- Fusion cross sections measured down to values ~20 μb.
- Barrier distributions and excitation functions look very similar for the two systems
- CCFULL code was used for the $^{36}S+^{50}Ti$ system including the couplings of the 2^+ vibrational states of ^{36}S and ^{50}Ti. A modified CCFULL code was used for the $^{36}S+^{51}V$ reaction to include the ^{51}V excitations. The theoretical predictions are in good agreement.
- Similar behavior can be explained in the weak-coupling scheme, where the relatively stiff ^{50}Ti is not much affected by the adding of one proton to form ^{51}V.

G. Montagnoli, C. Broggini, A. Caciolli, R. Depalo, M. Mazzocco, F. Scarlassara, E. Strano
Dept. of Physics and Astronomy, Univ. of Padova and INFN-Padova, Italy

A. M. Stefanini, L.Corradi, E.Fioretto, A. Goasduff, F.Galtarossa
INFN, Laboratori Nazionali di Legnaro, Legnaro (Padova), Italy

K. Hagino
Department of Physics, Tohoku University and Research Center for Electron Photon Science, Tohoku University, Sendai, Japan

S. Szilner, T. Mijatovic, P. Colovic, N. Vukman
Ruder Boskovic Institute, Zagreb, Croatia

D. Montanari
IPHC, CNRS-IN2P3, Univ. Louis Pasteur, Strasbourg Cedex 2, France

G.Jaworski
Heavy Ion Laboratory, University of Warsaw, PL-02-093 Warsaw, Poland

M. Siciliano
Irfu/DPhN/CEA, Université de Paris-Saclay, F-91191 Gif-sur-Yvette, France

J.Grebosz
Institute of Nuclear Physics, Cracow, Poland

Istituto Nazionale di Fisica Nucleare
Laboratori Nazionali di Legnaro

Heavy Ion Laboratory

Thank you for your attention

Sub-barrier fusion reactions with radioactive beams

Extra slide

Neutron transfer couplings and the use of neutron-rich exotic beams have been predicted to provide enhanced fusion probabilities for the synthesis of superheavy elements

No differences between ^{132}Sn + ^{58,64}Ni and no enhancement with respect to ^{58,64}Ni + ^{124}Sn.

Extra-enhancement appreciable at cross sections <1 mb).

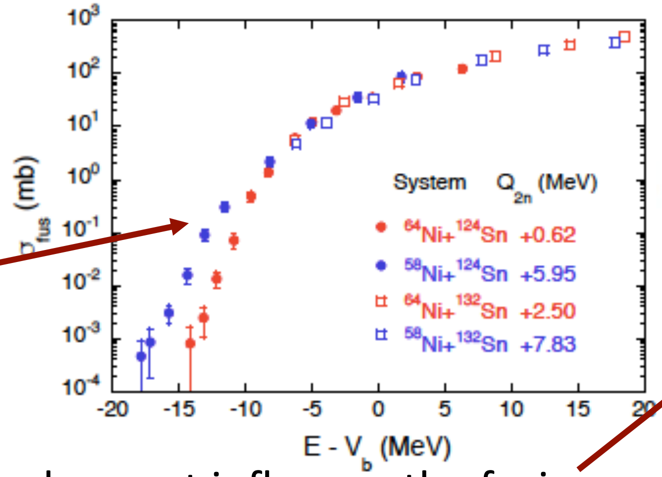

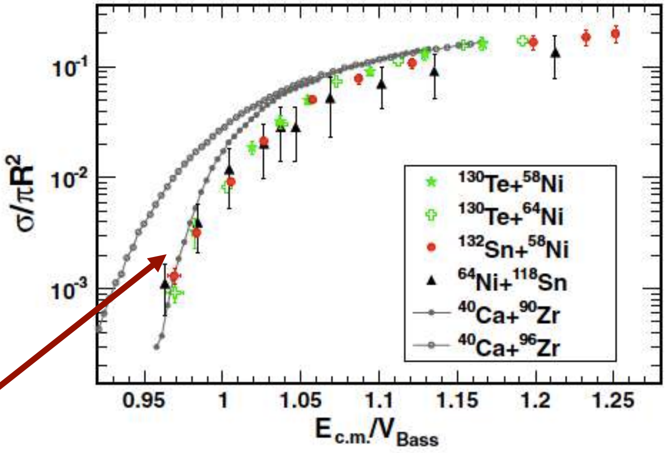

Positive Q-value transfer channels does not influence the fusion

Z. Kohley et al. , Phys. Rev. Let. 107.20 (2011)

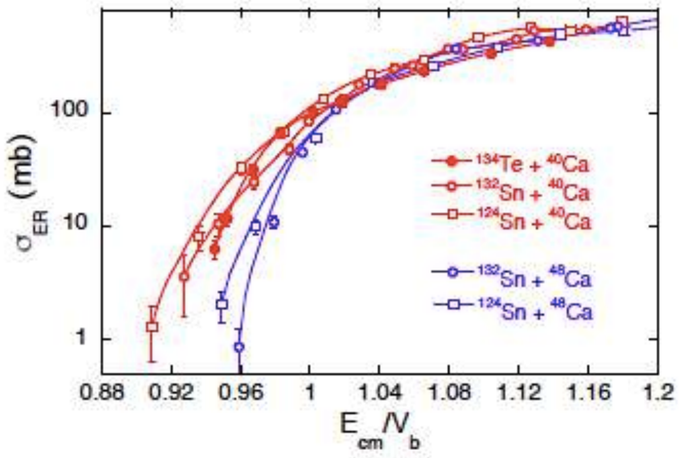

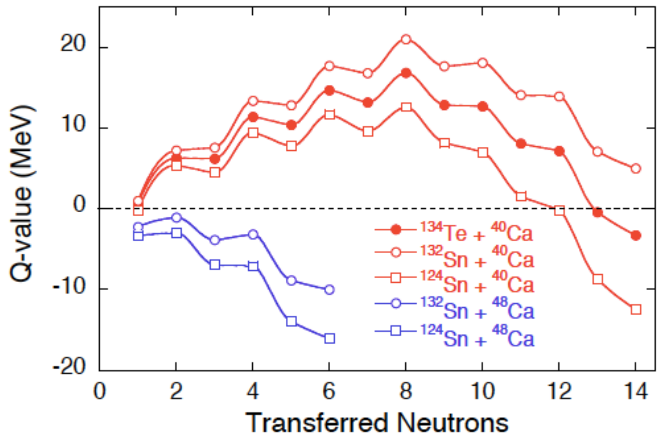

Negative Q-values for neutron transfer channels have smaller cross sections with respect to positive Q-value cases.

Very neutron rich exotic ^{132}Sn and ^{134}Te confirmed effect observed with stable beams .

Z. Kohley et al. Phys. Rev. C 87.6 (2013)

J. J. Kolata et al., Phys. Rev. C 85.5 (2012)

Istituto Nazionale di Fisica Nucleare
Laboratori Nazionali di Legnaro

Heavy Ion Laboratory

Extra slide

- **SPES Phase 1** : 5μA proton current on Ucx target (10^5 pps)

  ^{96}Sr, ^{94}Kr on ^{40}Ca and ^{28} Si targets neutron pick-up reactions Q-value +26MeV

  ^{134}Sn, ^{136}Te on light targets transfer channel effects on fusion < 1mb

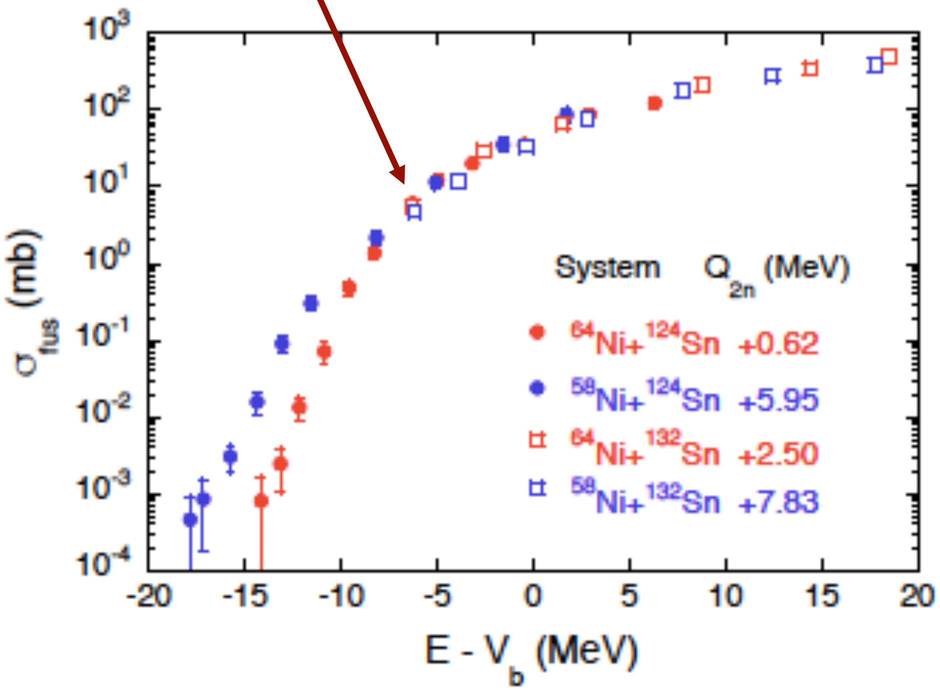

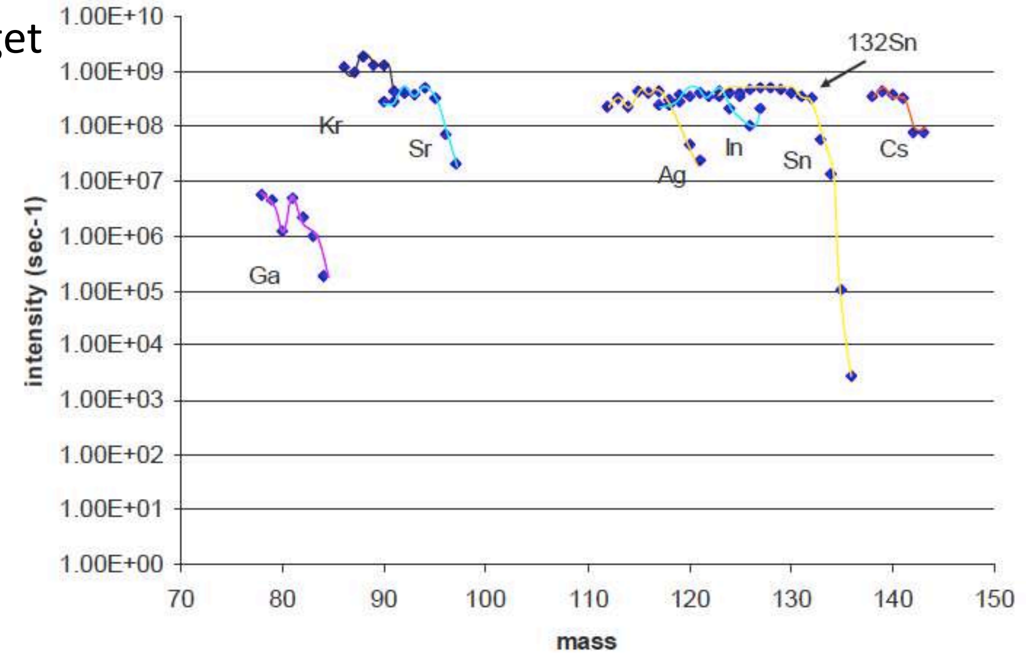

- **SPES Phase 2** : 200μA proton current on SiC and B4C targets

  ^{94}Sr, ^{92}Kr, ^{132}Sn, ^{134}Te, ^{140,142}Xe (higher intensity 10^6 – 10^8 pps)

- **SPES Phase 3** : 200μA proton current on all targets (mainly Ucx)

G. Prete et al., 'Theoretical Nuclear Physics in Italy' 1120 (2009)
https://web.infn.it/spes/index.php/characteristics/spes-beams-7037/spesbeamstable
Z. Kohley et al. , Phys. Rev. Let. 107.20 (2011)

Extra slide

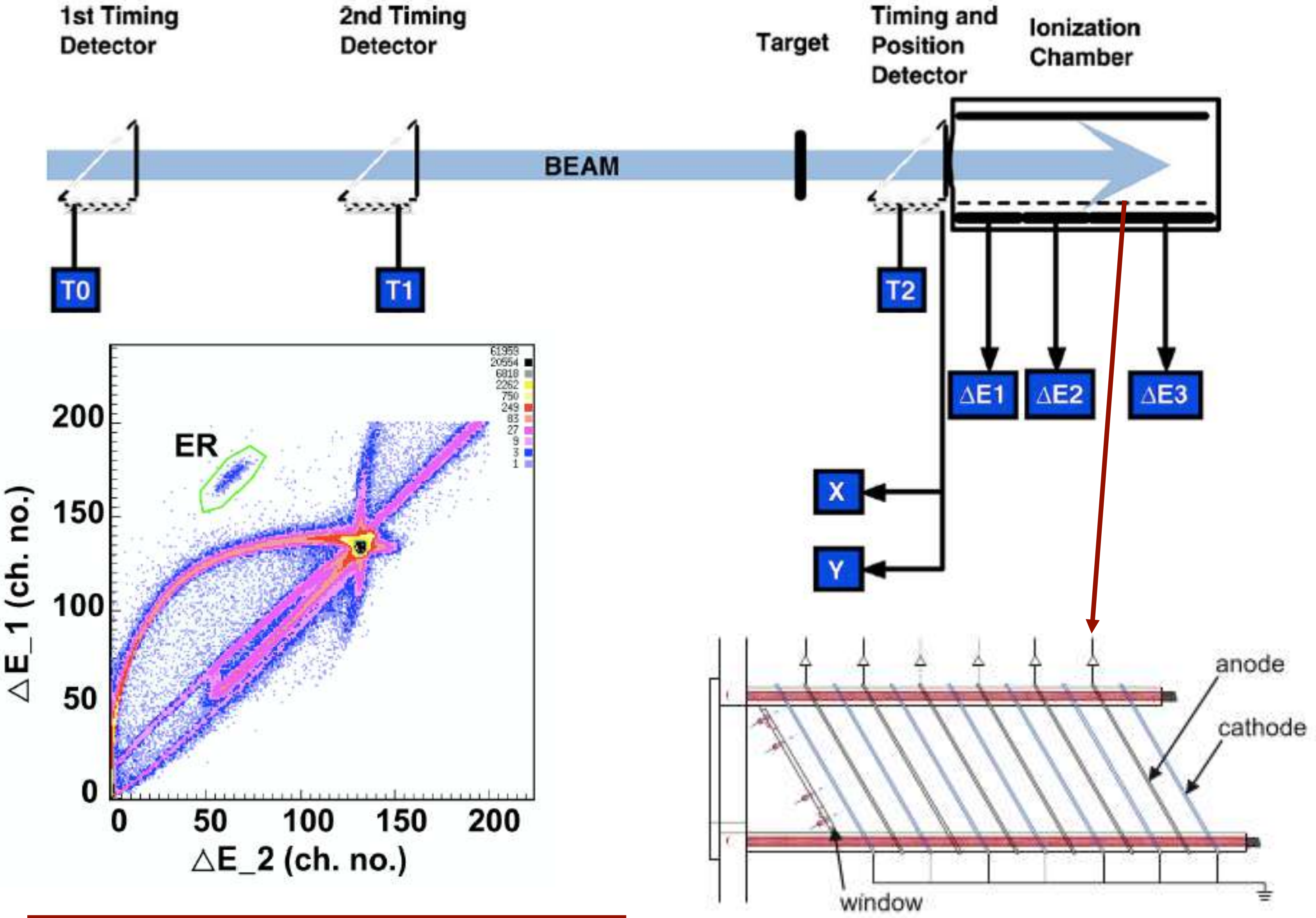

Maximum rate $\sim 10^3 - 10^4$ pps

J. F. Liang, D. Shapira, Phys.Rev. Lett. **91**. 152701, (2003)
D. Shapira et al., Nuclear Instruments and Methods in Physics Research A **551** (2005) 330–338

Extra slide

Measurement of low-energy fusion of ^{12}C + ^{30}Si in inverse kinematics at θ_{Lab}=3°

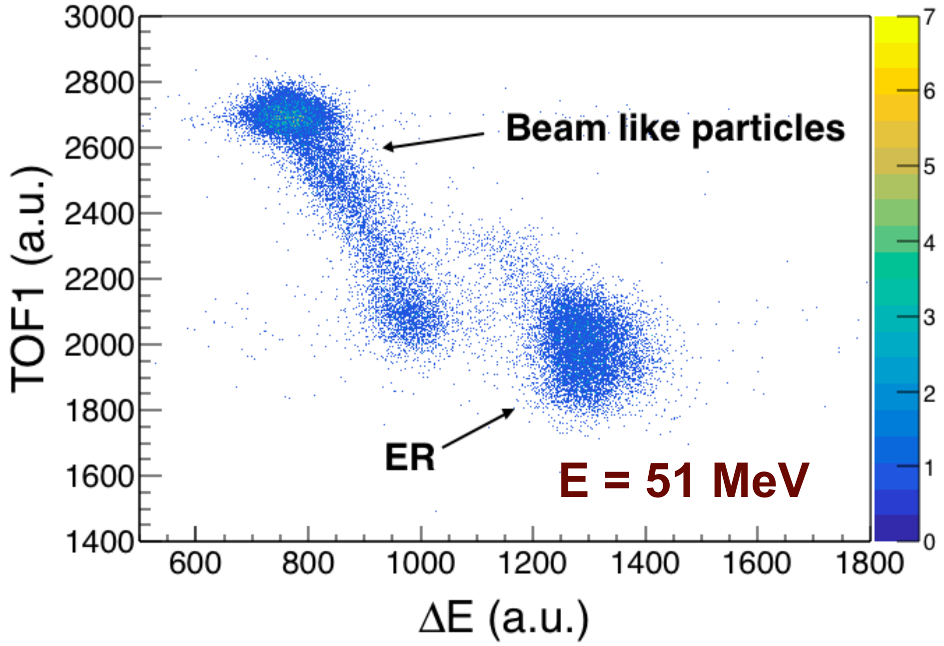

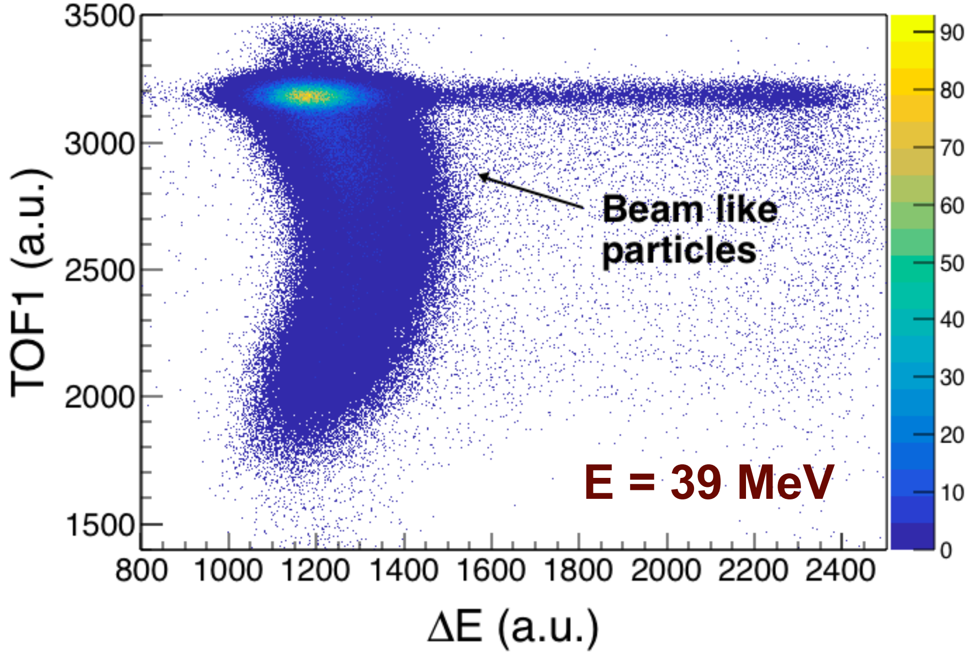

High background mainly due to the DAQ gate of 6μs, due to the slow response of the IC compared to the MCPs and Si detectors

We need a fast IC

Extra slide

GARFIELD field simulation

Equipotential lines

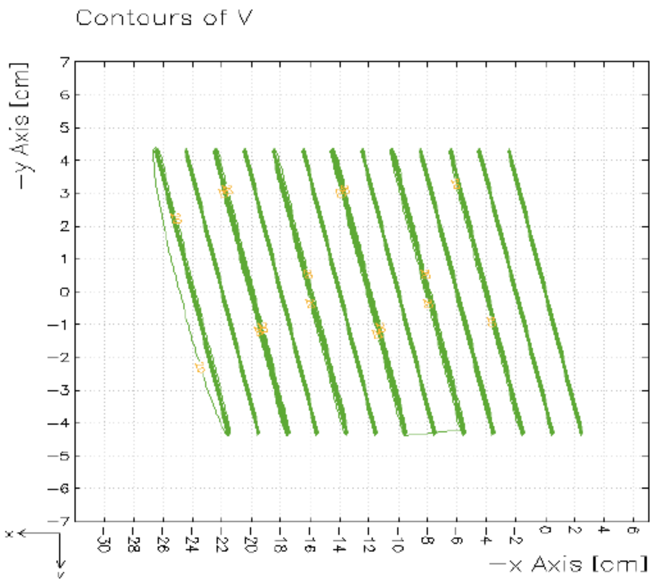

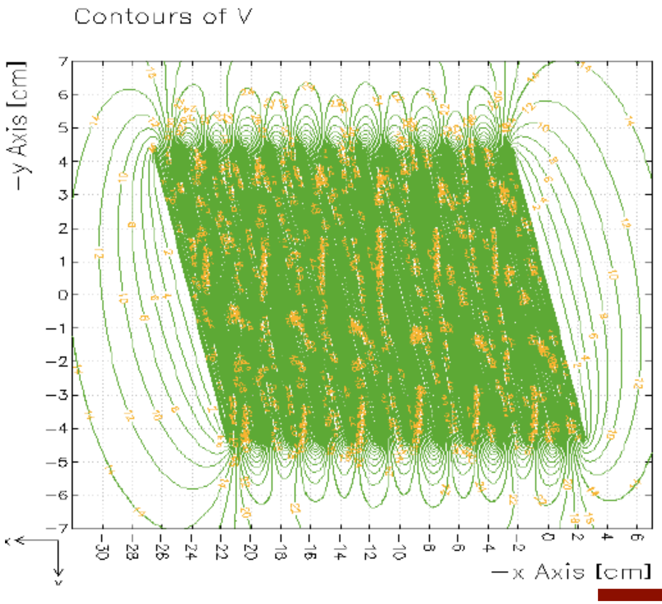

Electric field between two series of wires

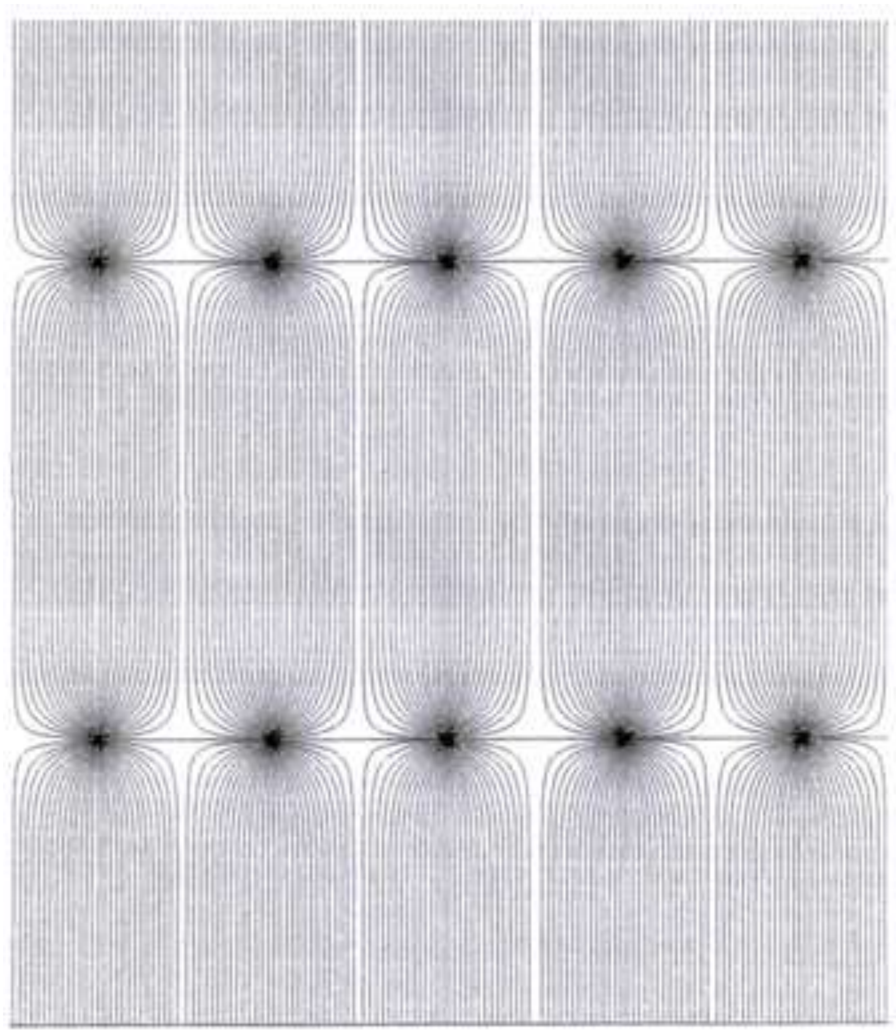

Extra slide

Low-intensity beams of 2 10^4 ion/s and target thick 1 mg/cm^2 → Fusion excitation function down to **1 mb**.

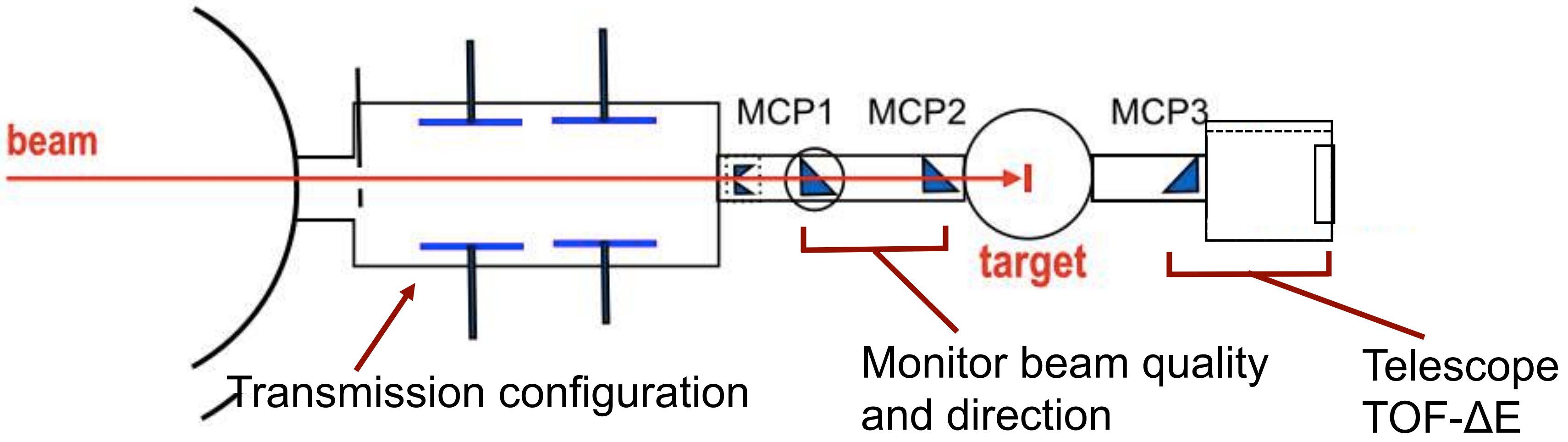

Low-intensity beams 10^5 ion/s → Fusion excitation function down to around **100 μb**.

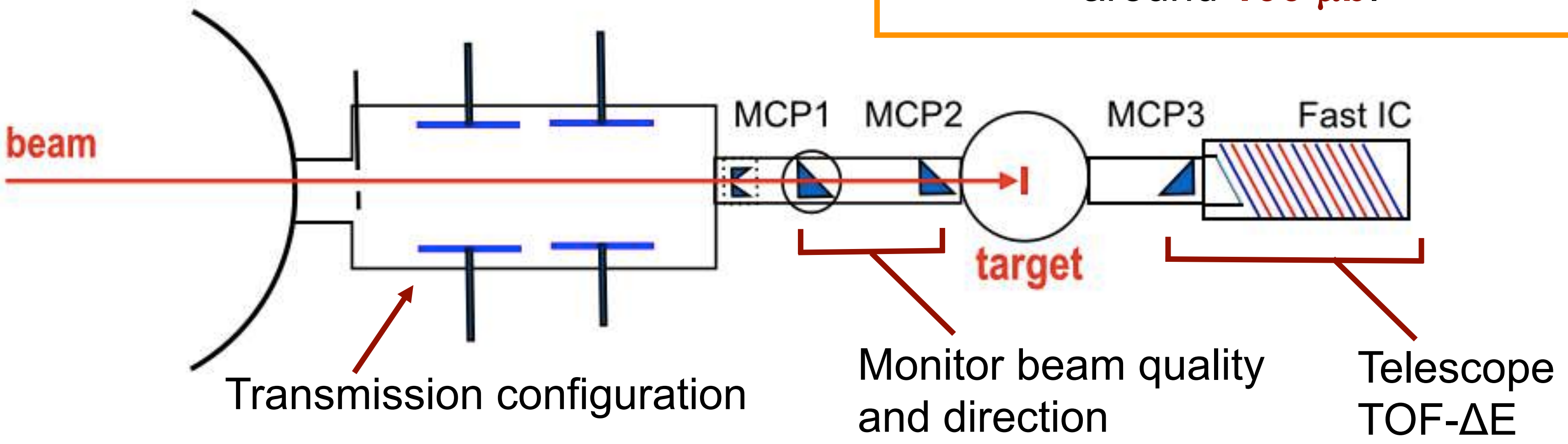

Istituto Nazionale di Fisica Nucleare
Laboratori Nazionali di Legnaro
HIL Heavy Ion Laboratory

^{64}Zn at the ALPI-Piave beam energy of E_{lab}=275 MeV on a ^{197}Au target

Extra slide

CH4 gas pressure 200 mbar → ^{197}Au recoils stopped in the IC

Detection angle 30 °

MCP$_1$ signal used as trigger of DAQ

Transmission of each electrode of 98%

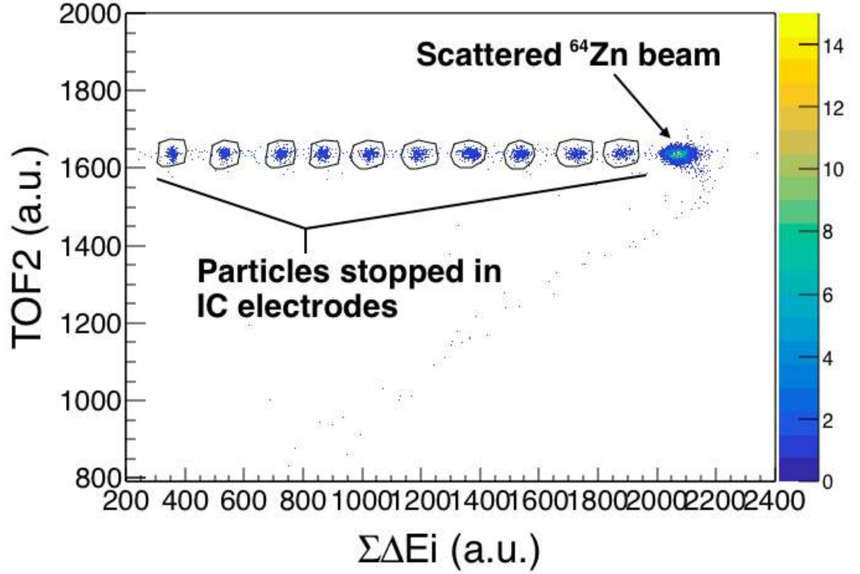

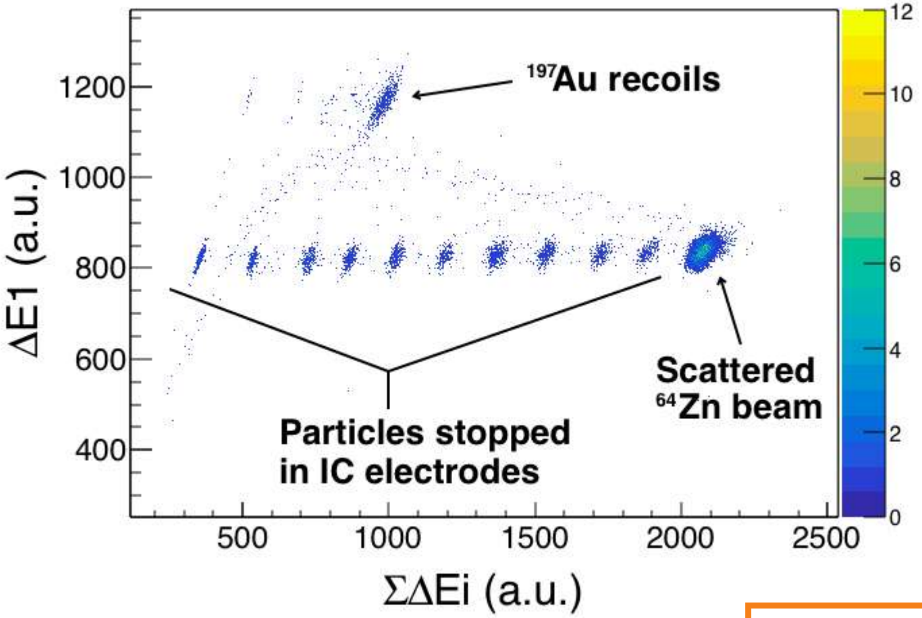

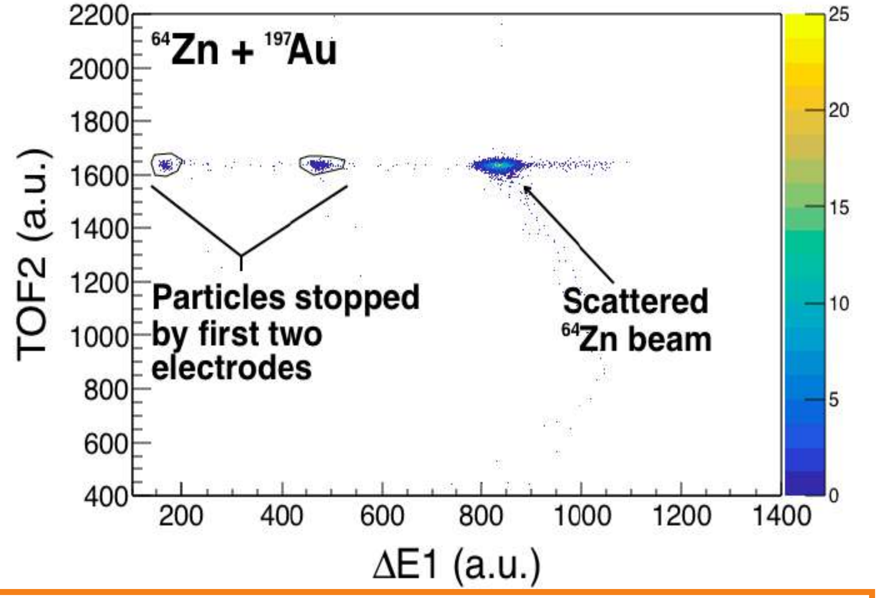

Total transparency of the total of 13 electrodes of **75%**

Extra slide

^{58}Ni beam at the energy of E_{lab}=190 MeV on a ^{28}Si target

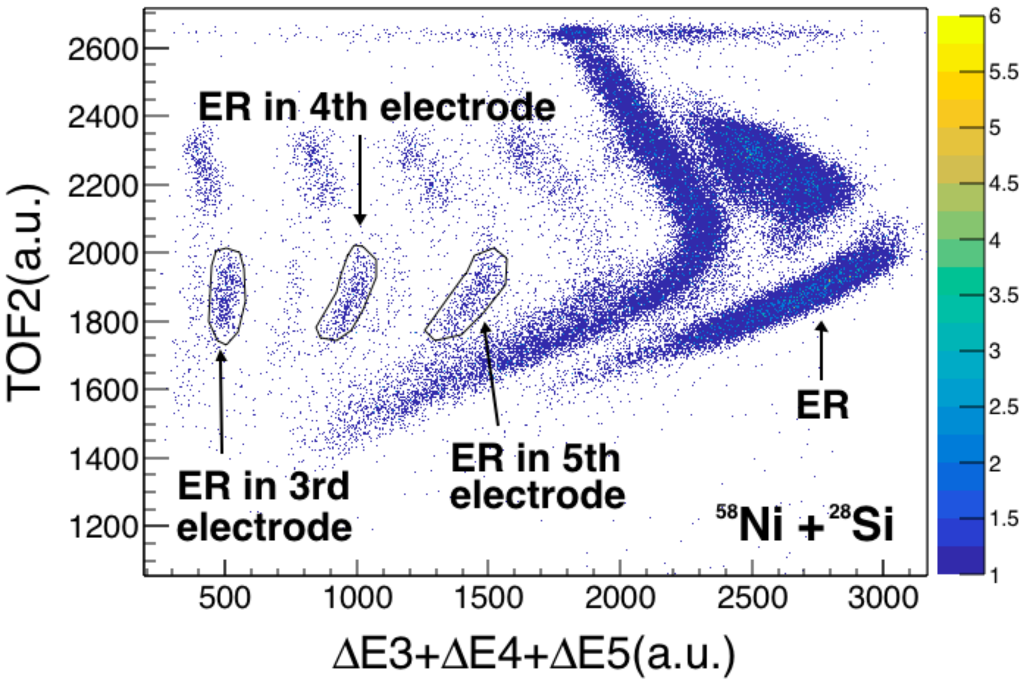

MCP$_1$ signal used as trigger of DAQ

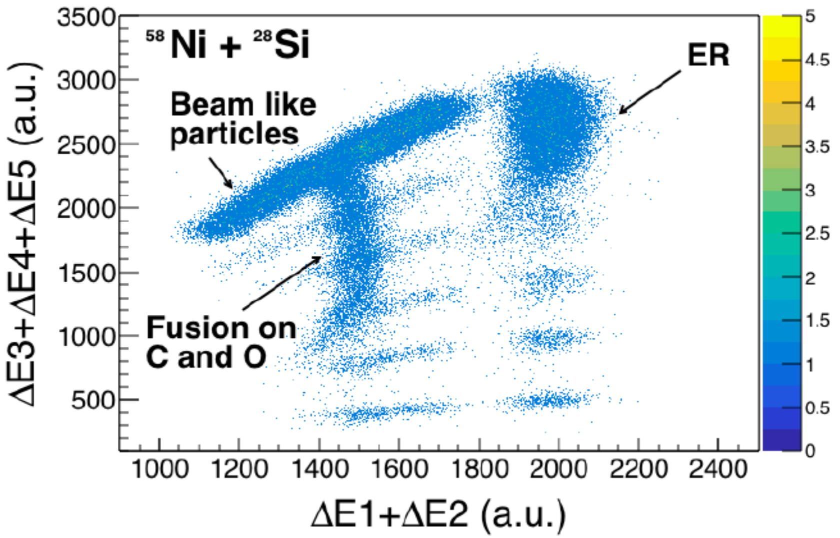

Transmission of each electrode of **98%**

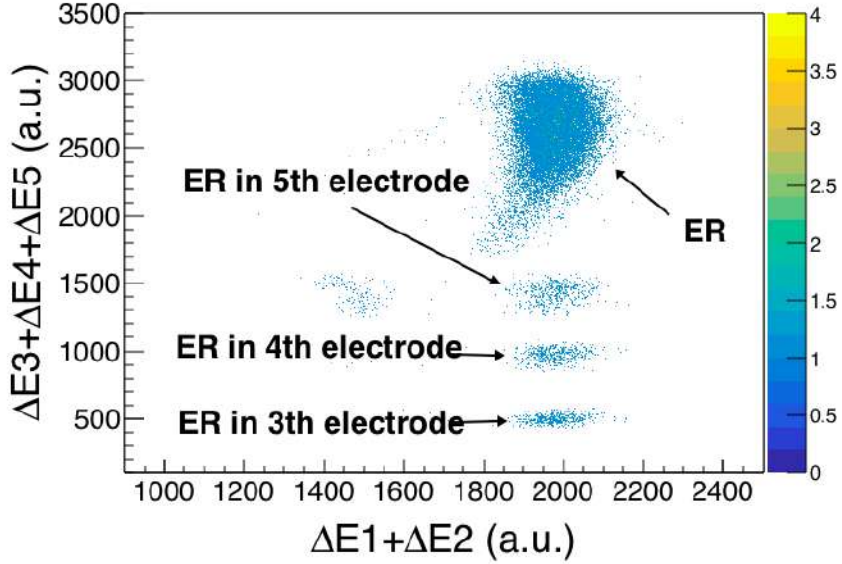

Applying a condition on the TOF2-$\Delta E_{3,4,5}$ matrix makes possible a clear identification of ER stopped in the three anodes.

Extra slide

^{28}Si beam at the energy of E_{lab}=125 MeV on a ^{100}Mo target

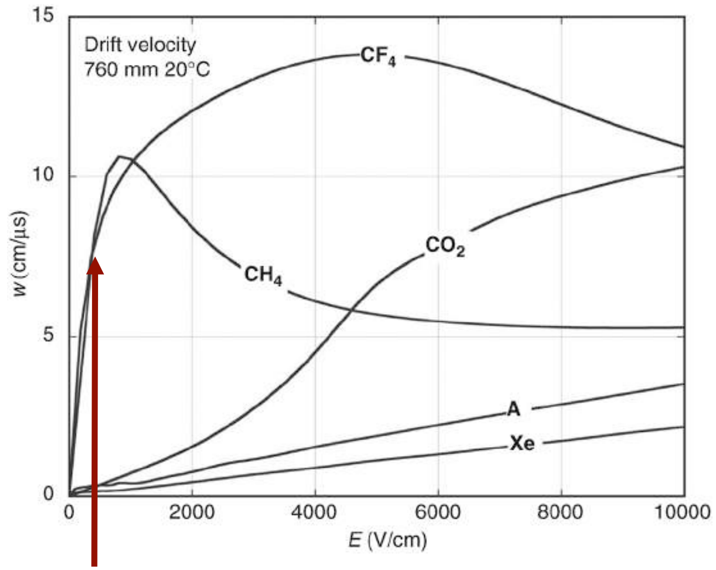

Voltage applied to IC does not exceed 500 V

Counting rate of 139 kHz

Electron drift velocity in freon is not higher in this voltage range

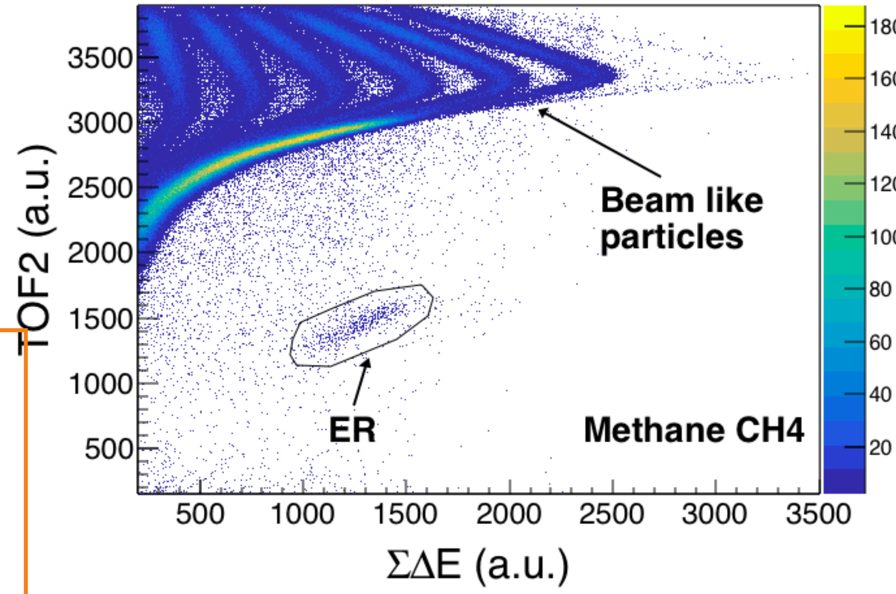

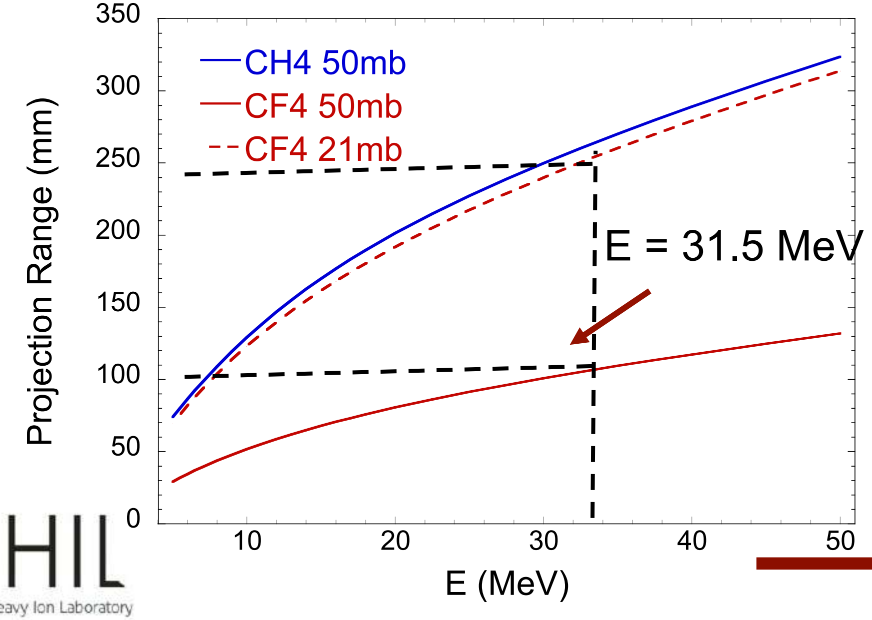

Range vs. energy of the compound nucleus ^{123}Cs

Increase of Noise/Total of **10%**

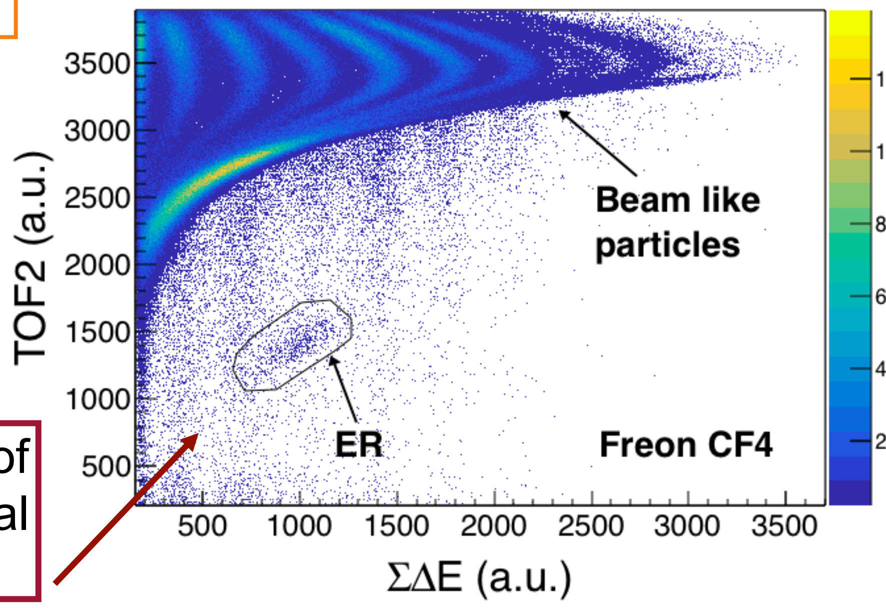

H. W. Fulbright. Nuclear Instruments and Methods 162 (1979), pp. 21–28

^{64}Zn at the ALPI-Piave beam energy of E_{lab}=275 MeV on a ^{54}Fe target

Extra slide

CH4 gas pressure 200 mbar → ^{64}Zn grazing angle 34.5°

Detection angle 30°

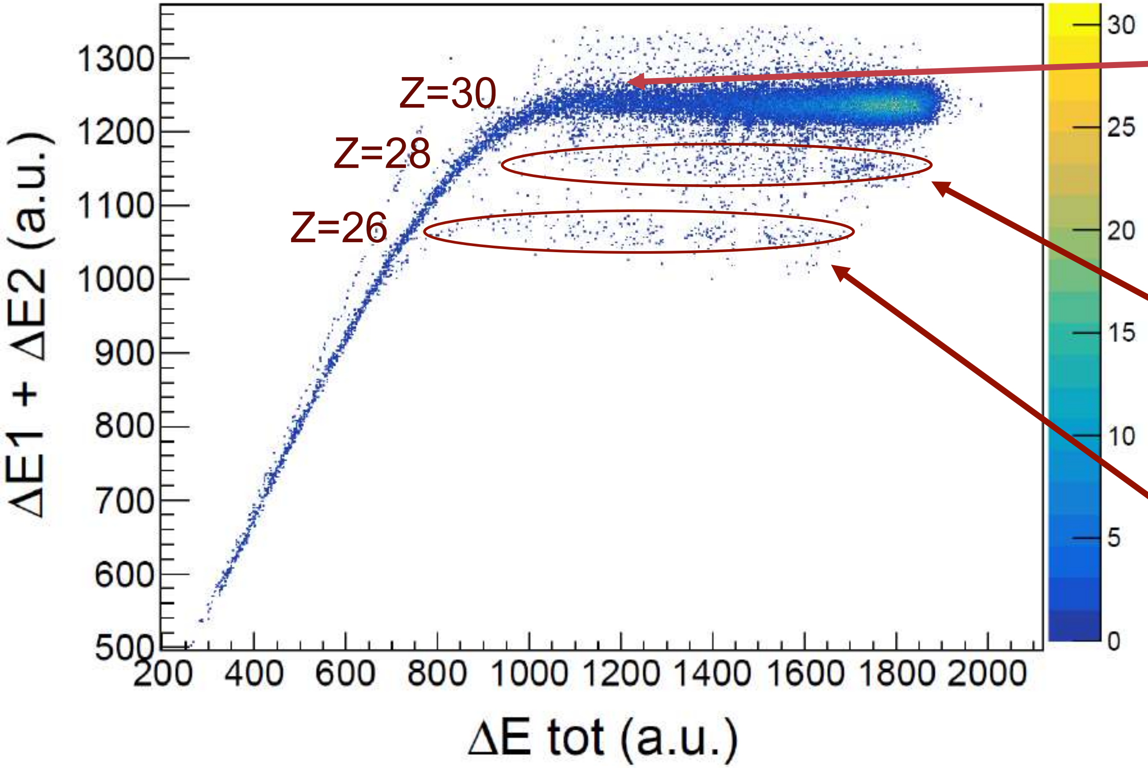

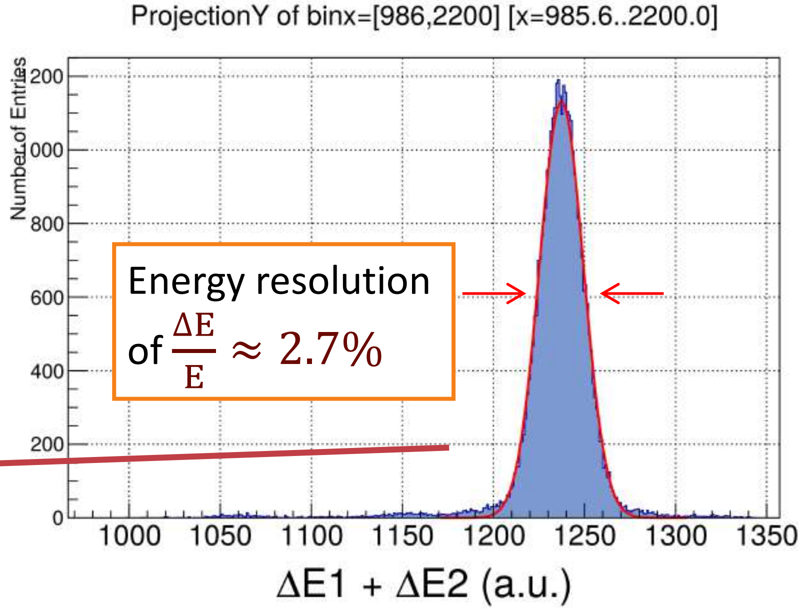

Energy resolution of $\frac{\Delta E}{E} \approx 2.7\%$

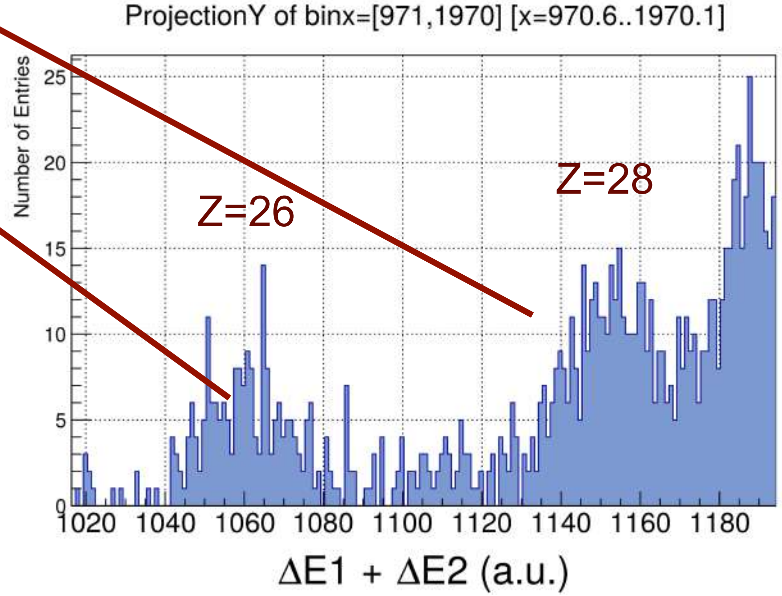

^{64}Zn at the ALPI-Piave beam energy of E_{lab}=275 MeV on a ^{54}Fe target

Extra slide

CH4 gas pressure 200 mbar → ^{64}Zn grazing angle 34.5°

Detection angle 30°

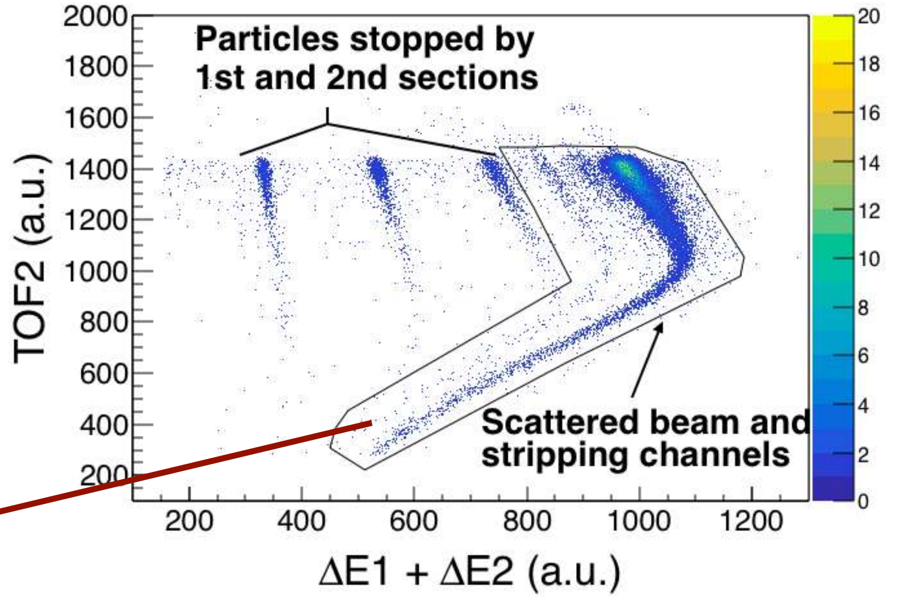

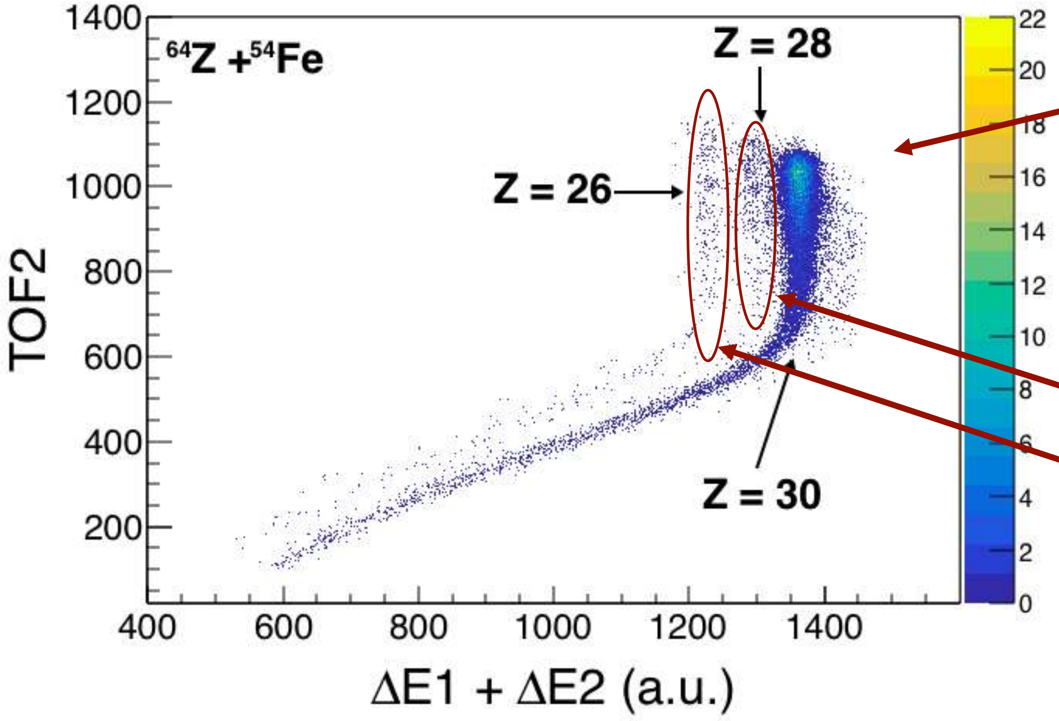

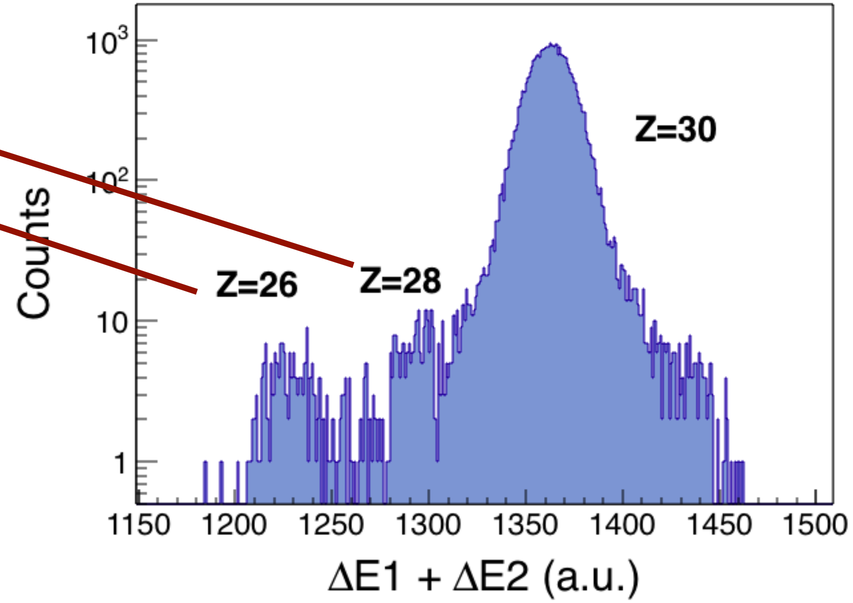

Z resolution of $\frac{\Delta Z}{Z} \approx \frac{1}{35}$

Extra slide

^{28}Si beam at the energy of E_{lab}=125 MeV on a ^{100}Mo target

Bipolar shaping of the spectroscopy amplifier to filter the residual positive ion tails, which lead to baseline fluctuation of the amplifier output.

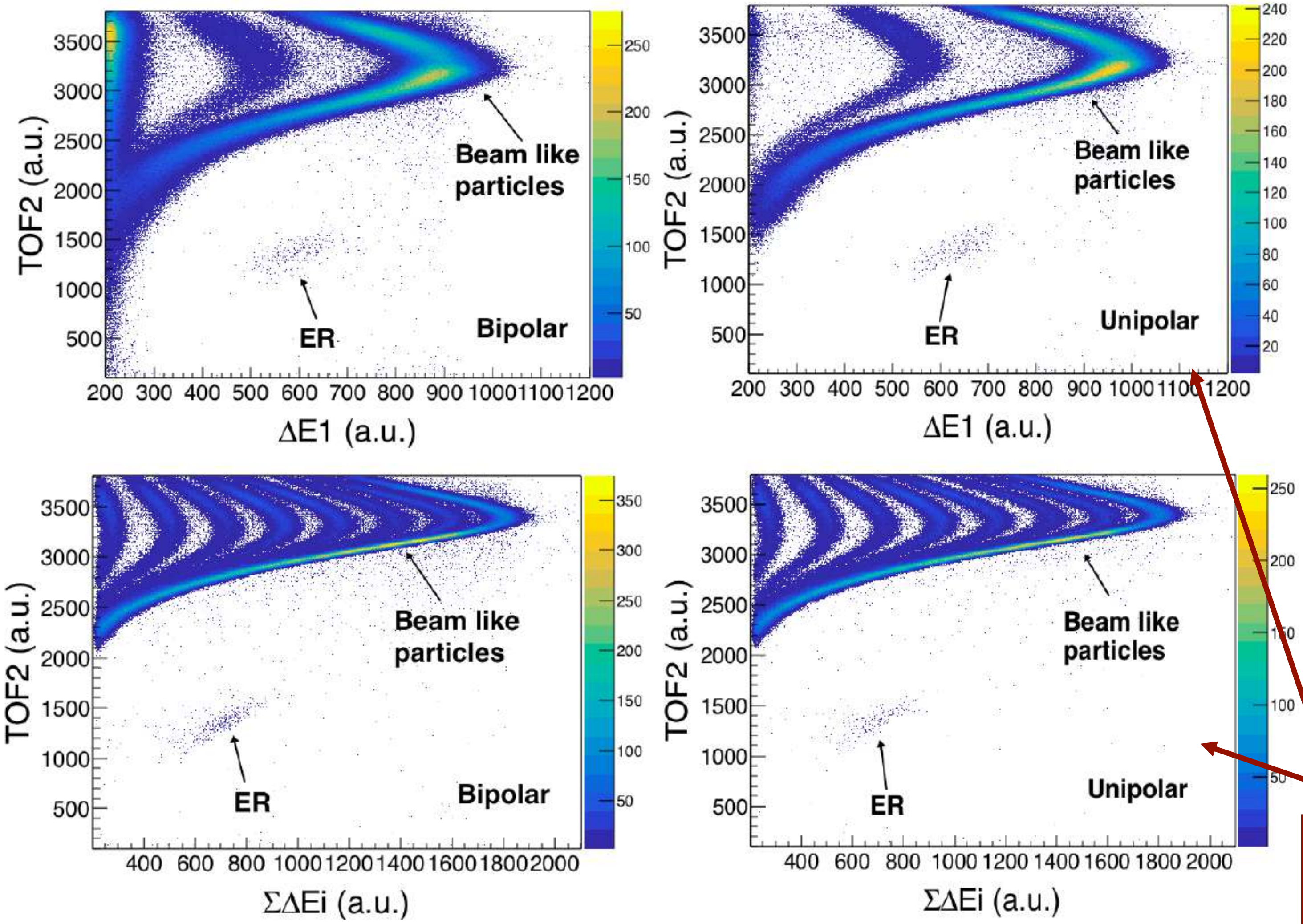

Bipolar shaping restore the baseline of the spectroscopy amplifier

Counting rate 14 kHz

MCP_1 as trigger of DAQ

Background reduction of **14%**

Extra slide

Differential fusion cross section normalized with respect to Rutherford cross section:

$$\frac{d\sigma_{fus}}{d\Omega} = \frac{N_{ER}}{N_{Mon}} \frac{\Delta\Omega_{mon}}{\Delta\Omega_{fus}^{geom}} \frac{d\sigma_{Ruth}}{d\Omega}(E) \frac{1}{T\ t\ t_{IC} t_{el}^{11}}$$

Two angular distributions for each system have been performed

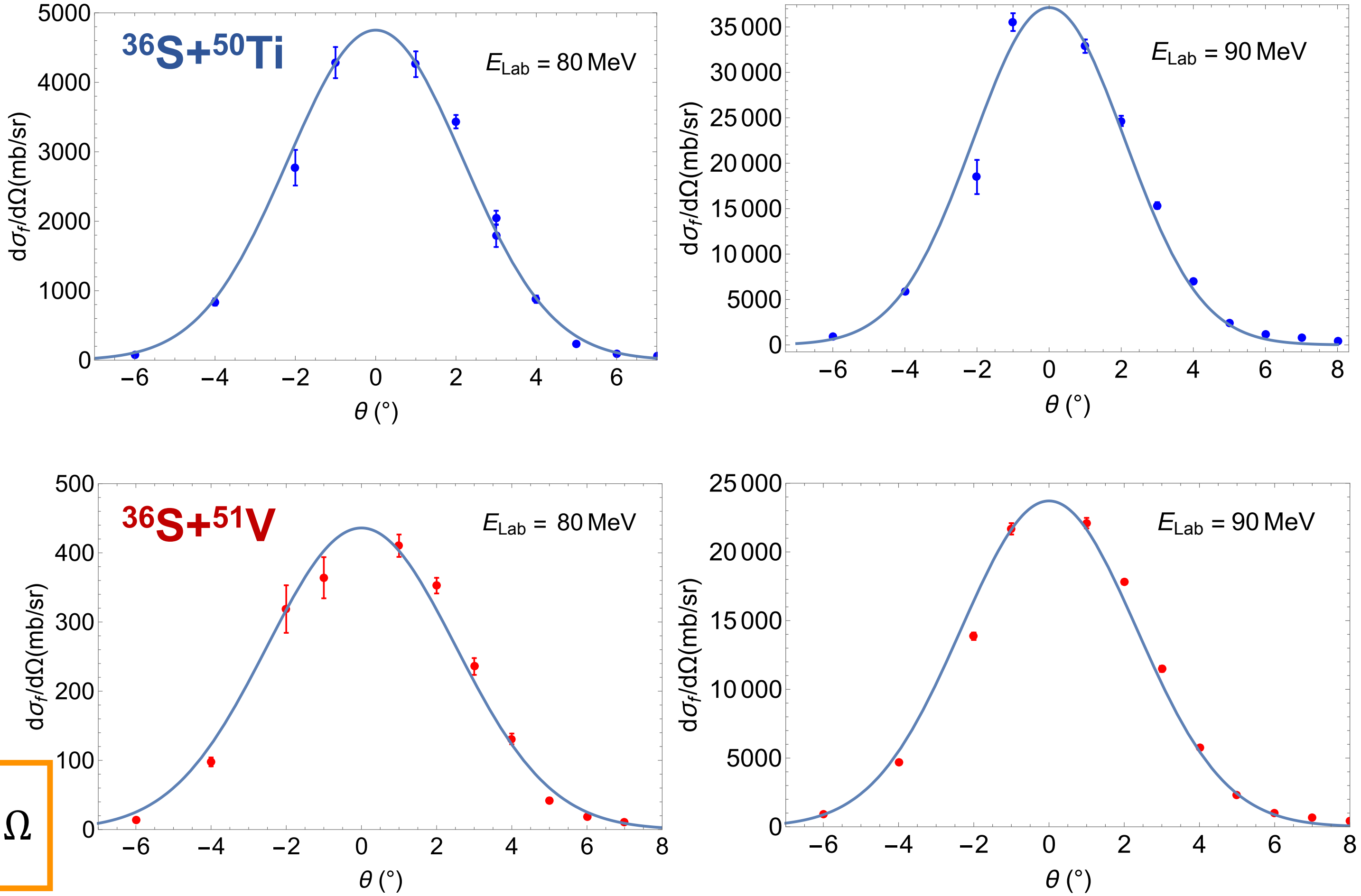

By integrating over all the solid angle, the fusion cross section is obtained

$$\sigma_{fus}(E) = \int \frac{d\sigma_{fus}}{d\Omega}(E,\theta)d\,\Omega$$

Extra slide

CC fusion cross sections underestimate the experimental data

Adiabatic coupling to high-energy states

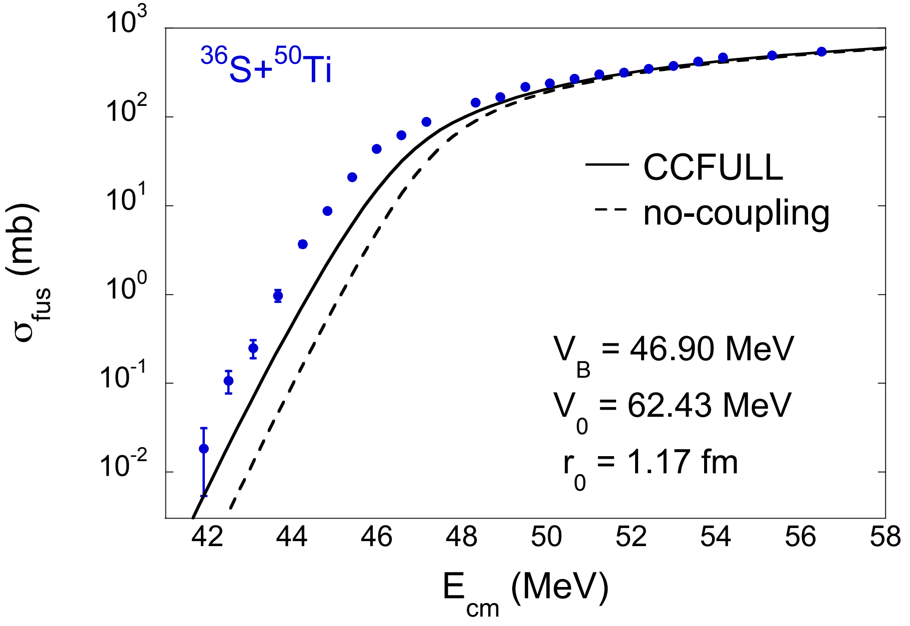

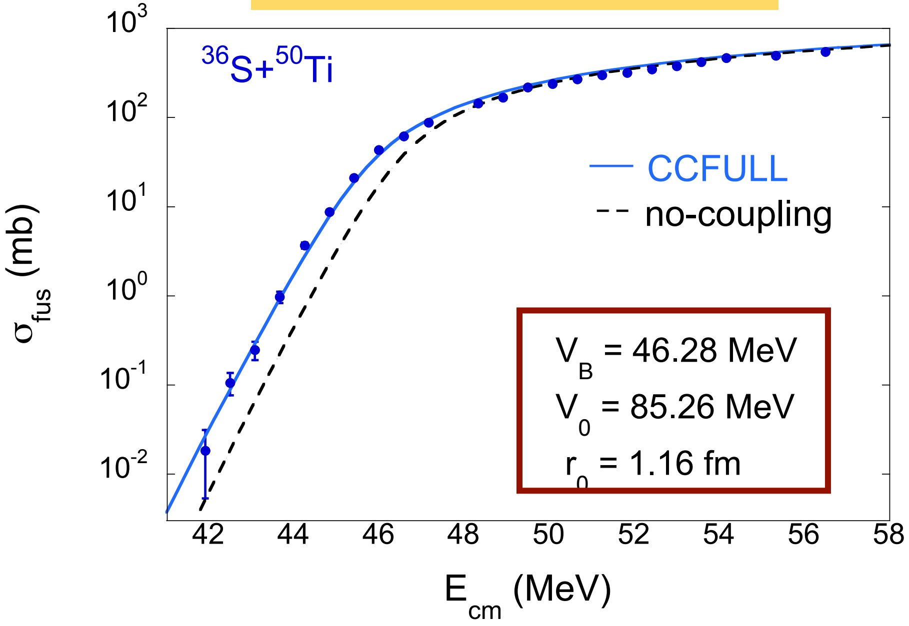

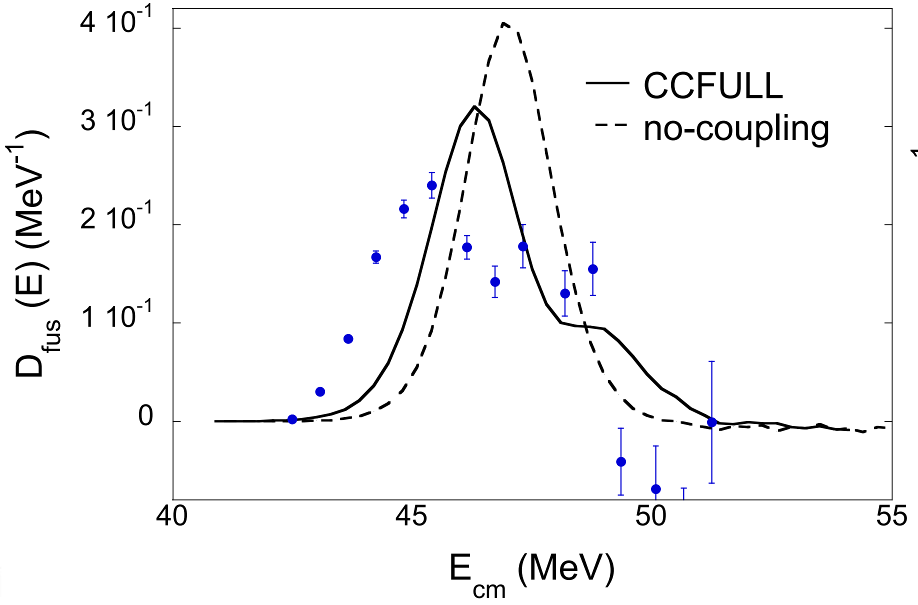

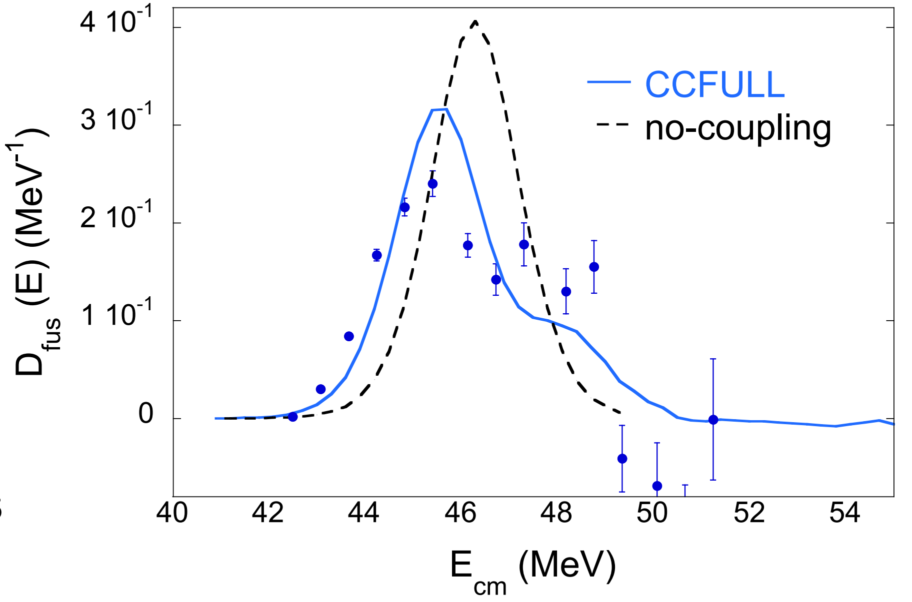

Istituto Nazionale di Fisica Nucleare

Laboratori Nazionali di Legnaro

Heavy Ion Laboratory

G. Colucci

Extra slide

CC fusion cross sections underestimate the experimental data

Adiabatic coupling to high-energy states

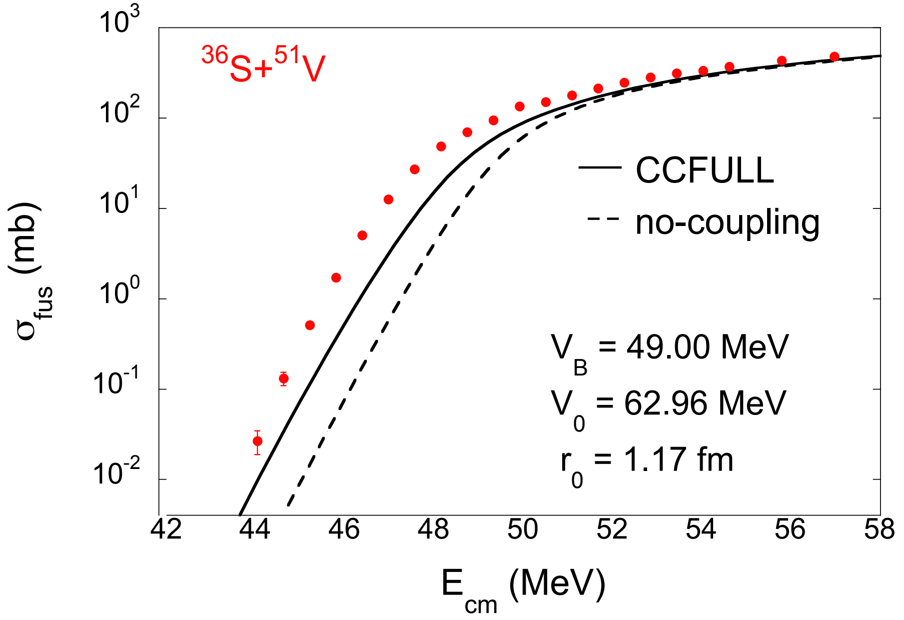

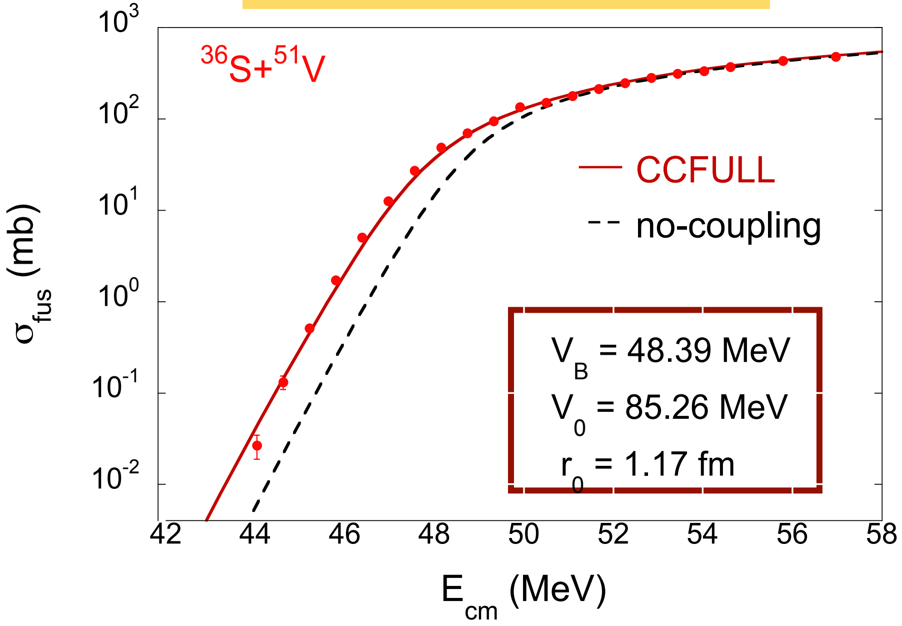

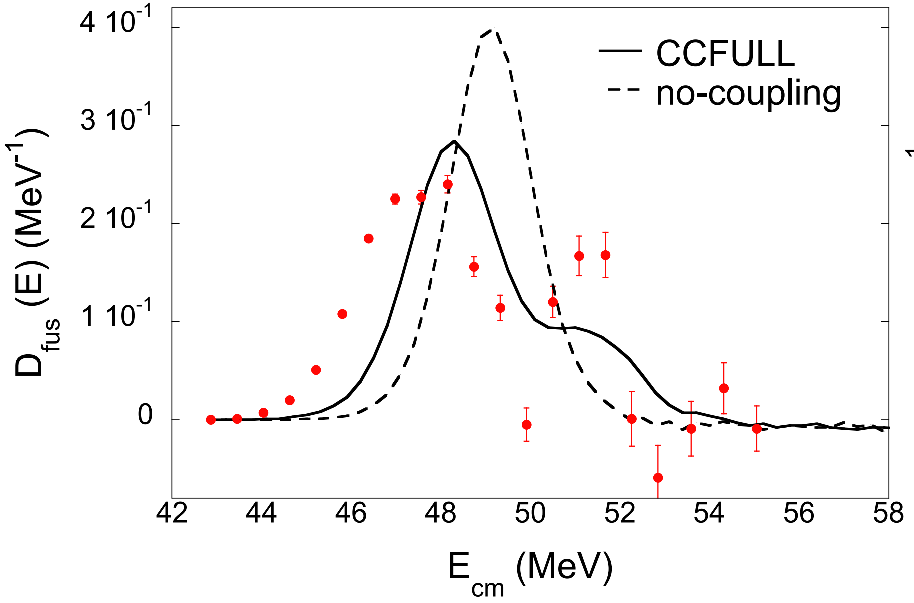

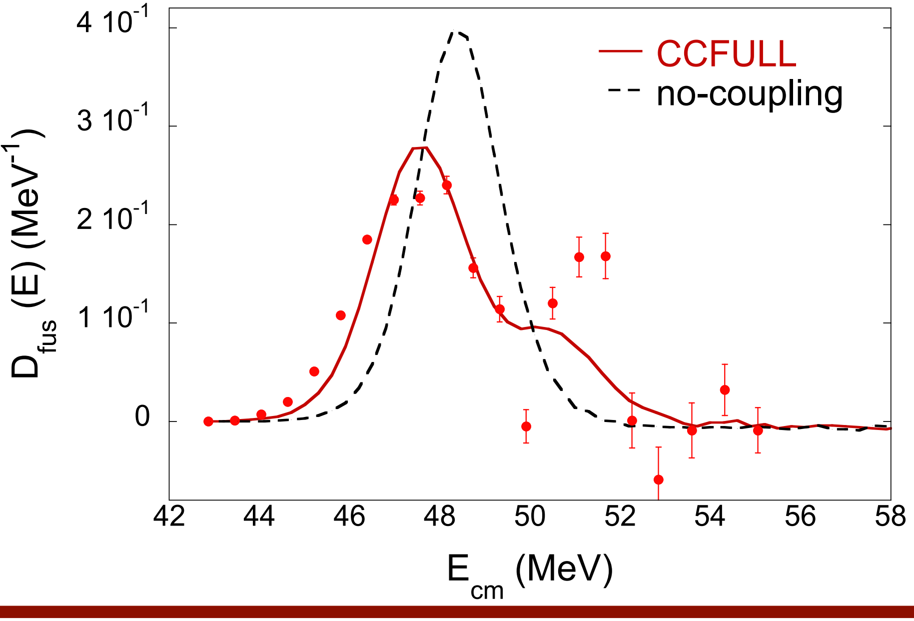

Extra slide

A total of **eight** couplings have been included in the calculations, according to the transitions among the states in ^{51}V .

Level Coupling	Spin I	B(E2) (W.u.)	β
1 - 2	$5/2^- \rightarrow 7/2^-$	14.5	
	$\pm 1/2$		+ 0.06
	$\pm 3/2$		+0.165
	$\pm 5/2$		+ 0.21
2 - 3	$3/2^- \rightarrow 5/2^-$	10.0	
	$\pm 1/2$		-0.069
	$\pm 3/2$		-0.169
1 - 3	$3/2^- \rightarrow 7/2^-$	7.6	
	$\pm 1/2$		+0.127
	$\pm 3/2$		+0.095
1 - 4	$11/2^- \rightarrow 7/2^-$	8.5	
	$\pm 1/2$		+0.188
	$\pm 3/2$		+0.172
	$\pm 5/2$		+0.140
	$\pm 7/2$		+0.0919
1 - 5	$9/2^- \rightarrow 7/2^-$	3.1	
	$\pm 1/2$		-0.0246
	$\pm 3/2$		-0.07
	$\pm 5/2$		-0.103
	$\pm 7/2$		-0.109
2 - 5	$9/2^- \rightarrow 5/2^-$	2.8	
	$\pm 1/2$		+0.110
	$\pm 3/2$		+0.095
	$\pm 5/2$		+0.0649
2 - 6	$3/2^- \rightarrow 5/2^-$	7.0	
	$\pm 1/2$		-0.0577
	$\pm 3/2$		-0.141
1 - 6	$3/2^- \rightarrow 7/2^-$	8.6	
	$\pm 1/2$		+0.136
	$\pm 3/2$		+0.101

The deformation parameters have been calculated for each coupling between the i-th and the j-th channel

The sign of the deformation parameter was established by using the weak-coupling

Extra slide

Four magnetic substates m = 1/2, 3/2, 5/2 and 7/2 of the 7/2− ground state of ^{51}V produce different Coulomb barriers.

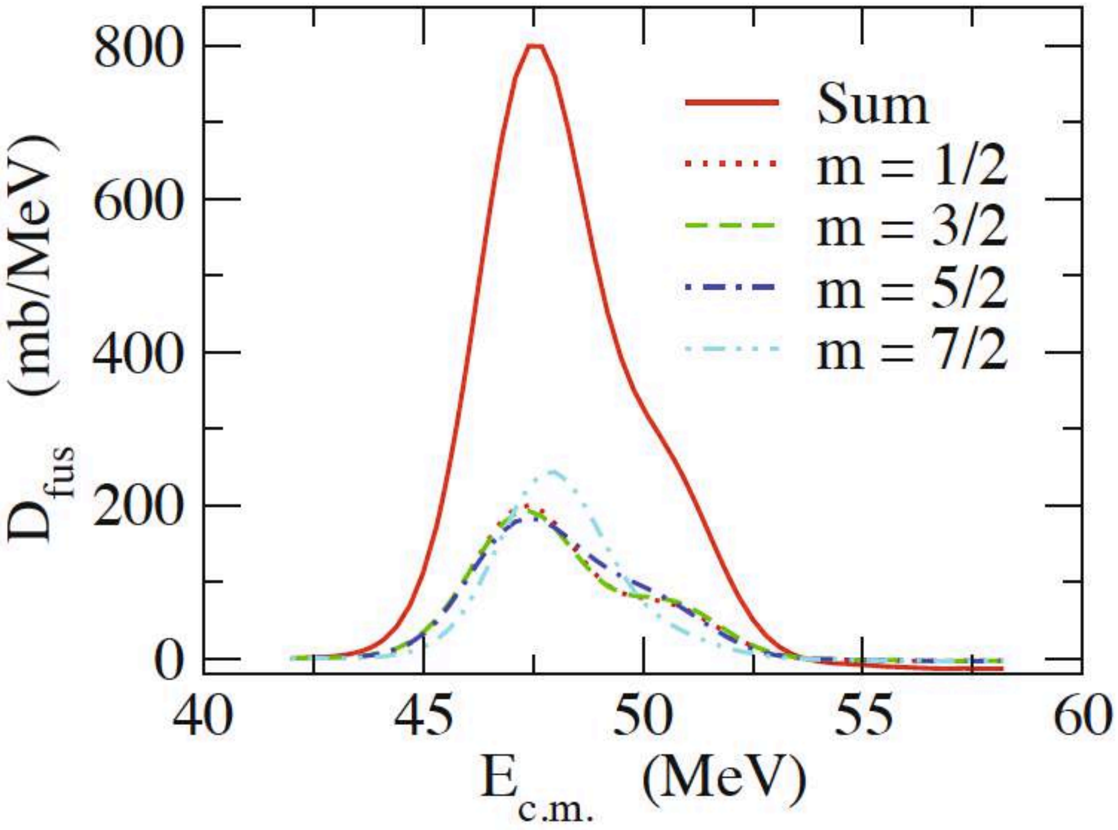

- Barrier distributions for m = 1/2 and 3/2 are almost equal, and similar to m = 5/2
- Barrier distribution for m = 7/2 is shifted towards high energies

Absence of the coupling between g.s - 5/2− state

The shift towards high energies of the barrier distribution for m = 7/2 yields the difference between the barrier CC calculations of the two systems.